6.21
The Geologic History of Seawater

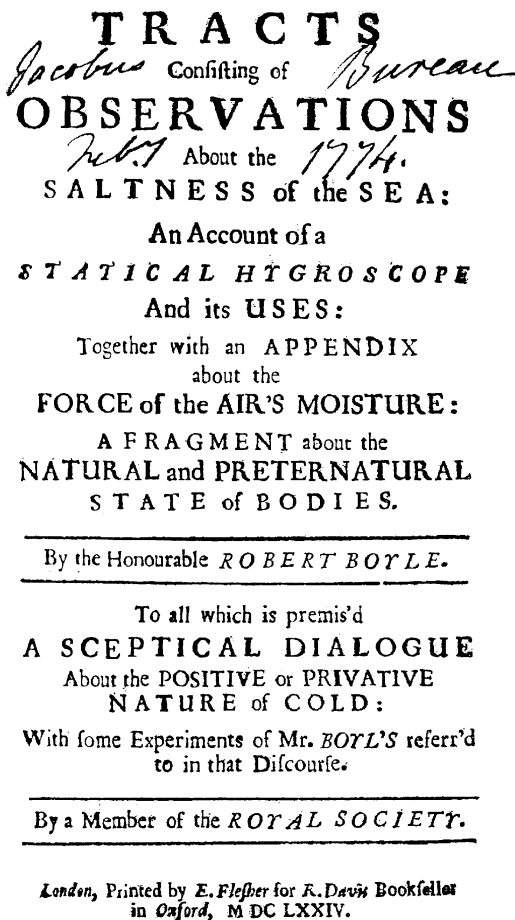## H. D. Holland

Harvard University, Cambridge, MA, USA

6.21.1 INTRODUCTION

Aristotle proposed that the saltness of the sea was due to the effect of sunlight on water. Robert Boyle took strong exception to this view and—in the manner of the Royal Society—laid out a program of research in the opening paragraph of his *Observations and Experiments about the Saltness of the Sea* (1674) (Figure 1):

The Cause of the Saltness of the Sea appears by *Aristotle's* Writings to have busied the Curiosity of Naturalists before his time; since which, his Authority, perhaps much more than his Reasons, did for divers Ages make the Schools and the generality of Naturalists of his Opinion, till towards the end of the last Century, and the beginning of ours, some Learned Men took the boldness to question the common Opinion; since when the Controversie has been kept on foot, and, for ought I know, will be so, as long as 'tis argued on both sides but by Dialectical Arguments, which may be probable on both sides, but are not convincing on either. Wherefore I shall here briefly deliver some particulars about the Saltness of the Sea, obtained by my own trials, where I was able; and where I was not, by the best Relations I could procure, especially from Navigators.

Boyle measured and compiled a considerable set of data for variations in the saltness of surface seawater. He also designed an improved piece of

TRACTS

Jacobus Confifting of *Bureau*

OBSERVATIONS

Feb.7 About the *1774.*

S A L T N E S S of the S E A :

An Account of a

S T A T I C A L   H Y G R O S C O P E

And its U S E S :

Together with an A P P E N D I X
about the

FOR CE of the AIR'S MOISTURE :

A F R A G M E N T about the

NATURAL and PRETERNATURAL

S T A T E of B O D I E S.

By the Honourable *R O B E R T B O Y L E.*

To all which is premis'd

A S C E P T I C A L D I A L O G U E

About the POSITIVE or PRIVATIVE
N A T U R E of C O L D :

With fome Experiments of Mr. *BOYL'S* referr'd
to in that Difcourfe.

By a Member of the *R O Y A L S O C I E T Y.*

London, Printed by *E. Flefher* for *R. Davis* Bookfeller
in *Oxford,* M DC LXXIV.

Figure 1 Title page of Robert Boyle's Tracts consisting of Observations about the Saltness of the Sea and other essays (1674).

equipment for sampling seawater at depth, but the depths at which it was used were modest: 30 m with his own instrument, 80 m with another, similar sampler. However, the younger John Winthrop (1606–1676), an early member of the Royal Society, an important Governor of Connecticut, and a benefactor of Harvard College, was asked to collect seawater from the bottom of the Atlantic Ocean during his crossing from England to New England in the spring of 1663. The minutes of the Royal Society's meeting on July 20, 1663, give the following account of his unsuccessful attempt to do so (Birch, 1756; Black, 1966):

> Mr. Winthrop's letter written from Boston to Mr. Oldenburg was read, giving an account of the trials made by him at sea with the instrument for sounding of depths without a line, and with the vessel for drawing water from the bottom of the sea; both which proved successless, the former by reason of too much wind at the time of making soundings; the latter, on account of the leaking of the vessel. Capt. Taylor being to go soon to Virginia, and offering himself to make the same experiments, the society

recommended to him the trying of the one in calm weather, and of the other with a stanch vessel.

> Mr. Hooke mentioning, that a better way might be suggested to make the experiment above-mentioned, was desired to think farther upon it, and to bring in an account thereof at the next meeting.

A little more than one hundred years later, in the 1780s, John Walker (1966) lectured at Edinburgh on the saltness of the oceans. He marshaled all of the available data and concluded that "these reasons seem all to point to this, that the water of the ocean in respect to saltness is pretty much what it ever has been."

In this opinion he disagreed with Halley (1715), who suggested that the salinity of the oceans has increased with time, and that the ratio of the total salt content of the oceans to the rate at which rivers deliver salt to the sea could be used to ascertain the age of the Earth. The first really serious attempt to measure geologic time by this method was made by Joly (1899). His calculations were refined by Clarke (1911), who inferred that the age of the ocean, since the Earth assumed its present form, is somewhat less than 100 Ma. He concluded, however, that "the problem cannot be regarded as definitely solved until all available methods of estimation shall have converged on one common conclusion." There was little appreciation in his approach for the magnitude of: (i) the outputs of salt from the oceans, (ii) geochemical cycles, and (iii) the notion of a steady-state ocean. In fact, Clarke's "age" of the ocean turns out to be surprisingly close to the oceanic residence time of Na^+ and Cl^-.

The modern era of inquiry into the history of seawater can be said to have begun with the work of Conway (1943, 1945), Rubey (1951), and Barth (1952). Much of the progress that was made between the appearance of these publications and the early 1980s was summarized by Holland (1984). This chapter describes a good deal of the progress that has been made since then.

6.21.2   THE HADEAN (4.5–4.0 Ga)

The broad outlines of Earth history during the Hadean are starting to become visible. The solar system originated 4.57 Ga (Allègre *et al.*, 1995). The accretion of small bodies in the solar nebula occurred within ~10 Myr of the birth of the solar system (Lugmaier and Shukolyukov, 1998). The Earth reached its present mass between 4.51 Ga and 4.45 Ga (Halliday, 2000; Sasaki and Nakazawa, 1986; Porcelli *et al.*, 1998). The core formed in <30 Ma (Yin *et al.*, 2002; Kleine *et al.*, 2002). The early Earth was covered by a magma ocean, but this must have cooled quickly at the end

of the accretion process, and the first primitive crust must have formed shortly thereafter.

At present we do not have any rocks older than 4.03 Ga (Bowring and Williams, 1999). There are, however, zircons older than 4.03 Ga which were weathered out of their parent rocks and incorporated in 3 Ga quartzitic rocks in the Murchison District of Western Australia (Froude *et al.*, 1983; Compston and Pidgeon, 1986; Nutman *et al.*, 1991; Nelson *et al.*, 2000). A considerable number of 4.2–4.3 Ga zircon grains have been found in the Murchison District. A single 4.40 Ga zircon grain has been described by Wilde *et al.* (2001). The oxygen of these zircons has apparently retained its original isotopic composition. Mojzsis *et al.* (2001), Wilde *et al.* (2001), and Peck *et al.* (2001) have shown that the $\delta^{18}O$ values of the zircons which they have analyzed are significantly more positive than those of zircons which have crystallized from mantle magmas (see Figure 2). The most likely explanation for this difference is that the melts from which the zircons crystallized contained a significant fraction of material enriched in ^{18}O. This component was probably a part of the pre-4.0 Ga crust. Its enrichment in ^{18}O was almost certainly the result of subaerial weathering, which generates ^{18}O-enriched clay minerals (see, e.g., Holland, 1984, pp. 241–251). If this interpretation is correct, the data imply the presence of an active hydrologic cycle, a significant quantity of water at the Earth surface, and an early continental crust. However, as Halliday (2001) has pointed out, inferring the existence of entire continents from zircon grains in a single

area requires quite a leap of the imagination. We need more zircon data from many areas to confirm the inferences drawn from the small amount of available data. Nevertheless, the inferences themselves are reasonable and fit into a coherent model of the Hadean Earth.

At present, little can be said with any degree of confidence about the composition of the proposed Hadean ocean, but it was probably not very different from that of the Early Archean ocean, about which a good deal can be inferred.

6.21.3 THE ARCHEAN (4.0–2.5 Ga)

6.21.3.1 The Isua Supracrustal Belt, Greenland

The Itsaq Gneiss complex of southern West Greenland contains the best preserved occurrences of ≥3.6 Ga crust. The gneiss complex had a complicated early history. It was added to and modified during several events starting ca. 3.9 Ga (Nutman *et al.*, 1996). Supracrustal, mafic, and ultramafic rocks comprise ~10% of the complex; these range in age from ≥3.87 Ga to ca. 3.6 Ga. A large portion of the Isua supracrustal belt (Figure 3) contains rocks that may be felsic volcanics and volcaniclastics, and abundant, diverse chemical sediments (Nutman *et al.*, 1997). The rocks are deformed, and many are substantially altered by metasomatism. However, transitional stages can be seen from units with relatively well-preserved primary volcanic and sedimentary features to schists in which all primary features have been
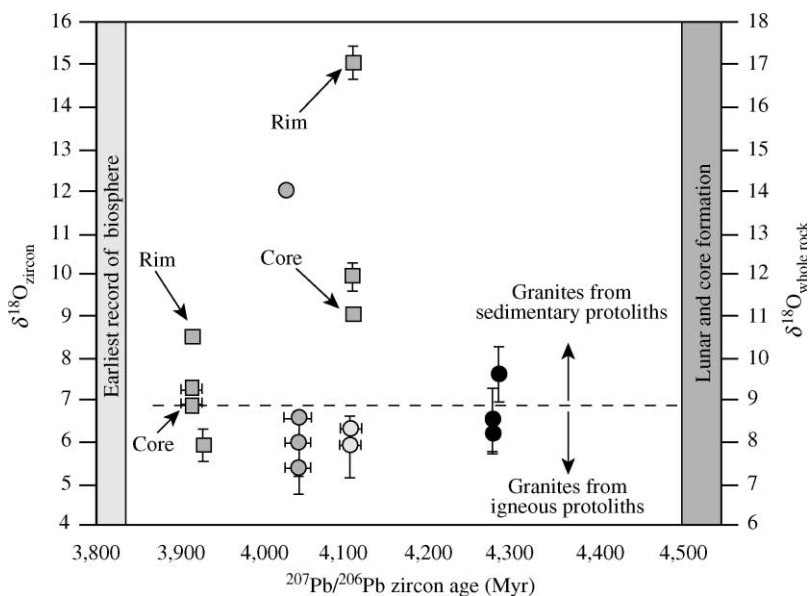
Figure 2 Ion microprobe $\delta^{18}O$ data for individual zircon spot analyses versus $^{207}Pb/^{206}Pb$ zircon age. The right vertical axis shows the estimated $\delta^{18}O$ data for the whole rock ($\delta^{18}O_{WR}$) from which the zircon crystallized (source Mojzsis *et al.*, 2001).
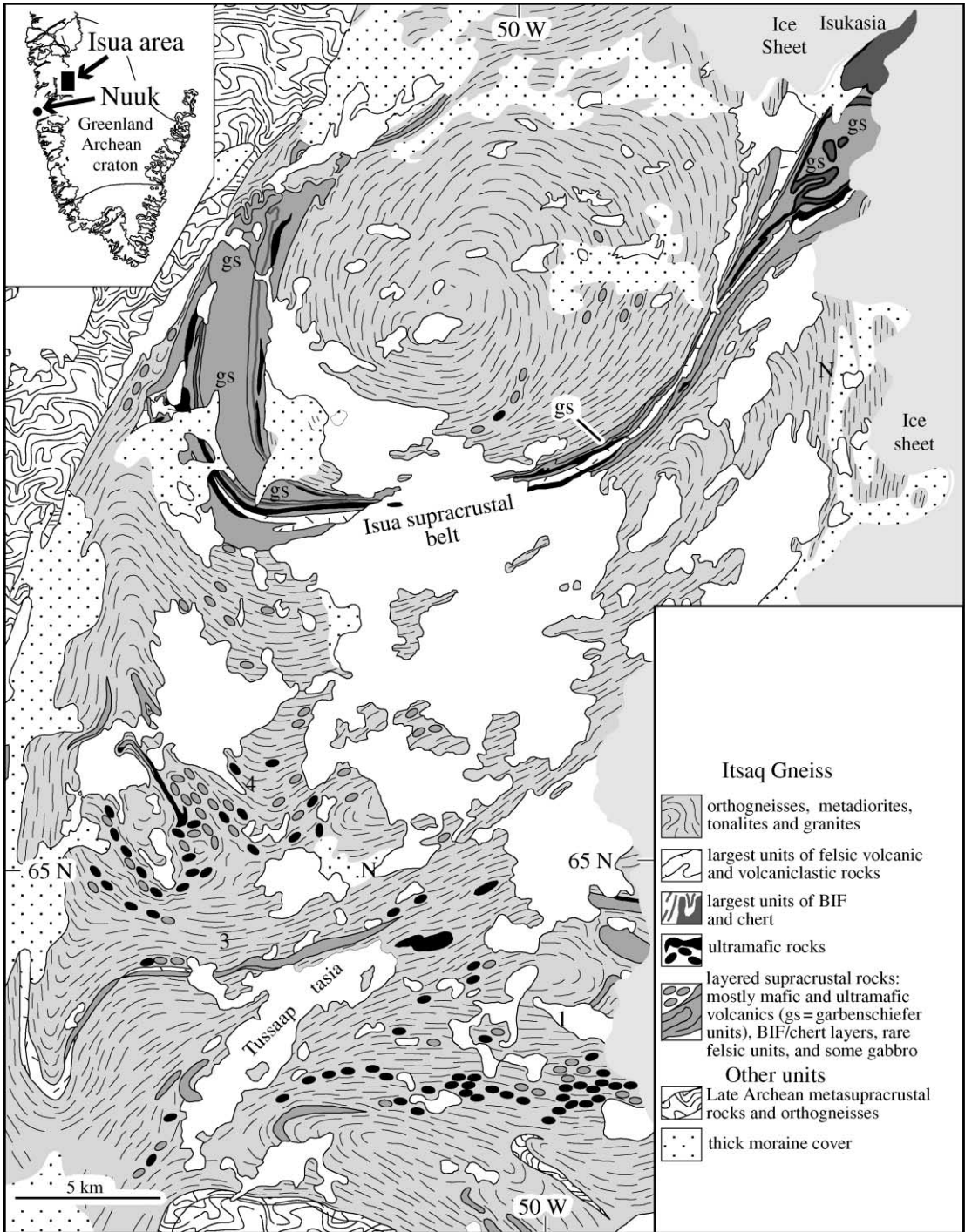
Figure 3   Map of the northern part of the Itsaq Gneiss complex (source Nutman *et al*., 2002).

obliterated. Most of the Isua greenstone belt consists of fault-bounded rock packages mainly derived from basaltic and high-manganese basaltic pillow lava and pillow lava breccia, chert-banded iron formation (chert-BIF), and a minor component of clastic sedimentary rocks derived from chert and basaltic volcanic rocks (Myers, 2001). The Isua sequence, as we now see it, resembles deep-sea sequences rather than platform deposits. The Isua rocks could have been deposited in a purely oceanic environment without a significant sialic detrital component, and intruded by the felsic gneisses during or after tectonic emplacement into the Amitsoq protocontinent (Rosing *et al*., 1996).

The most compelling evidence for an ocean during the deposition of the Isua greenstone belt is

provided by the BIF deposits which occur in this sequence. They are highly metamorphosed. Boak and Dymek (1982) have shown that the pelitic rocks in the sequence were exposed to temperatures of ~550 °C at pressures of ~5 kbar. Temperatures during metamorphism could not have exceeded ~600 °C. The mineralogy and the chemistry of the iron formations have obviously been altered by metamorphism, but their major features are still preserved. Magnetite-quartz BIFs are particularly common. Iron enrichment can be extensive, as shown by the presence of a two-billion ton body at the very north-easternmost limit of the supracrustal belt (Bridgewater *et al.*, 1976).

In addition to the quartz-magnetite iron formation, Dymek and Klein (1988) described magnesian iron formation, aluminous iron formation, graphitic iron formation, and carbonate rich iron formation. They pointed out that the composition of the iron formation as a whole is very similar to that of other Archean and Proterozoic iron formations that have been metamorphosed to the amphibolite facies.

The source of the iron and probably much of the silica in the BIF was almost certainly seawater that had cycled through oceanic crust at temperatures of several hundred degree celsius. The low concentration of sulfur and of the base metals that are always present in modern solutions of this type indicates that these elements were removed, probably as sulfides of the base metals before the deposition of the iron oxides and silicates of the Isua iron formations.

The molar ratio of Fe_2O_3/FeO in the BIFs is less than 1.0 in all but one of the 28 analyses of Isua iron formation reported by Dymek and Klein (1988). In the one exception the ratio is 1.17. Unless the values of this ratio were reduced significantly during metamorphism, the analyses indicate that magnetite was the dominant iron oxide, and that hematite was absent or very minor in these iron formations. This, in turn, shows that some of the hydrothermal Fe^{2+} was oxidized to Fe^{3+} prior to deposition, but that not enough was oxidized to lead to the precipitation of Fe_2O_3 and/or Fe^{3+} oxyhydroxide precursors, or that these phases were subsequently replaced by magnetite.

The process(es) by which the precursor(s) of magnetite in these iron formations precipitated is not well understood. A possible explanation involves the oxidation of Fe^{2+} by reaction with seawater to produce Fe^{3+} and H_2 followed by the precipitation of "green rust"—a solid solution of $Fe(OH)_2$ and $Fe(OH)_3$—and finally by the dehydration of green rust to magnetite (but see below). Figure 4 shows that the boundary between the stability field of $Fe(OH)_2$ and amorphous $Fe(OH)_3$ is at a rather low value of $p\varepsilon$. The field of green rust probably straddles this boundary. Saturation of solutions with siderite along this
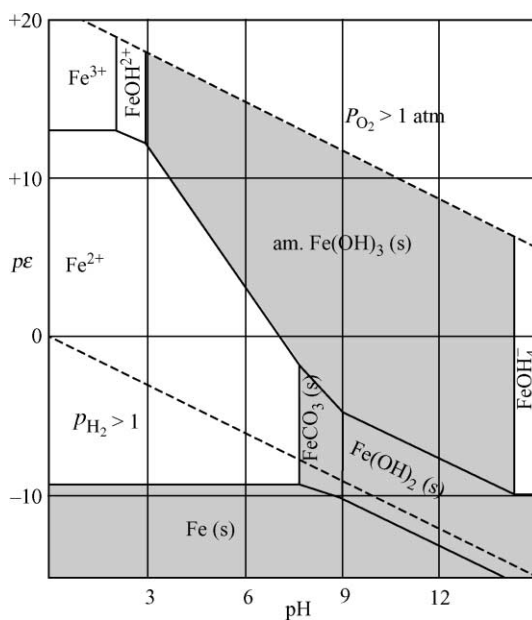
Figure 4 Diagram $p\varepsilon$ versus pH for the system $Fe–CO_2–H_2O$. The solid phases are $Fe(OH)_3$ (amorphous), $FeCO_3$ (siderite), $Fe(OH)_2(s)$, and $Fe(s)$; $C_T = 10^{-3}$ M. Lines are calculated for Fe(II) and Fe(III) = 10^{-5} M at 25 °C. The possible conversion of carbonate to methane at low $p\varepsilon$ values was ignored (source Stumm and Morgan, 1996).

boundary at a total carbon concentration of 10^{-3} M and a total Fe concentration of 10^{-5} M lies within a reasonable range for the pH of Archean seawater. However, the sequence of mineral deposition was probably more complex (see below).

The reaction of Fe^{2+} with H_2O is greatly accelerated by solar UV (see, e.g., Braterman *et al.*, 1984), and it has been suggested that solar UV played an important role in the deposition of oxide facies iron formation (Cairns-Smith, 1978; Braterman *et al.*, 1983; Sloper, 1983; François, 1986, 1987; Anbar and Holland, 1992). However, it now appears that solar UV played no more than a minor role in the deposition of oxide facies BIF. The reasons for this conclusion are detailed later in the chapter. The absence of significant quantities of hematite indicates that seawater from which the precursor of the magnetite-quartz iron formation was deposited was mildly reducing. This is corroborated by the mineralogy of the silicates, in which iron is present exclusively or nearly so in the divalent state. The only possible indication of a relatively high oxidation state is the presence of cerium anomalies reported in some of Dymek and Klein's (1988) rare earth element (REE) analyses. However, the validity of these anomalies is somewhat uncertain, because the analyses do not include praseodymium, and

because neodymium measurements are lacking in a number of cases. Fryer (1983) had earlier observed that no significantly anomalous behavior of cerium has been found in any Archean iron formations, and neither Appel (1983) and Shimizu et al. (1990), nor Bau and Möller (1993) were able to detect cerium anomalies in samples of the Isua iron formation.

One of the most intriguing sedimentary units described by Dymek and Klein (1988) is the graphitic iron formation. Four samples of this unit contained between 0.70% and 2.98% finely dispersed graphite. Quartz, magnetite, and cummingtonite are their main mineral constituents. The origin of the graphite has been a matter of considerable debate. Schidlowski et al. (1979) reported a range of $-5.9‰$ to $-22.2‰$ for the $\delta^{13}C$ value of 13 samples of graphite from Isua. They proposed that the graphite represents the metamorphosed remains of primary Isua organisms, that the isotopically light carbon in some of their graphite samples reflects the isotopic composition of these organisms, and that the isotopically heavy carbon in some of their graphite samples reflects the redistribution of carbon isotopes between organic and carbonate carbon during amphibolite grade metamorphism. Perry and Ahmad (1977) found $\delta^{13}C$ values between $-9.3‰$ and $-16.3‰$ in Isua supracrustal rocks and pointed out that the fractionation of the carbon isotopes between siderite and graphite in their samples is consistent with inorganic equilibrium of these phases at $\sim 400–500$ °C. Oehler and Smith (1977) found graphite with $\delta^{13}C$ values of $-11.3‰$ to $-17.4‰$ in Isua metapelites (?) containing $150–4,800$ ppm reduced carbon, and graphite with a $\delta^{13}C$ range between $-21.4‰$ and $-26.9‰$ in metasediments from the Isua iron formation which contain only trace amounts of graphite ($4–56$ ppm). The carbon in the latter samples is thought to be due to postdepositional contamination.

Since then Mojzsis et al. (1996) have used *in situ* ion microprobe techniques to measure the isotopic composition of carbon in Isua BIF and in a unit from the nearby Akilia Island that may be BIF. $\delta^{13}C$ in carbonaceous inclusions in the BIF ranged from $-23‰$ to $-34‰$; those in carbon inclusions occluded in apatite micrograins from the Akilia Island BIF ranged from $-21‰$ to $-49‰$. Since the carbon grains embedded in apatite were small and irregular, the precision and accuracy of the individual $\delta^{13}C$ measurements was typically $\pm 5‰$ (1σ). These measurements tend to confirm the Schidlowski et al. (1979) interpretation, and suggest that the graphite in the Isua and Akilia BIFs could well be the metamorphosed remains of primitive organisms. However, other interpretations have been advanced very forcefully (see, e.g., Holland, 1997; Van Zuilen et al., 2002).

Naraoka et al. (1996) have added additional $\delta^{13}C$ measurements, which fall in the same range as those reported previously. They emphasize that graphite with $\delta^{13}C$ values around $-12‰$ was probably formed by an inorganic, rather than by a biological process. Rosing (1999) reported $\delta^{13}C$ values ranging from $-11.4‰$ to $-20.2‰$ in $2–5$ μm graphite globules in turbiditic and pelagic sedimentary rocks from the Isua supracrustal belt. He suggests that the reduced carbon in these samples represents biogenic detritus, which was perhaps derived from planktonic organisms.

This rather large database certainly suggests that life was present in the $3.7–3.9$ Ga oceans, but it is probably best to treat the proposition as likely rather than as proven. One of the arguments against the presence of life before 3.8 Ga is based on the likelihood of large extraterrestrial impacts during a late heavy bombardment (LHB). The craters of the moon record an intense bombardment by large bodies, ending abruptly ca. 3.85 Ga (Dalrymple and Ryder, 1996; Hartmann et al., 2000; Ryder, 1990). The Earth was probably impacted at least as severely as the moon, and there is a high probability that impacts large enough to vaporize the ocean's photic zone occurred as late as 3.8 Ga (Sleep et al., 1989). The environment of the early Earth, therefore, may have been extremely challenging to life (Chyba, 1993; Appel and Moorbath, 1999). There has, however, been little direct examination of the Earth's surface environment during this period. The metasediments at Isua and on Akilia Island supply a small window on the effects of extraterrestrial bombardment between ca. 3.8 Ga and 3.9 Ga. Anbar et al. (2002) have determined the concentration of iridium and platinum in three samples of a ~ 5 m thick BIF chert unit and in three samples of mafic–ultramafic flows interposed with BIF in a relatively undeformed section on Akilia Island. The iridium and platinum concentrations in the Akilia metasediments are all extremely low. The iridium content of only one of the BIF/chert samples is above 3 ppt, the detection limit of the ID–ICP–MS techniques. The concentration of platinum is below the detection limit (40 ppt) in nearly all of the BIF/chert samples. Both elements were readily detected in the mafic–ultramafic samples. The extremely low concentration of iridium and platinum in the BIF/chert samples shows that their composition was not significantly affected by extraterrestrial impacts. It is difficult, however, to extrapolate from these few analyses to other environments between 3.8 Ga and 3.9 Ga, especially because it has been proposed that these rocks are not sedimentary (Fedo and Whitehouse, 2002). As Anbar et al. (2002) have pointed out, the large time gaps between the large, life-threatening impact events require

extensive sampling of the rock record for the detection of the impact events. The slim evidence supplied by the Anbar *et al.* (2002) study encourages the view that conditions were sufficiently benign for the existence of life on Earth during the deposition of the sediments at Isua and on Akilia, but optimism on this point must surely be tempered, and it is premature to speculate on the effects of the potential biosphere on the state of the oceans 3.8–3.9 Ga.

6.21.3.2 The Mesoarchean Period (3.7–3.0 Ga)

Evidence for the presence of life is abundant during the later part of the Mesoarchean period. Unmetamorphosed carbonaceous shales with $\delta^{13}C$ values that are consistent with a biological origin of the contained carbon are reasonably common (see, e.g., Schidlowski *et al.*, 1983; Strauss *et al.*, 1992). The nature of the organisms that populated the Mesoarchean oceans is still hotly disputed. The description of microfossils in the 3.45 Ga Warrawoona Group of Western Australia by Schopf and Packer (1987) and Schopf (1983) suggested that some of these microfossils were probably the remains of cyanobacteria. If so, oxygenic photosynthesis is at least as old as 3.45 Ga. Brasier *et al.* (2002) have re-examined the type sections of the material described by Schidlowski *et al.* (1983) and have reinterpreted all of his 11 holotypes as artifacts formed from amorphous graphite within multiple generations of metalliferous hydrothermal vein chert and volcanic glass. However, Schopf *et al.* (2002) maintain that the laser Raman imagery of this material not only establishes the biogenicity of the fossils which they have studied, but also provides insight into the chemical changes that accompanied the metamorphism of these organics. Whatever the outcome of this debate, it is most likely that the oceans contained an upper, photic zone, that ~20% of the volcanic CO_2 added to the atmosphere was reduced and buried as a constituent of organic water, and that the remaining 80% were buried as a constituent of marine carbonates (see, e.g., Holland, 2002).

The influence of these processes on the composition of Mesoarchean seawater is still unclear. De Ronde *et al.* (1997) have studied the fluid chemistry of what they believe are Archean seafloor hydrothermal vents, and have explored the implications of their analyses for the composition of contemporary seawater. They estimate that seawater contained 920 mmol L^{-1} Cl, 2.25 mmol L^{-1} Br, 2.3 mmol L^{-1} SO_4, 0.037 mmol L^{-1} I, 789 mmol L^{-1} Na, 5.1 mmol L^{-1} NH_4, 18.9 mmol L^{-1} K, 50.9 mmol L^{-1} Mg, 232 mmol L^{-1} Ca, and 4.52 mmol L^{-1} Sr. This composition, if correct, implies that Archean seawater was rather similar to modern seawater.

Unfortunately, there is considerable doubt about the correctness of these concentrations. First, the composition of seawater is altered significantly during passage through the oceanic crust, and the reconstruction of the composition of seawater from that of hydrothermal fluids is not straightforward. Second the charge balance of the proposed seawater is quite poor. Third, the quartz which contained the fluid inclusions analyzed by De Ronde *et al.* (1997) is intimately associated with hematite and goethite. The former mineral is most unusual as an ocean floor mineral at 3.2 Ga. The latter is also unusual, because these sediments passed through a metamorphic event at 2.7 Ga during which the temperature rose to >200 °C (De Ronde *et al.*, 1994). It is not unlikely that the inclusion fluids analyzed by De Ronde *et al.* were trapped more recently than 3.2 Ga, and that they are not samples of 3.2 Ga seawater (Lowe, personal communication, 2002).

The direct evidence for the composition of Mesoarchean seawater is, therefore, quite weak. For the time being it seems best to rely on indirect evidence derived from the mineralogy of sediments from this period, the composition of these minerals, and the isotopic composition of their contained elements. The carbonate minerals in Archean sediments are particularly instructive (see, e.g., Holland, 1984, chapter 5). Calcite, aragonite, and dolomite were the dominant carbonate minerals. Siderite was only a common constituent of BIFs. These observations imply that the Archean oceans were saturated or, more likely, supersaturated with respect to $CaCO_3$ and $CaMg(CO_3)_2$. Translating this observation into values for the concentration of Ca^{2+}, Mg^{2+}, HCO_3^-, and CO_3^{2-} in seawater is difficult in the absence of other information, but it can be shown that for the likely range of values of atmospheric P_{CO_2} (≤0.03 atm; Rye *et al.*, 1995), the pH of seawater was probably ≥6.5. At saturation with respect to calcite and dolomite at 25 °C, the ratio $m_{Mg^{2+}}/m_{Ca^{2+}}$ in solutions is close to 1.0. This does not have to be the value of the ratio in Archean seawater. In Phanerozoic seawater (see below), the Mg^{2+}/Ca^{2+} ratio varied considerably from values as low as 1 up to its present value of 5.3 (Lowenstein *et al.*, 2001; Horita *et al.*, 2002).

A rough upper limit to the Fe^{2+}/Ca^{2+} ratio in Archean seawater can be derived from the scarcity of siderite except as a constituent of carbonate iron formations. At saturation with respect to siderite and calcite, the ratio $m_{Fe^{2+}}/m_{Ca^{2+}}$ is approximately equal to the ratio of the solubility product of siderite (Bruno *et al.*, 1992) and calcite (Plummer and Busenberg, 1982):

$$\frac{m_{Fe^{2+}}}{m_{Ca^{2+}}} \approx \frac{K_{sid}}{K_{cal}} = \frac{10^{-10.8}}{10^{-8.4}} = 4 \times 10^{-3} \quad (1)$$

The absence of siderite from normal Archean carbonate sequences indicates that this is a reasonable upper limit for the Fe^{2+}/Ca^{2+} ratio in normal Archean seawater. An approximate lower limit can be set by the Fe^{2+} content of limestones and dolomites. These contain significantly more Fe^{2+} and Mn^{2+} than their Phanerozoic counterparts (see, e.g., Veizer et al., 1989), a finding that is consistent with a much lower O_2 content in the atmosphere and in near-surface seawater than today.

The strongest evidence for no more than a few ppm O_2 in the Archean and Early Paleoproterozoic atmosphere is the evidence for mass-independent fractionation (MIF) of the sulfur isotopes in pre-2.47 Ga sulfides and sulfates (Farquhar et al., 2000, 2001; Pavlov and Kasting, 2002; Bekker et al., 2002). In the absence of O_2, solar UV interacts with SO_2 and generates MIF of the sulfur isotopes in the reaction products. The MIF signal is probably preserved in the sedimentary record, because this signal in elemental sulfur produced by this process differs from that of the gaseous products. The fate of the elemental sulfur and sulfur gases is not well understood, but S^0 may well be deposited largely as a constituent of sulfide minerals and the sulfur that is present as a constituent of sulfur gases in part as a constituent of sulfates. Today very little of the MIF signal is preserved, because all of the products are gases that become isotopically well mixed before the burial of their contained sulfur.

It is not surprising that the geochemical cycle of sulfur during the low-O_2 Archean differed from that of the present day. As shown in Figure 5, the mass-dependent fractionation of the sulfur isotopes in sedimentary sulfides was smaller prior to 2.7 Ga than in more recent times. Several explanations have been advanced for this observation. The absence of microbial sulfate reduction is one. However, the presence of microscopic sulfides in ca. 3.47 Ga barites from north pole, Australia with a maximum sulfur fractionation of 21.1% and a mean of 11.6% clearly indicates that microbial sulfate reduction was active during the deposition of these, probably evaporitic sediments (Shen et al., 2001). A second explanation involves high temperatures in the pre-2.7 Ga oceans (Ohmoto et al., 1993; Kakegawa et al., 1998). However, Canfield et al. (2000) have shown that at both high and low temperatures large fractionations are expected during microbial sulfate reduction in the presence of abundant sulfate. A third possibility is that the concentration of sulfate in the Mesoarchean oceans was very much smaller than its current value of 28 mm. At present it appears that, until ca. 2.3 Ga, $m_{SO_4^{2-}}$ was ≤ 200 μmol L^{-1}, the concentration below which isotopic fractionation during sulfate reduction is greatly reduced (Harrison and Thode, 1958; Habicht et al., 2002). Such a low sulfate concentration in seawater prior to 2.3 Ga is quite reasonable. In the absence of atmospheric O_2, sulfide minerals would not have been oxidized during weathering, and this source of river SO_4^{2-} would have been extremely small. The other major source of river SO_4^{2-}, the solution of evaporite minerals, would also have been minimal. Constructing a convincing, quantitative model of the Archean sulfur cycle is still, however, very difficult. Volcanic SO_2 probably disproportionated, at least partially, into H_2S and H_2SO_4 by reacting with H_2O at temperatures below 400 °C. SO_4^{2-} from this source must have cycled through the biosphere. Some of it was probably lost during passage through the oceanic crust at hydrothermal temperatures. Some was lost as a constituent of sulfides (mainly pyrite) and relatively rare sulfates (mainly barite).
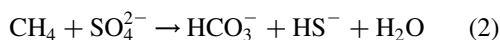
Another potentially major loss of SO_4^{2-} may well have been the anaerobic oxidation of
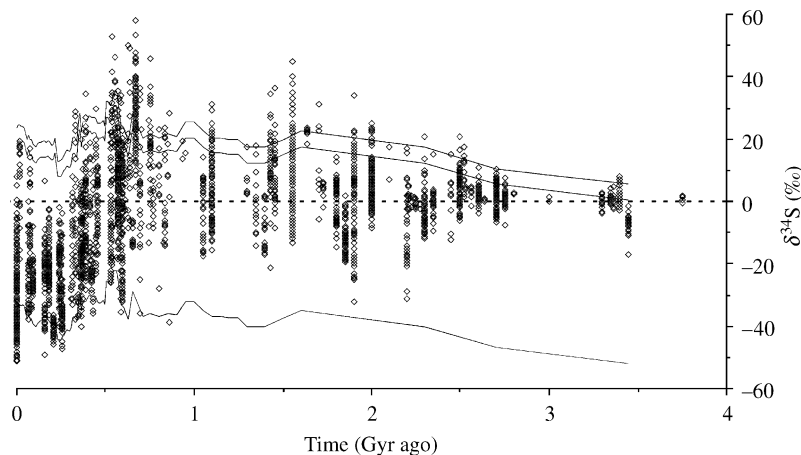
Figure 5 The isotopic composition of sedimentary sulfides over geologic time (sources Canfield and Raiswell, 1999).

methane via the overall reaction

$$CH_4 + SO_4^{2-} \rightarrow HCO_3^- + HS^- + H_2O \quad (2)$$

(Iversen and Jørgensen, 1985; Hoehler and Alperin, 1996; Orphan *et al.*, 2001). It seems likely that the reaction is accomplished in part by a consortium of Archaea growing in dense aggregates of ~100 cells, which are surrounded by sulfate-reducing bacteria (Boetius *et al.*, 2000; De Long, 2000). In sediments rich in organic matter SO_4^{2-} is depleted rapidly. Below the zone of SO_4^{2-} depletion CH_4 is produced. The gas diffuses upward and is destroyed, largely in the transition zone, where the concentration of SO_4^{2-} in the interstitial water is in the range of $0.1–1$ mmol kg^{-1} (Iversen and Jørgensen, 1985). The rate of CH_4 oxidation is highest where its concentration is equal to that of SO_4^{2-}. In two stations studied by Iversen and Jørgensen, the total anaerobic methane oxidation was close to 1 mmol m^{-2} d^{-1}, of which 96% occurred in the sulfate–methane transition zone. If this rate were characteristic of the ocean floor as a whole, SO_4^{2-} reduction within marine sediments would occur at a rate of ~(1×10^{14}) mol yr^{-1}, which exceeds the present-day input of volcanic SO_2 by ca. two orders of magnitude. The process is, therefore, potentially important for the global geochemistry of sulfur and carbon.

The anaerobic oxidation of CH_4 also occurs in anoxic water masses. In the Black Sea only ~2% of the CH_4 which escapes from sediments reaches the atmosphere. The remainder is largely lost by sulfate reduction in the anoxic parts of the water column (Reeburgh *et al.*, 1991). In an ocean containing ≤ 1 mmol L^{-1} SO_4^{2-} the rate of CH_4 loss in the water column would almost certainly be smaller than in the Black Sea today, and the flux of CH_4 to the atmosphere would almost certainly be greater than today. Pavlov *et al.* (2000) have shown that the residence time of CH_4 in an anoxic atmosphere is ~3×10^4 yr, i.e., some 1,000 times longer than today. The combination of a higher rate of CH_4 input and a longer residence time in the atmosphere virtually assures that the partial pressure of CH_4 was much higher in the Archean atmosphere than its present value of ~(1×10^{-6}) atm. A CH_4 pressure of $10^{-4}–10^{-3}$ atm is not unlikely (Catling *et al.*, 2001). At these levels CH_4 generates a very significant greenhouse warming, enough to overcome the likely lower luminosity of the Sun during the early part of Earth history (Kasting *et al.*, 2001). The recent discovery of microbial reefs in the Black Sea fueled by the anaerobic oxidation of methane by SO_4^{2-} (Michaelis *et al.*, 2002) suggests that this process was important during the Archean, and that it can account for some of the organic matter generated in the oceans before the rise of atmospheric O_2.

### 6.21.3.3 The Neoarchean (3.0–2.5 Ga)

The spread in the $\delta^{34}S$ value of sulfides and sulfates increased significantly between 3.0 Ga and 2.5 Ga. The first major increase in the $\delta^{34}S$ range occurred ~2.7 Ga (see Figure 5). However, sulfate concentrations probably stayed well below the present value of 28 mmol kg^{-1} until the Neoproterozoic. Grotzinger (1989) has reviewed the mineralogy of Precambrian evaporites and has shown that calcium sulfate minerals (or their pseudomorphs) are scarce before ~1.7–1.6 Ga. Bedded or massive gypsum/anhydrite formed in evaporitic environments is absent in the Archean and Paleoproterozoic record. A low concentration of SO_4^{2-} in the pre-1.7 Ga oceans is the most reasonable explanation for these observations (Grotzinger and Kasting, 1993).

Rather interestingly, the oldest usable biomarkers in carbonaceous shales date from the Neoarchean. Molecular fossils extracted from 2.5 Ga to 2.7 Ga shales of the Fortescue and Hamersley groups in the Pilbara Craton, Western Australia, indicate that the photic zone of the water column in the areas where these shales were deposited was probably weakly oxygenated, and that cyanobacteria were part of the microbial biota (Brocks *et al.*, 1999, 2002; Summons *et al.*, 1999). The similarity of the timing of the rise in the range of $\delta^{34}S$ in sediments and the earliest evidence for the presence of cyanobacteria may, however, be coincidental, because to date no sediments older than 2.7 Ga have been found that contain usable biomarker molecules (Brocks, personal communication, 2002).

Despite the biomarker evidence for the generation of O_2 at 2.7 Ga, the atmosphere seems to have contained very little or no O_2, and much of the ocean appears to have been anoxic. Pyrite, uraninite, gersdorffite, and, locally, siderite occur as unequivocally detrital constituents in 3,250–2,750 Ma fluvial siliciclastic sediments in the Pilbara Craton in Australia (Rasmussen and Buick, 1999). These sediments have never undergone hydrothermal alteration. Some grains of siderite display evidence of several episodes of erosion, rounding, and subsequent authigenic overgrowth (see Figure 6). Their frequent survival after prolonged transport in well-mixed and, therefore, well-aerated Archean rivers that contained little organic matter strongly implies that the contemporary atmosphere was much less oxidizing than at present. The paper by Rasmussen and Buick (1999) was criticized by Ohmoto (1999), but staunchly defended by Rasmussen *et al.* (1999).

These observations complement those made since the early 1990s on the gold–uranium ores of the Witwatersrand Basin in South Africa and on the uranium ores of the Elliot Lake District in
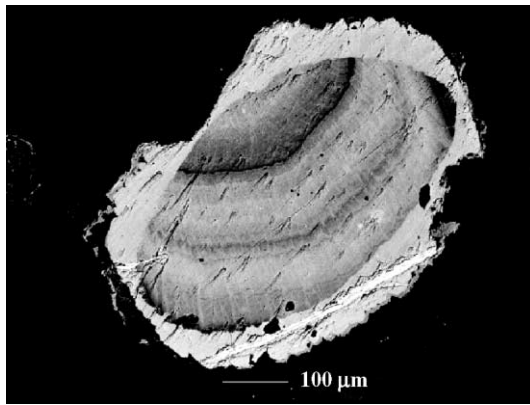
Figure 6 Rounded siderite grain, with core of compositionally banded siderite and gray to black syntaxial overgrowths (source Rasmussen and Buick, 1999).


Figure 7 Detrital grains of uraninite with characteristic dusting of galena, partly surrounded by PbS overgrowths. The big grain displays a typical "muffin shape." Basal Reef, footwall; Loraine Gold Mines, South Africa oil immersion; 375× (source Schidlowski, 1966).

Canada. The origin of these ores has been hotly debated (see, e.g., Phillips *et al*., 2001). The rounded shape of many of the pyrite and uraninite grains (see Figures 7 and 8) are in a geologic setting appropriate for the placer accumulation of heavy minerals. Figure 7 shows some of the muffin-shaped uraninite grains described by Schidlowski (1966), and Figure 8 shows rounded grains of pyrite described by Ramdohr (1958). It is clear that some of the rounded pyrite grains are replacements of magnetite, ilmenite, and other minerals. The origin of any specific rounded pyrite grain if based on textural evidence alone is, therefore, somewhat ambiguous. However, the Re–Os age of some pyrite grains indicates that they are older than the depositional age of the sediments (Kirk *et al*., 2001). The detrital origin of the uraninite muffins is essentially established by their chemical composition. As shown in Table 1 these contain significant concentrations of ThO_2, which are characteristic of uraninite derived from pegmatites but not of hydrothermal pitchblende. It is, therefore, very difficult to assign anything but a detrital origin to the uraninite in the Witwatersrand ores (see, e.g., Hallbauer, 1986).

Experiments by Grandstaff (1976, 1980) and more recently by Ono (2002) on the oxidation and dissolution or uraninite can be used to set a rough upper limit of 10^{-2}–10^{-3} atm on the O_2 content of the atmosphere during the formation of the Au–U deposits of the Witwatersrand Basin (Holland, 1984, chapter 7). This maximum O_2 pressure is much greater than that permitted by the presence of MIF of sulfur isotopes during the last 0.5 Ga of the Archean; the observations do, however, complement each other.

The chemical composition of soils developed during the Late Archean and during the Paleoproterozoic also fit the pattern of a low- or
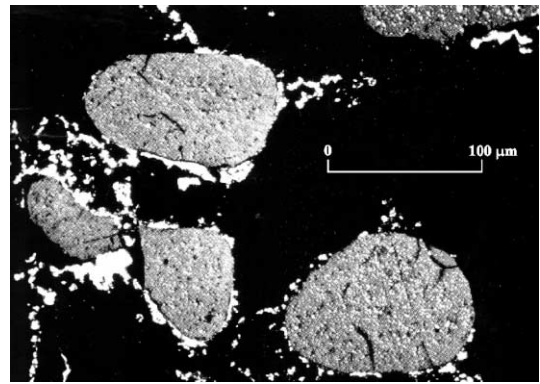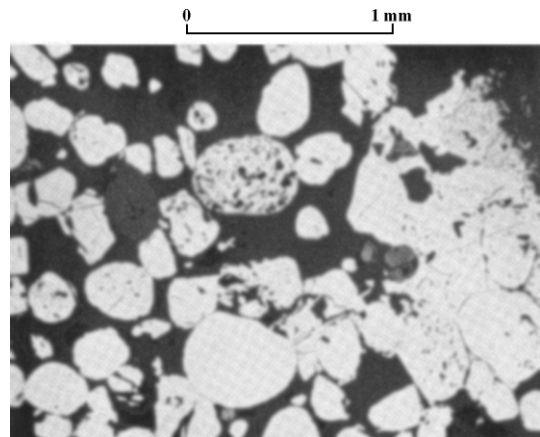
Figure 8 Conglomerate consisting of several types of pyrite together with zircon, chromite, and other heavy minerals. The large pyrite grain in the right part of the figure is a complex assemblage of older pyrite grains which have been cemented by younger pyrite (source Ramdohr, 1958).

no-O_2 atmosphere. During weathering on such an Earth, elements which are oxidized in a high-O_2 atmosphere remain in their lower valence states and behave differently within soils, in groundwaters, and in rivers. The theory connecting this qualitative statement to the expected behavior of redox sensitive elements has been developed in papers by Holland and Zbinden (1988), Pinto and Holland (1988), and Yang and Holland (2003). The available data for the chemical evolution of paleosols have been summarized by Rye and Holland (1998) and by Yang and Holland (2003). The composition of paleosols is consistent with a change from a low- or no-O_2 atmosphere to a highly oxygenated atmosphere between 2.3 Ga and 2.0 Ga; a different interpretation of the

Table 1 Electron microprobe analyses of uraninite in some Witwatersrand ores.

Source	Grain no.	UO$_2$ (%)	ThO$_2$ (%)	PbO$_2$ (%)	FeO (%)	TiO$_2$ (%)	CaO (%)	Total (%)	UO$_2$/ThO$_2$
Cristaalkop Reef (171)	T21	65.8	5.3	23.3	0.8	<0.01	0.6	95.8	12.4
(Vaal Reefs South Mine)	T22	66.5	6.1	21.9	0.5	0.02	0.7	95.7	10.9
	T23	70.5	1.7	23.8	0.5	0.04	0.8	97.3	41.5
	T23	62.4	6.1	24.7	0.4	<0.01	1.1	94.7	10.2
	T25	63.0	8.0	23.0	0.5	<0.01	1.0	95.5	7.9
	T27	66.6	3.2	23.3	1.0	0.04	0.9	95.0	20.8
	T28	66.3	1.4	28.0	0.6	0.02	0.9	97.2	47.4
	T29	63.5	3.9	28.5	0.6	<0.01	0.8	97.3	16.3
	T30	65.7	10.2	18.9	0.7	0.08	1.1	96.7	6.4
	Average	65.6	5.1	23.9	0.6	0.02	0.9	96.1	12.9
Carbon Leader (135)	T13	69.6	2.7	26.1	0.2	0.08	1.0	99.7	25.8
(Western Deep Levels Mine)	T14	66.4	2.5	27.8	0.2	0.12	0.7	97.7	26.6
	T15	63.8	2.0	30.3	0.2	0.06	0.7	97.1	31.9
	T16	62.6	7.0	24.5	0.2	0.04	0.8	95.1	8.9
	T17	67.1	5.2	21.1	0.2	0.06	0.7	94.4	12.9
	T18	69.2	2.1	28.0	0.2	0.10	0.7	100.3	33.0
	T19	67.9	7.2	18.3	0.2	0.06	0.6	94.3	9.4
	Average	66.7	4.1	25.2	0.2	0.07	0.7	97.0	16.3
Carbon Leader (167)	B43	61.1	5.4	27.9	1.1	0.25	0.4	96.2	11.3
(West Driefontein Mine)	B44	71.3	2.6	24.2	0.6	0.25	0.6	99.6	27.4
	B46	68.2	4.3	28.2	0.4	0.10	0.5	101.7	15.9
	B47	70.0	2.1	23.6	0.4	0.10	0.6	96.8	33.3
	B48	68.2	3.5	24.7	0.5	0.12	0.3	97.3	19.5
	B49	67.3	6.4	21.6	0.4	0.16	0.5	96.4	10.5
	B52	67.6	9.2	22.8	0.9	0.14	0.3	100.9	7.3
	Average	68.1	4.2	24.7	0.6	0.16	0.5	98.3	16.2
Main Reef (151)	B31	68.7	3.3	14.7	2.3	1.20	0.4	90.6	20.8
(SA Lands Mine)	B32	69.1	2.1	21.0	1.1	0.50	0.4	94.2	32.9
	B36	67.3	1.5	24.4	0.9	0.19	0.3	94.6	44.9
	B37	63.5	2.9	17.3	5.0	2.03	0.5	91.2	21.9
	Average	67.2	2.5	19.4	2.3	0.98	0.4	92.8	26.9
Basal Reef (184)	U4	68.2	6.3	19.6	2.4	<0.1	0.4	96.9	10.8
(Welkom Mine)	U5	70.5	3.3	16.8	4.1	0.2	0.4	95.3	21.4
	U7	70.1	5.2	24.8	1.1	0.1	0.5	101.8	13.5
	U8	66.6	4.5	25.2	0.9	<0.1	0.3	97.5	14.8
	U9	72.5	2.6	26.1	1.6	<0.1	0.5	103.3	27.9
	U10	64.8	3.3	23.7	5.2	0.2	0.5	97.7	19.6
	Average	68.8	4.2	22.7	2.6	0.1	0.4	98.7	16.4
Overall average:		67.2	3.9	23.6	1.0	0.16	0.6	93.8	17.2

Source: Feather (1980).

available data has been proposed by Ohmoto (1996) and by Beukes *et al.* (2002a,b).

One consequence of the proposed great oxidation event (GOE) of the atmosphere between 2.3 Ga and 2.0 Ga is that trace elements such as molybdenum, rhenium, and uranium, which are mobile during weathering in an oxidized environment, would have been essentially immobile before 2.3 Ga. Their concentration in seawater would then have been very much lower than today, and their enrichment in organic carbon-rich shales would have been minimal. This agrees with the currently available data (Bekker *et al.*, 2002; Yang and Holland, 2002). Carbonaceous shales older than ca. 2.3 Ga are not enriched in molybdenum, rhenium, and uranium. A transition

to highly enriched shales occurs ~2.1 Ga; by 1.6 Ga the enrichment of carbonaceous shales in these elements was comparable to that in their Phanerozoic counterparts (see, e.g., Werne *et al.*, 2002).

The data for the mineralogy of BIFs tell much the same story. These sediments provide strong evidence for the view that the deep oceans were anoxic throughout Archean time (James, 1992). Evidence regarding the oxidation state of the shallow parts of the Archean oceans is still very fragmentary. The shallow water facies of the 2.49 ± 0.03 Griquatown iron formation (Nelson *et al.*, 1999) in the Transvaal Supergroup of South Africa (Beukes, 1978 , 1983; Beukes and Klein, 1990) were deposited on the ~800 km × 800 km

shelf shown in the somewhat schematic Figure 9. The stratigraphic relations are illustrated in the south–north cross-section of Figure 10. Several of the units in the Danielskuil Member of the Griquatown iron formation can be traced across the shallow platform from the subtidal, low-energy epeiric sea, through the high-energy zone of the shelf, into the lagoonal, near-shore parts of the platform. In the deeper parts of the shelf, siderite and iron silicates dominate the mineralogy of the iron formation. Siderite and minor ($<10\%$) hematite dominate the sediments of the high-energy zone. Greenalite and siderite lutites are most common in the platform lagoonal zone.

The dominance of Fe^{2+} minerals in even the shallowest part of the platform can only be explained if the O_2 content of the ambient atmosphere was very low. The half-life of Fe^{2+} oxidation in the Gulf Stream and in Biscayne Bay, Florida is only a few minutes (Millero *et al.*, 1987). The half-life of Fe^{2+} oxidation is similar in the North Sea, the Sargasso Sea, Narragansett Bay, and Puget Sound (for summary see Millero *et al.*, 1987).

The half-life of Fe^{2+} in the solutions from which the Griquatown iron formation was deposited was obviously many orders of magnitude longer than this, and it is useful to inquire into the cause for the difference. Stumm and Lee (1961) have shown that the rate of oxidation of Fe^{2+} in aqueous solutions is governed by the equation

$$-dm_{Fe^{2+}}/dt = k m_{OH^-}^2 m_{O_2} m_{Fe^{2+}} \qquad (3)$$
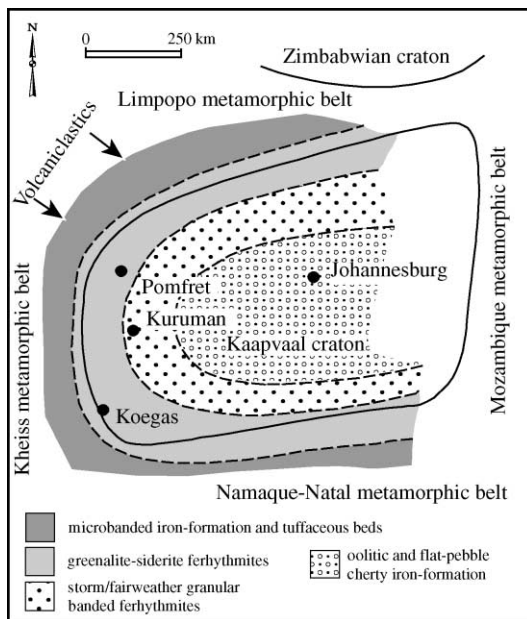
Figure 9 Depositional model for the Kuruman–Griquatown transition zone in a plan view, illustrating lithofacies distribution during drowning of the Kaapvaal craton (source Beukes and Klein, 1990).

where

$$m_{OH^-} = \text{concentration of free } OH^-$$

$$m_{O_2} = \text{concentration of dissolved } O_2$$

Integration of Equation (3) yields

$$\ln m_{Fe^{2+}}/_o m_{Fe^{2+}} = -k m_{OH^-}^2 m_{O_2} t \qquad (4)$$

where $_o m_{Fe^{2+}}$ is the initial concentration of Fe^{2+} in the solution. If we substitute a_{OH^-} for m_{OH^-}, the value of k for modern seawater is $\sim 0.9 \times 10^{15} \text{ min}^{-1}$ (Millero *et al.*, 1987). An upper limit for $\ln m_{Fe^{2+}}/_o m_{Fe^{2+}}$ can be obtained from the field data for the Griquatown iron formation on the Campbellrand platform. Hematite accounts for $\leq 10\%$ of the iron in the near-shore iron formation. If all of the iron that was oxidized to Fe^{3+} was precipitated as a constituent of Fe_2O_3 during the passage of seawater across the platform,

$$m_{Fe^{2+}}/_o m_{Fe^{2+}} \geq 0.9 \qquad (5)$$

The time, t, required for the passage of water across the Campbellrand platform is uncertain. The modern Bahamas are probably a reasonable analogue for the Campbellrand platform. On the Bahama Banks tidal currents of 25 cm s^{-1} are common, and velocities of 1 m s^{-1} have been recorded in channels (Sellwood, 1986). At a rate of 25 cm s^{-1} it would have taken seawater ~ 1 month (4×10^4 min) to traverse the ~ 800 km diameter of the Campbellrand platform. This period is much longer than the time required to precipitate Fe^{3+} oxyhydroxide after the oxidation of Fe^{2+} to Fe^{3+} (Grundl and Delwiche, 1993). The best estimate of the residence time of seawater on the Grand Bahama Bank is ~ 1 yr (Morse *et al.*, 1984; Millero, personal communication). The pH of the solutions from which the iron formations were deposited was probably less than that of seawater today, but probably not lower than 7.0.

If we combine all of these rather uncertain values for the terms in Equation (4), we obtain

$$m_{O_2} \sim (<0.10)/0.9 \times 10^{15} \times (\geq 10^{-14.0})$$
$$\times 4 \times 10^4 \text{ mol kg}^{-1}$$
$$< 3 \times 10^{-7} \text{ mol kg}^{-1} \qquad (6)$$

In an atmosphere in equilibrium with seawater containing this concentration of dissolved O_2,

$$P_{O_2} = 2.4 \times 10^{-4} \text{ atm}$$

The maximum value of atmospheric P_{O_2} estimated in this manner is consistent with inferences from the MIF of the sulfur isotopes during the deposition of the Griquatown iron formation that $P_{O_2} \leq 1 \times 10^{-5}$ PAL.

A rather curious observation in the light of these observations is that in many unmetamorphosed
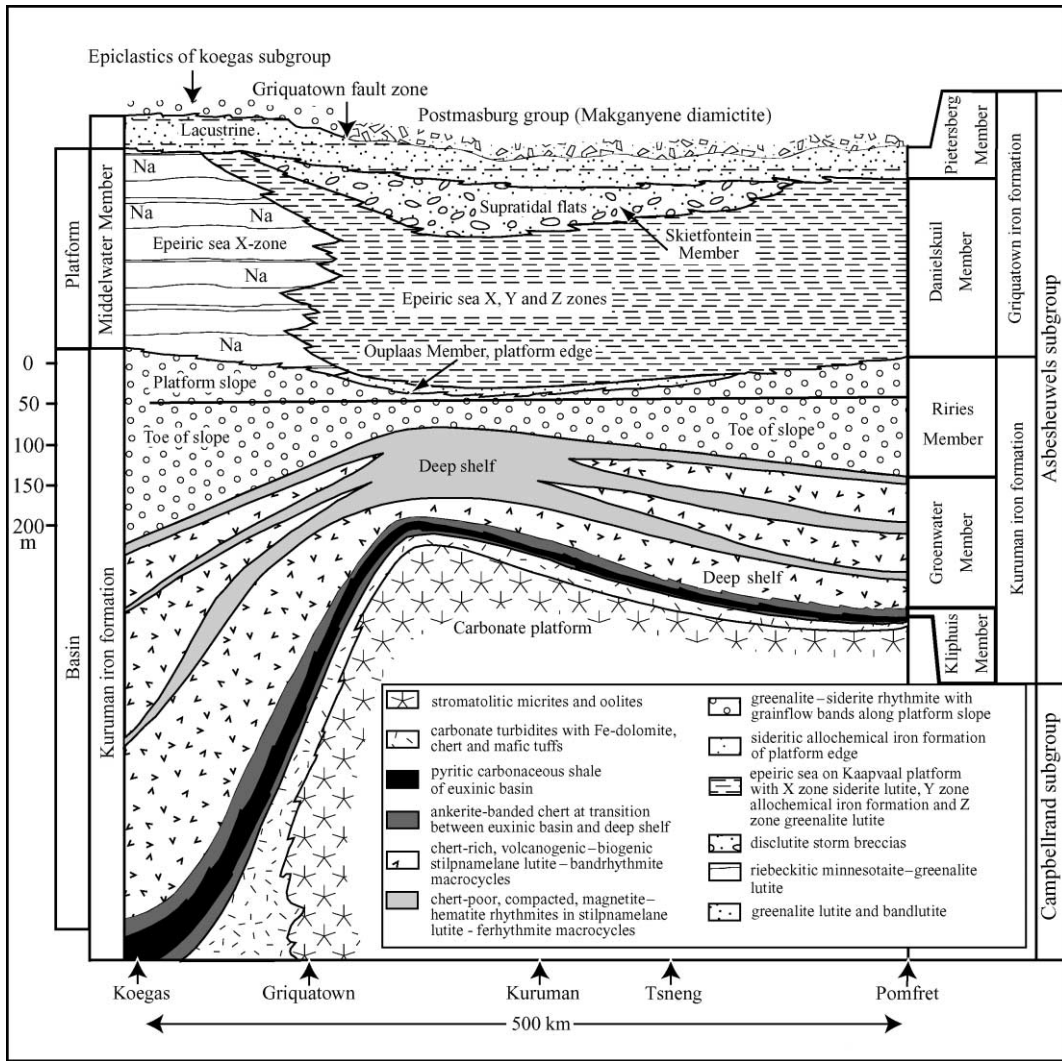
Figure 10 Longitudinal cross-section illustrating stratigraphic relationships and inferred palaeodepositional environments of the Asbesheuwels Subgroup in the Griqualand West basin (after Beukes, 1978).

oxide facies BIFs, the first iron oxide mineral precipitated was frequently hematite (Han, 1982, 1988). This phase was later replaced by magnetite. Klein and Beukes (1989) have reported the presence of hematite as a minor component in iron formations of the Paleoproterozoic Transvaal Supergroup, South Africa. The hematite occurs in two forms: as fine hematite dust and as very fine grained specularite. The former could well be a very early phase in these BIFs. The early deposition of hematite in BIFs followed by large-scale replacement by magnetite could simply be the result of reactions in mixtures of hydrothermal vent fluids with ambient O_2-free seawater. High-temperature hydrothermal vent fluids are strongly undersaturated with respect to hematite. However, on mixing with ambient O_2-free seawater their pH rises, and path calculations indicate that they can become supersaturated

with respect to hematite. During hematite precipitation P_{H_2} would increase, and the early hematite could well be replaced by magnetite during early diagenesis. The sequence of mineral deposition from such solutions depends not only on the composition of the vent fluids and that of the ambient seawater, but also on the kinetics of the precipitation mechanisms. These, in turn, could have been influenced by bacterial processes (Konhauser *et al.*, 2002). A thorough study of the effects of these parameters remains to be done.

6.21.4 THE PROTEROZOIC

6.21.4.1 The Paleoproterozoic (2.5–1.8 Ga)

In 1962 the author divided the evolution of the atmosphere into three stages (Holland, 1962). On the basis of rather scant evidence from the

mineralogy of Precambrian sedimentary uranium deposits, it was suggested that free oxygen was not present in appreciable amounts until ca. 1.8 Ga, but that by the end of the Paleozoic the O_2 content of the atmosphere was already a large fraction of its present value. In a similar vein, Cloud (1968) proposed that the atmosphere before 1.8–2.0 Ga could have contained little or no free oxygen. In 1984 the author published a much more extensive analysis of the rise of atmospheric oxygen (Holland, 1984). Progress since 1962 had been rather modest. After reading the section on atmospheric O_2 in the Precambrian, Robert Garrels commented that this part of the book was very long but rather short on conclusions. Much more progress was reported in 1994 (Holland, 1994), and the last few years have shown a widespread acceptance of his proposed "great oxidation event" (GOE) between ca. 2.3 Ga and 2.0 Ga. This acceptance has not, however, been universal. Ohmoto and his group have steadfastly maintained (Ohmoto, 1996, 1999) that the level of atmospheric O_2 has been close to its present level during the past 3.5–4.0 Ga.

During the past few years the most exciting new development bearing on this question has been the discovery of the presence of mass-independent fractionation (MIF) of the sulfur isotopes in sulfides and sulfates older than ca. 2.47 Ga. Figure 11 summarizes the available data for the degree of MIF ($\Delta^{33}S$) in sulfides and sulfates during the past 3.8 Ga. The presence of values of $\Delta^{33}S > 0.5‰$ in sulfides and sulfates older than ca. 2.47 Ga indicates that the O_2 content of the atmosphere was $<10^{-5}$ PAL prior to 2.47 Ga

(Farquhar *et al.*, 2001; Pavlov and Kasting, 2002). The absence of significant MIF in sulfides and sulfates ≤2.32 Ga (Bekker *et al.*, 2002) is indicative of O_2 levels $>10^{-5}$ PAL. There are no data to decide when between 2.32 Ga and 2.47 Ga the level of atmospheric P_{O_2} rose, and whether the rise was a single event, or whether P_{O_2} oscillated before a final rise by 2.3 Ga.

The presence of O_2 in the atmosphere–ocean system at 2.32 Ga is supported strongly by the presence of a large body of shallow-water hematitic ironstone ore in the Timeball Hill Formation, South Africa (Beukes *et al.*, 2002a,b). Apparently, the shallow oceans have been oxidized ever since. The deeper oceans may have continued in a reduced state at least until the disappearance of the Paleoproterozoic BIFs ca. 1.7 Ga.

The rapidity of the rise of the O_2 content of the atmosphere after 2.3 Ga is a matter of dispute. The Hekpoort paleosols, which developed on the 2.25 Ga Hekpoort Basalt, consist of an oxidized hematitic upper portion and a reduced lower portion. Beukes *et al.* (2002a,b) have pointed out that the section through the Hekpoort paleosol near Gaborone in Botswana is similar to modern tropical laterites. Yang and Holland (2003) have remarked on the differences between the chemistry and the geology of the Hekpoort paleosols and Tertiary groundwater laterites, and have proposed that the O_2 level in the atmosphere during the formation of the Hekpoort paleosols was between ca. 2.5×10^{-4} atm and 9×10^{-3} atm, i.e., considerably lower than at present. Paleosols developed in the Griqualand Basin on the Ongeluk Basalt, which is of the same
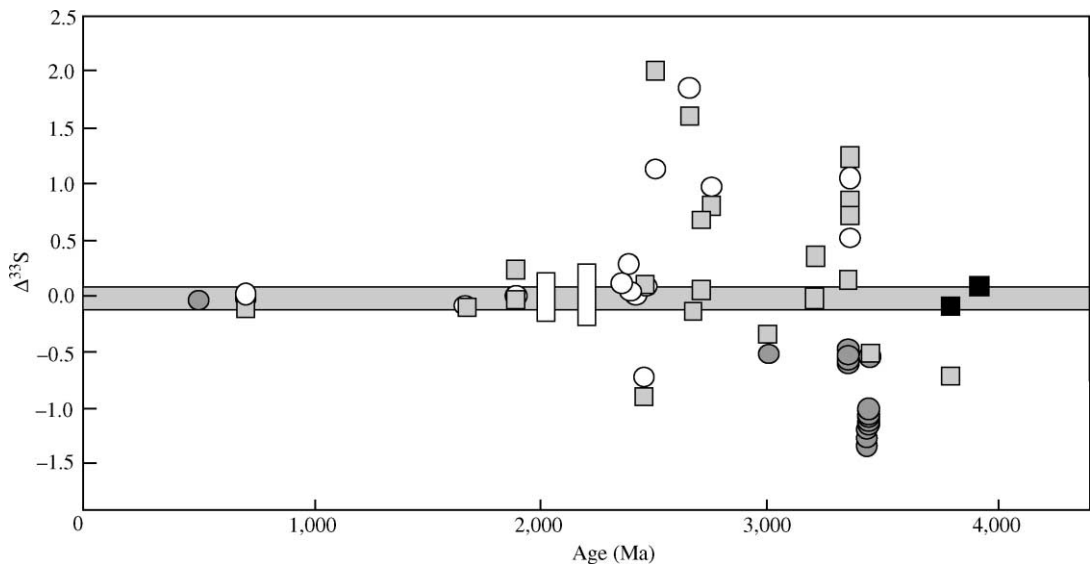
Figure 11 Summary of data for the degree of MIF of the sulfur isotopes in sulfides and sulfates. Data from Farquhar *et al.* (2000) (chemically defined sulfur minerals (▫) sulfides, (■) total sulfur, and (○) sulfates; (◉) macroscopic sulfate minerals) with updated ages and from Bekker *et al.* (2002) ((▯) range of values for pyrites in black shales). The gray band at $\Delta^{33}S \sim 0$ represents the mean and 1 SD of recent sulfides and sulfates from Farquhar *et al.* (2000).

age as the Hekpoort Basalt, are highly oxidized. The difference between their oxidation state and that of the Hekpoort paleosols may be due to a slightly younger age of the paleosols in the Griqualand Basin. They probably formed during the large, worldwide positive variation of Figure 12 in the $\delta^{13}C$ value of marine carbonates (Karhu and Holland, 1996). This excursion is best interpreted as a signal of the production of a large quantity of O_2 between 2.22 Ga and 2.06 Ga. Estimates of this quantity are perforce very rough. The average isotopic composition of organic carbon during the excursion is somewhat uncertain, as is the total rate of carbon burial with organic matter and carbonate sediments during the $\delta^{13}C$ excursion, and there is the possibility that the $\delta^{13}C$ excursion in Figure 12 was preceded by another, shorter excursion (Bekker *et al.*, 2001; Young, 1969). It seems likely, however, that the total excess quantity of O_2 produced during the ca. 160 Ma of the $\delta^{13}C$ excursion was ~12–22 times the inventory of atmospheric oxygen (Karhu, 1993;

Karhu and Holland, 1996). This large amount of O_2 must somehow have disappeared into the sedimentary record. The most likely sinks are crustal iron and sulfur. As indicated by the mineralogy of marine evaporites and the isotopic composition of sulfur in black shales, the SO_4^{2-} concentration of seawater probably remained very modest until well beyond 2.0 Ga (Grotzinger and Kasting, 1993; Shen *et al.*, 2002). Iron is, therefore, the most likely major sink for the O_2 produced during the $\delta^{13}C$ excursion between 2.22 Ga and 2.06 Ga. This is not unreasonable. Before the rise of atmospheric O_2, FeO was not oxidized to Fe_2O_3 during weathering, as shown by the record of the Fe_2O_3/FeO ratio in pre-2.3 Ga sedimentary rocks (Bekker *et al.*, 2003). The appearance of extensive red beds ca. 2.3 Ga indicates that a major increase in the Fe_2O_3/FeO ratio of sediments and sedimentary rocks occurred at that time. Shales before the GOE contained, on average, ~6.5% FeO and ~1.3% Fe_2O_3. Shales deposited between 2.3 Ga and 2.1 Ga contain, on average, ~4.1% FeO and
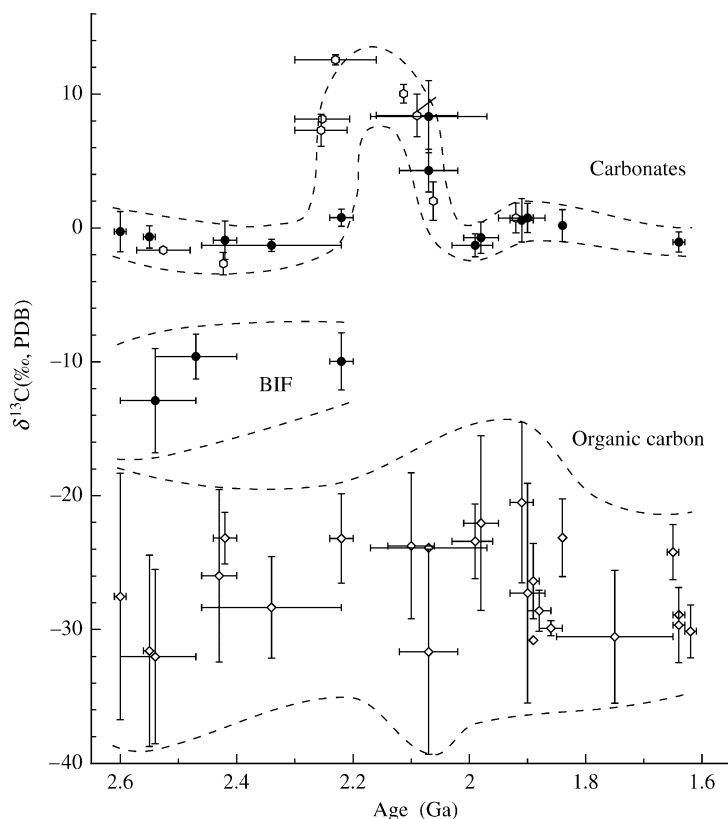
Figure 12 Variation in isotopic composition of carbon in sedimentary carbonates and organic matter during Paleoproterozoic time. Mean $\delta^{13}C$ values of carbonates from Fennoscandian Shield from Karhu (1993) are indicated by open circles. Vertical bars represent ±1 SD of $\delta^{13}C$ values, and horizontal bars indicate uncertainty in age of each stratigraphic unit. Arrows combine dated formations that are either preceded or followed by major $\delta^{13}C$ shift. BIF denotes field for iron and manganese formations. Note that uncertainties given for ages do not necessarily cover uncertainties in entire depositional periods of sample groups. PDB—Peedee belemnite (source Karhu and Holland, 1996).

2.5% Fe_2O_3. There seems to have been little change between 2.1 Ga and 1.0 Ga (Bekker *et al.*, 2003). Approximately 2% of the FeO in pre-GOE rocks seem to have been converted to Fe_2O_3 during weathering in the course of the GOE. Since each mole of FeO requires 0.25 mol O_2 for conversion to Fe_2O_3, $\sim$0.08 mol O_2 was used during the weathering of each kilogram of rock. If weathering rates during the GOE were comparable to current rates, some 1.6×10^{12} mol O_2 were used annually to convert FeO to Fe_2O_3 during weathering in the course of the $\delta^{13}C$ excursion. The total O_2 use was, therefore, $\sim$2.6 $\times 10^{20}$ mol, i.e., $\sim$6 times the present atmospheric O_2 inventory. Some of the excess O_2 was probably used to increase the redox state of the crustal sulfur cycle. The duration of the $\delta^{13}C$ excursion is roughly equal to the half-life of sedimentary rocks at 2 Ga. The Fe_2O_3/FeO ratio of rocks subjected to weathering at the end of the $\delta^{13}C$ excursion was, therefore, greater than at its beginning and was approaching a value typical of Mesoproterozoic sedimentary rocks. Post-$\delta^{13}C$ excursion weathering of sediments produced during the $\delta^{13}C$ excursion, therefore, required much less additional O_2 than the weathering of pre-GOE rocks.

Although this is a likely explanation for the fate of most of the "extra" O_2 generated during the $\delta^{13}C$ excursion between ca. 2.22 Ga and 2.06 Ga, it does not account for the GOE itself or for the cause of the $\delta^{13}C$ excursion. The appearance of O_2 in the atmosphere between ca. 2.47 Ga and 2.32 Ga could be explained easily if cyanobacteria evolved at that time. However, this explanation has been rendered very unlikely by the discovery of biomarkers that are characteristic of cyanobacteria and eukaryotes in 2.5–2.7 Ga sedimentary rocks (Brocks *et al.*, 1999). An alternative explanation involves a change in the redox state of volcanic gases as the trigger for the change of the oxidation state of the atmosphere (Kasting *et al.*, 1993). These authors pointed out that the loss of H_2 from the top of a reducing atmosphere into interplanetary space would have increased the overall oxidation state of the Earth as a whole, and almost certainly that of the mantle. This, in turn, would have led to an increase in the f_{O_2} of volcanic gases and to a change in the redox state of the atmosphere.

In a more detailed analysis of this mechanism, Holland (2002) showed that the change in the average f_{O_2} of volcanic gases required for the transition of the atmosphere from an anoxygenic to an oxygenic state is quite small. There is no inconsistency between the required change in f_{O_2} and the limits set on such changes by the data of Delano (2001) and Canil (1997, 1999, 2002) for the evolution of the redox state of the upper mantle during the past 4.0 Ga. The estimated changes in f_{O_2} due to H_2 loss are consistent with

the likely changes in the redox state of the upper mantle if the major control on that state is exerted by the Fe_2O_3/FeO buffer. In this explanation the average composition of volcanic gases before the GOE was such that 20% of their contained CO_2 could be reduced to CH_2O, and all of the sulfur gases to FeS_2. Excess H_2 present in the gases would have escaped from the atmosphere, possibly via the decomposition of CH_4 in the upper atmosphere. The loss of H_2 would have produced an irreversible oxidation of the early Earth (Catling *et al.*, 2001). The GOE began when the composition of volcanic gases had changed, so that not enough H_2 was present to convert 20% of the contained CO_2 to CH_2O and all of the sulfur gases to FeS_2. Before the GOE the only, or nearly the only, sulfate mineral deposited in sediments seems to have been barite. Since barium is a trace element, its precipitation as $BaSO_4$ accounted for only a small fraction of the atmospheric input of volcanic sulfur. After the GOE a fraction of volcanic sulfur began to leave the atmosphere–ocean system as a constituent of other sulfate minerals as well, largely as gypsum ($CaSO_4 \cdot 2H_2O$) and anhydrite ($CaSO_4$).

During the Phanerozoic close to half of the volcanic sulfur in volcanic gases has been removed as a constituent of FeS_2, the other half as a constituent of gypsum and anhydrite (see, e.g., Holland, 2002). The shift from the essentially complete removal of volcanic sulfur as a constituent of FeS_2 to the present state was gradual (see below). It was probably controlled by a feedback mechanism involving an increase in the sulfur content of volcanic gases. This was probably the result of an increase in the rate of subduction of $CaSO_4$ added to the oceanic crust by the cycling of sea water at temperatures above ca. 200 °C.

The burial of excess organic matter during the $\delta^{13}C$ excursion between 2.22 Ga and 2.06 Ga almost certainly required an excess of PO_4^{3-}. It seems likely that this excess was released from rocks during weathering due to the lower pH of soil waters related to the generation of H_2SO_4 that accompanied the oxidative weathering of sulfides. Toward the end of the $\delta^{13}C$ excursion, this excess PO_4^{3-} was probably removed by adsorption on the Fe^{3+} hydroxides and oxyhydroxides produced by the oxidative weathering of Fe^{2+} minerals (Colman and Holland, 2000). Although this sequence of events is reasonable, and although some parts of it can be checked semiquantitatively, the proposed process by which the anoxygenic atmosphere became converted to an oxygenic state should be treated with caution. Too many pieces of the puzzle are still either missing or of questionable shape.

A most interesting and geochemically significant change in the oceans may have occurred

ca. 1.7 Ga. BIFs ceased to be deposited. They are apparently absent from the geologic record until their reappearance 1 Ga later in association with the very large Neoproterozoic ice ages (Beukes and Klein, 1992). Three explanations have been advanced for the hiatus in BIF deposition between 1.7 Ga and 0.7 Ga. The first proposes that the deposition of BIF ended when the deep waters of the oceans became aerobic (Cloud, 1972; Holland, 1984). After 1.7 Ga, Fe^{2+} from hydrothermal vents was oxidized to Fe^{3+} close to the vents and was precipitated as Fe^{3+} oxides and/or oxyhydroxides on the floor of the oceans. The second explanation proposes that anoxic bottom waters persisted until well after the deposition of BIFs ceased, and that an increase in the concentration of H_2S rather than the advent of oxygen was responsible for removing iron from deep ocean water (Canfield, 1998). The sulfur isotope record indicates that the concentration of oceanic sulfate began to increase ~2.3 Ga leading to increasing rates of sulfide production by bacterial sulfate reduction. Canfield (1998) has suggested that sulfide production became sufficiently intense ~1.7 Ga to precipitate the total hydrothermal flux of iron as a constituent of pyrite in the deep oceans. As a basis for this contention, he points out that the generation of aerobic deep ocean water would have required levels of atmospheric O_2 within a factor of 2 or 3 of the present level, a level which he believes was not attained until the Neoproterozoic. However, Canfield's (1998) analysis of his three-box model of the oceans assumes that the rate of sinking of organic matter into the deep ocean was the same during the Paleoproterozoic as at present. This is unlikely. Organic matter requires ballast to make it sink. Today most of the ballast is supplied by siliceous and carbonate tests (Logan *et al.*, 1995; Armstrong *et al.*, 2002; Iglesias-Rodriguez *et al.*, 2002; Sarmiento *et al.*, 2002). Clays and dust seem to be minor constituents of the ballast, although they may have been more important before the advent of soil-binding plants. There is no evidence for the production of siliceous or calcareous tests in the Paleoproterozoic oceans. Inorganically precipitated SiO_2 and/or $CaCO_3$ could have been important, but precipitation of these phases probably occurred mainly in shallow-water evaporitic settings. It is, therefore, likely that ballast was much scarcer during the Paleoproterozoic than today, and that the quantity of particulate organic matter (POC) transported annually from shallow water into the deep oceans was much smaller than today. This, in turn, implies that the amount of dissolved O_2 that was required to oxidize the rain of POC was much smaller than today. Evidence from paleosols suggests that atmospheric O_2 levels ca. 2.2 Ga were $\geq$15% PAL (Holland and Beukes, 1990). This implies

that the proposal for the end of BIF deposition based on the development of oxygenated bottom waters ca. 1.7 Ga is quite reasonable. It does not, of course, prove that the proposal is correct. For one thing, too little is known about the mixing time of the Paleoproterozoic oceans. Data for the oxidation state of the deep ocean since 1.7 Ga are needed to settle the issue. The third explanation posits that no large hydrothermal inputs such as are required to produce BIFs occurred between 1.7 Ga and 0.7 Ga. This seems unlikely but not impossible.

6.21.4.2 The Mesoproterozoic (1.8–1.2 Ga)

Sedimentary rocks of the McArthur Basin in Northern Australia provide one of the best windows on the chemistry of the Mesoproterozoic ocean. Some 10 km of 1.6–1.7 Ga sediments accumulated in this intracratonic basin (Southgate *et al.*, 2000). In certain intervals, they contain giant strata-bound Pb–Zn–Ag mineral deposits (Jackson *et al.*, 1987; Jackson and Raiswell, 1991; Crick, 1992). The sediments have experienced only low grades of metamorphism.

Shen *et al.* (2002) have reported data for the isotopic composition of sulfur in carbonaceous shales of the lower part of the 1.72–1.73 Ga Wollogorang Formation and in the lower part of the 1.63–1.64 Ga Reward Formation of the McArthur Basin. These shales were probably deposited in a euxinic intracratonic basin with connection to the open ocean. The $\delta^{34}S$ of pyrite in black shales of the Wollogorang Formation ranges from −1‰ to +6.3‰ with a mean and SD of 4.0 ± 1.9‰ ($n = 14$). Donnelly and Jackson (1988) reported similar values. The $\delta^{34}S$ values of pyrite in the lower Reward Formation range from +18.2‰ to +23.4‰ with an average and SD of 18.4 ± 1.8‰ ($n = 10$). The spread of $\delta^{34}S$ values within each formation is relatively small. The sulfur is quite ^{34}S-enriched compared to compositions expected from the reduction of seawater sulfate with a $\delta^{34}S$ of 20–25‰ (Strauss, 1993). This is especially true of the sulfides in the Reward Formation. Shen *et al.* (2002) propose that the Reward data are best explained if the concentration of sulfate in the contemporary seawater was between 0.5 mmol kg^{-1} and 2.4 mmol kg^{-1}. Sulfate concentrations in the Mesoproterozoic ocean well below those of the present oceans have also been proposed on the basis of the rapid change in the value of $\delta^{34}S$ in carbonate associated sulfate of the 1.2 Ga Bylot Supergroup of northeastern Canada (Lyons *et al.*, 2002). However, the value of $m_{SO_4^{2-}}$ in Mesoproterozoic seawater is still rather uncertain.

Somewhat of a cross-check on the SO_4^{2-} concentration of seawater can be obtained from the evaporite relics in the McArthur Group

(Walker *et al.*, 1977). Up to 40% of the measured sections of the Amelia Dolomite consist of such relics in the form of carbonate pseudomorphs after a variety of morphologies of gypsum and anhydrite crystals, chert pseudomorphs after anhydrite nodules, halite casts, and microscopic remnants of original, unaltered sulfate minerals. Muir (1979) and Jackson *et al.* (1987) have pointed out the similarity of this formation to the recent sabkhas along the Persian Gulf coast. The pseudomorphs crosscut sedimentary features such as bedding and laminated microbial mats, suggesting that the original sulfate minerals crystallized in the host sediments during diagenesis.

Pseudomorphs after halite are common throughout the McArthur Group. The halite appears to have formed by almost complete evaporation of seawater in shallow marine environments and probably represents ephemeral salt crusts. The general lack of association of halite and calcium sulfate minerals in these sediments probably resulted in part from the dissolution of previously deposited halite during surface flooding, but also indicates that evaporation did not always proceed beyond the calcium sulfate facies.

This observation allows a rough check on the reasonableness of the Shen *et al.* (2002) estimate of the sulfate concentration in seawater during the deposition of the McArthur Group. On evaporating modern seawater, gypsum begins to precipitate when the degree of evaporation is ~3.8. As shown in Figure 13, the onset of gypsum and/or anhydrite precipitation occurs at progressively greater degrees of evaporation as the product $m_{Ca^{2+}} m_{SO_4^{2-}}$ in seawater decreases. Today $m_{Ca^{2+}} m_{SO_4^{2-}} = 280$ (mmol kg^{-1})^2. If this product is reduced to 23 (mmol kg^{-1})^2, anhydrite

begins to precipitate simultaneously with halite at a degree of evaporation of 10.8. The presence of gypsum casts without halite in the sediments of the McArthur Group indicates that in seawater at that time $m_{Ca^{2+}} m_{SO_4^{2-}} > 23$ (mmol kg^{-1})^2 provided the salinity of seawater was the same as today. If $m_{SO_4^{2-}}$ was 2.4 mmol kg^{-1}, the upper limit suggested by Shen *et al.* (2002), $m_{Ca^{2+}}$, must then have been >10 mmol kg^{-1}, the concentration of Ca^{2+} in modern seawater. An SO_4^{2-} concentration of 2.4 mmol kg^{-1} is, therefore, permissible. Sulfate concentrations as low as 0.5 mmol kg^{-1} require what are probably unreasonably high concentrations of Ca^{2+} in seawater to account for the precipitation of gypsum before halite in the McArthur Group sediments.

The common occurrence of dolomite in the McArthur Group indicates that the $m_{Mg^{2+}}/m_{Ca^{2+}}$ ratio in seawater was >1 (see below). This is also indicated by the common occurrence of aragonite as the major primary $CaCO_3$ phase of sediments on Archean and Proterozoic carbonate platforms (Grotzinger, 1989; Winefield, 2000). Although these hints regarding the composition of Mesoproterozoic seawater are welcome, they need to be confirmed and expanded by analyses of fluid inclusions in calcite cements.

Perhaps the most interesting implication of the close association of gypsum, anhydrite, and halite relics in the McArthur Group is that the temperature during the deposition of these minerals was not much above 18 °C, the temperature at which gypsum, anhydrite, and halite are stable together (Hardie, 1967). At higher temperatures anhydrite is the stable calcium sulfate mineral in equilibrium with halite. The coexistence of gypsum and anhydrite with halite suggests that the temperature
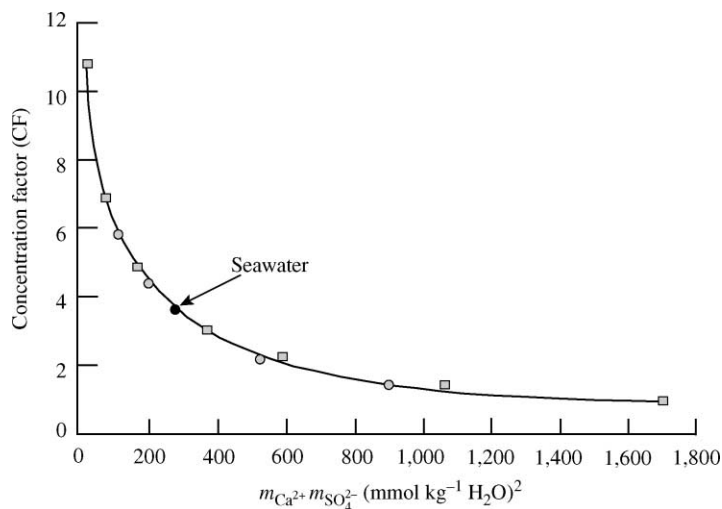
Figure 13 The relationship between the value of the product $m_{Ca^{2+}} m_{SO_4^{2-}}$ in seawater and the concentration factor at which seawater becomes saturated with respect to gypsum at 25 °C and 1 atm (source Holland, 1984).

during their deposition was possibly lower but probably no higher than in the modern sabkhas of the Persian Gulf, where anhydrite is the dominant calcium sulfate mineral in association with halite (Kinsman, 1966).

In their paper on the carbonaceous shales of the McArthur Basin, Shen *et al.* (2002) comment that euxinic conditions were common in marine-connected basins during the Mesoproterozoic, and they suggest that low concentrations of seawater sulfate and reduced levels of atmospheric oxygen at this time are compatible with euxinic deep ocean waters. Anbar and Knoll (2002) echo this sentiment. They point out that biologically important trace metals would then have been scarce in most marine environments, potentially restricting the nitrogen cycle, affecting primary productivity, and limiting the ecological distribution of eukaryotic algae. However, some of the presently available evidence does not support the notion of a Mesoproterozoic euxinic ocean floor. Figure 14 shows that the redox sensitive elements molybdenum, uranium, and rhenium are well correlated with the organic carbon content of carbonaceous shales in the McArthur Basin. The slope of the correlation lines is close to that in many Phanerozoic black shales, suggesting that the concentration of these elements in McArthur

Basin seawater was comparable to their concentration in modern seawater. Preliminary data for the isotopic composition of molybdenum in the Wollogorang Formation of the McArthur Basin (Arnold *et al.*, 2002) suggest somewhat more extensive sulfidic deposition of molybdenum in the Mesoproterozoic than in the modern oceans. Their data may, however, reflect a greater extent of shallow water euxinic basins rather than an entirely euxinic ocean floor. The good correlation of the concentration of sulfur and total iron in the McArthur Basin shales (Shen *et al.*, 2002) confirms the euxinic nature of the Basin; the large value of the ratio of sulfur to total iron indicates that this basin cannot have been typical of the oceans as a whole. Additional data for the concentration of redox sensitive elements in carbonaceous shales and more data for the isotopic composition of molybdenum and perhaps of copper in carbonaceous shales will probably clarify and perhaps settle the questions surrounding the redox state of the deep ocean during the Mesoproterozoic.

6.21.4.3 The Neoproterozoic (1.2–0.54 Ga)

After what appears to have been a relatively calm and uneventful climatic, atmospheric, and marine history during the Mesoproterozoic, the
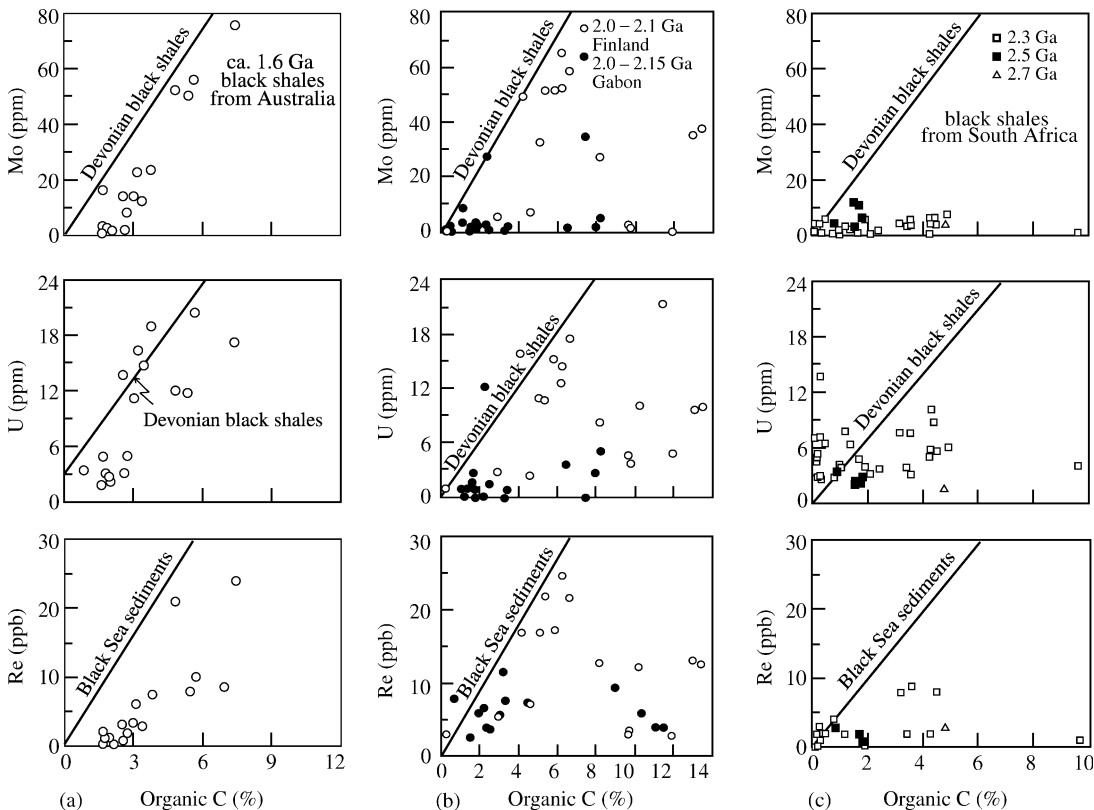

Figure 14 The concentration of Mo, U, and Re in carbonaceous shales: (a) McArthur Basin, Australia, 1.6 Ga; (b) Finland and Gabon, 2.0–2.15 Ga; and (c) South Africa, ≥2.3 Ga.

Neoproterozoic returned to the turbulence of the Paleoproterozoic era. The last 300 Ma of the Proterozoic were times of extraordinary global environmental and biological change. Major swings in the $\delta^{13}C$ value of marine carbonates were accompanied by several very large glaciations, the sulfate content of seawater rose to values comparable to that of the modern oceans (Horita et al., 2002), and the level of atmospheric O_2 probably attained modern values by the time of the biological explosion at the end of the Precambrian and the beginning of the Paleozoic. A great deal of research has been done on the last few hundred million years of the Proterozoic, stimulated in part by the discovery of the extensive glacial episodes of this period. Nevertheless, many major questions remain unanswered. The description of the major events and particularly their causes are still quite incomplete.

Figure 15 is a recent compilation of measurements of the $\delta^{13}C$ values of marine carbonates between 800 Ma and 500 Ma (Jacobsen and Kaufman, 1999). The $\delta^{13}C$ values experienced a major positive excursion interrupted by sharp negative spikes. The details of these spikes are still quite obscure (see, e.g., Melezhik et al., 2001), but the negative excursions associated with major glaciations between ca. 720 Ma and 750 Ma and between 570 Ma and 600 Ma were almost certainly separated by a 100 Ma plateau of very strongly positive $\delta^{13}C$ values (see, e.g., Walter et al., 2000; Shields and Veizer, 2002; Halverson, 2003). In some ways the Late

Neoproterozoic positive $\delta^{13}C$ excursion is reminiscent of the Paleoproterozoic excursion between 2.22 Ga and 2.06 Ga. Their duration and magnitude are similar. However, the Paleoproterozoic ice ages preceded the large positive $\delta^{13}C$ excursion, whereas in the Neoproterozoic they occur close to the beginning and close to the end of the excursion. Figure 15 can be used to estimate the "excess O_2" produced during the Neoproterozoic excursion. The average value of $\delta^{13}C$ between 700 Ma and 800 Ma was +3.0‰; between 595 Ma and 700 Ma it was +8.0‰, and between 540 Ma and 595 Ma it was −0.4‰. The average $\delta^{13}C$ value for the period between 595 Ma and 800 Ma was +5.6‰. The variation of $\delta^{13}C$ during this time interval has been defined much more precisely by Halverson (2003). Although his $\delta^{13}C$ curve differs considerably from that of Jacobsen and Kaufman (1999), Halverson's (2003) average value of $\delta^{13}C$ between 595 Ma and 800 Ma is very similar to that of Jacobsen and Kaufman (1999). This indicates that ~40% of the carbon in the sediments of this period were deposited as a constituent of organic matter.

The rate of excess O_2 generation was probably ~6×10^{12} mol yr^{-1}, and the total excess O_2 produced between 600 Ma and 800 Ma was ~12×10^{20} mol. This quantity is ~30 times the O_2 content of the present atmosphere, 0.4×10^{20} mol. O_2 buildup in the atmosphere could, therefore, have been only a small part of the effect of the large $\delta^{13}C$ excursion. The excess O_2
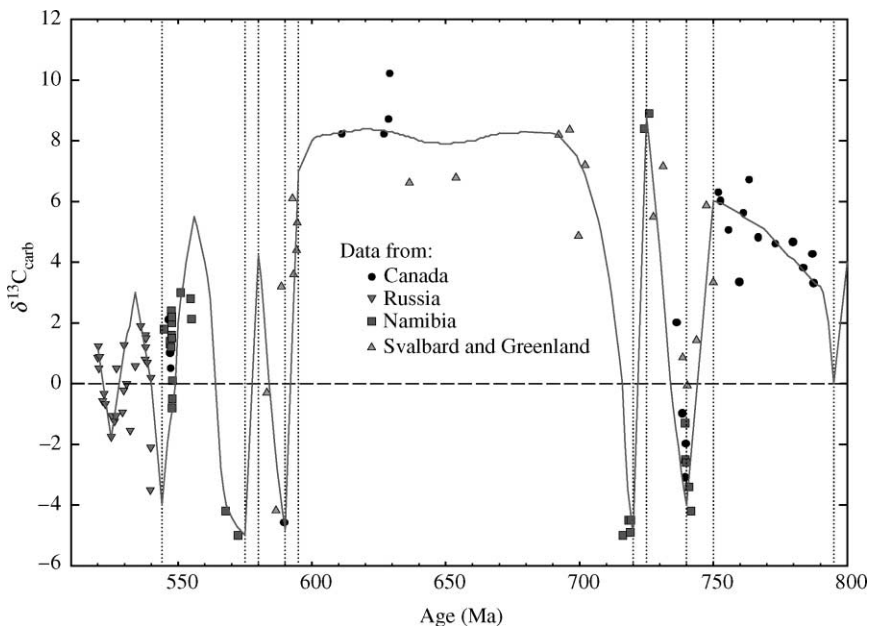

Figure 15 Temporal variations in $\delta^{13}C$ values of marine carbonates between 800 Ma and 500 Ma (source Jacobsen and Kaufman, 1999).

is also much larger than 0.8×10^{20} mol, the quantity required to raise the SO_4^{2-} concentration of seawater from zero to its present value by oxidizing sulfide. Fortunately, additional sulfate sinks are available to account for the estimated excess O_2: $CaSO_4$ and $CaSO_4 \cdot 2H_2O$ in evaporites, $CaSO_4$ precipitated in the oceanic crust close to MORs during the cycling of seawater at hydrothermal temperatures, and an increase in the Fe_2O_3/FeO ratio in sedimentary rocks. These sinks seem to be of the right order of magnitude to account for the use of the excess O_2. The magnitude of the $CaSO_4$ reservoir in sedimentary rocks during the last part of the Neoproterozoic has been estimated on the basis of models based on sulfur isotope data to be $(2 \pm 0.5) \times 10^{20}$ mol (Holser *et al.*, 1989). The conversion of this quantity of sulfur from sulfide to sulfate requires $(4 \pm 1) \times 10^{20}$ mol O_2.

At present the loss of $CaSO_4$ from seawater to the oceanic crust seems to be $\sim 1.0 \times 10^{12}$ mol yr^{-1} (Holland, 2002). At this rate the loss of SO_4^{2-} to the oceanic crust between 600 Ma and 800 Ma would have been 2×10^{20} mol. The total O_2 sinks due to the sulfur cycle during this period might, therefore, have amounted to $\sim 6 \times 10^{20}$ mol. The increase in the Fe_2O_3/FeO ratio in sedimentary rocks probably required $\sim 1 \times 10^{20}$ mol O_2. Given all the rather large uncertainties and somewhat shaky assumptions which have been made in this mass balance calculation, the agreement between the estimated quantity of excess O_2 and the estimated quantity of O_2 required to convert the sulfur cycle from its pre-1,200 Ma state to its state at the beginning of the Paleozoic is quite reasonable. The logic behind the change is also compelling. Carbon, iron, and sulfur are the three elements which dominate the redox state of the near-surface system. The carbon cycle seems to have been locked into its present state quite early in Earth history, probably by its linkage to the geochemical cycle of phosphorus. The iron cycle took on a more modern cast during the positive Paleoproterozoic $\delta^{13}C$ excursion. It is not unreasonable to propose that the positive $\delta^{13}C$ excursion during the Neoproterozoic was responsible for converting the sulfur cycle to its modern mode and for generating a further increase in the Fe_2O_3/FeO ratio.

Two questions now come to mind: (i) What triggered the Neoproterozoic $\delta^{13}C$ excursion? and (2) Are the strong negative excursions due to instabilities inherent in the long positive excursion? The answers that have been given to both questions are still speculative, but it seems worthwhile to attempt a synthesis. The $\delta^{13}C$ excursion was accompanied by the reappearance of BIFs (Klein and Beukes, 1993), which are related to glacial periods but in a somewhat irregular manner (Young, 1976; James, 1983).

They are widely distributed, and their tonnage is significant. Their reappearance virtually demands that the deeper parts of the oceans were anoxic. If, as suggested earlier, the deep oceans were oxidized during the Mesoproterozoic, they returned to their pre-1.7 Ga state during the last part of the Neoproterozoic. One possible cause for this return is the appearance of organisms which secreted SiO_2 or $CaCO_3$, that could serve as ballast for particulate organic matter. Recently discovered vase-shaped microfossils (VSMs) in the Chuar Group of the Grand Canyon could be members of one of these groups. The fossils appear to be testate amoebae (Porter and Knoll, 2000; Porter *et al.*, 2003). The structure and composition of testate amoebae tests are similar to those inferred for the VSMs. A number of testate amoebae have agglutinated tests; others have tests in which internally synthesized 1 μm to $>$10 μm scales of silica are arrayed in a regular pattern (Figure 16). The age of the VSM fossils in the Grand Canyon and in the Mackenzie Mountain Supergroup, NWT is between 742 ± 7 Ma and ca. 778 Ma. Their presence at this time suggests that they or other SiO_2-secreting organisms could have supplied ballast for the transport of particulate organic matter into the deep ocean near the beginning of the Neoproterozoic $\delta^{13}C$ excursion. If the O_2 content of the atmosphere at that time was still significantly less than today, the flux of organic matter required to make the deep oceans anoxic would only need to have been a small fraction of the present-day flux. An increase in the flux of organic matter to the deep ocean probably followed the Cambrian explosion (Logan *et al.*, 1995).
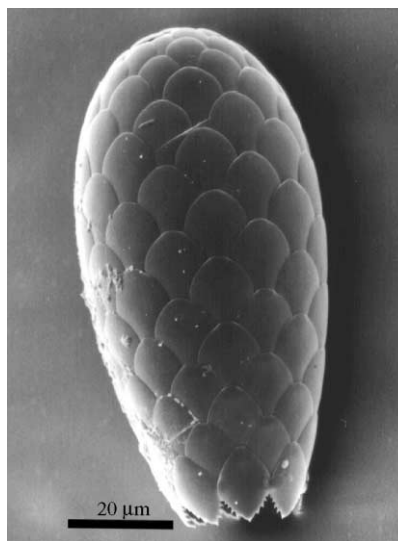
Figure 16 The test of *Euglypha tuberculata*. Note regularly arranged siliceous scales: scale bar, 20 μm (courtesy of Ralf Meisterfeld).

Arguments can be raised against the importance of the evolution of SiO_2-secreting organisms as ballast for organic matter. The VSM organisms were shallow water and benthic, not open ocean and planktonic, and the remains of SiO_2-secreting organisms have not been found in Neoproterozoic deep-sea sediments. Alternative explanations have been offered for the burial of "excess" organic carbon between 800 Ma and 600 Ma. Knoll (1992) and Hoffman et al. (1998) pointed out that the Late Proterozoic was a time of unusual, if not unique, formation of rapidly subsiding extensional basins flooded by marine waters. Organic matter buried with rapidly deposited sediments is preserved more readily than in slowly deposited sediments (Suess, 1980). However, the consequences of this effect on the total rate of burial of organic matter are small unless additional PO_4^{3-} becomes available. Anoxia would tend to provide the required addition (Colman and Holland, 2000). However, the evidence for anoxia is still limited. The reappearance of BIFs demands deep-ocean anoxia during their formation, but the Neoproterozoic BIFs are associated with the major glaciations, which may indicate—but surely does not prove—that deep-water anoxia between 800 Ma and 550 Ma was restricted to these cold periods. Other indications of deep-water anoxia are needed to define the oxidation state of deep water and the causes of anoxia during the Neoproterozoic.

In a low-sulfate ocean, anoxia would probably have increased the rate of methane production in marine sediments. Some of this methane probably escaped into the water column. In the deeper, O_2-free parts of the oceans, methane was oxidized in part by organisms using SO_4^{2-} as the oxidant. In the upper parts of the oceans, it was partly oxidized by O_2. The remainder escaped into the atmosphere. There it was in part decomposed and oxidized inorganically to CO_2; in part it was returned to the ocean in nonmethanogenic areas and was oxidized there biologically. Some methane generated in marine sediments was probably sequestered at least temporarily in methane clathrates. The methane concentration in the Neoproterozoic atmosphere could have been as high as 100–300 ppm (Pavlov et al., 2003). If methane concentrations were as high as this, it would have been a very significant greenhouse gas. At a concentration of 100 ppm, methane could well have increased the surface temperature by 12 °C (Pavlov et al., 2003).

It seems strange, therefore, that the Late Neoproterozoic should have been a time of severe glaciations (Kirschvink, 1992). In their review of the snowball Earth hypothesis, Hoffman and Schrag (2002) point out that in some sections a steep decline in δ^{13}C values by 10–15‰

preceded any physical evidence of glaciation or sea-level fall. The most likely explanation for such a sharp drop involves a major decrease in the burial rate of organic carbon. The reason(s) for this are still obscure. It is intriguing that major periods of phosphogenesis coincided roughly with the glaciations between 750–800 Ma and ca. 620 Ma (Cook and McElhinny, 1979). The first of these appears to coincide with the appearance of Rapitan-type iron ores. The second seems to have commenced shortly after the latest Neoproteroizc glaciation (Hambrey and Harland, 1981), reached a peak during the Early Cambrian, then declined rapidly, and finally ended in the Late Mid-Cambrian (Cook and Shergold, 1984, 1986). However, the time relationship between the glacial and the phosphogenic events is still not entirely resolved. The rapid removal of phosphate from the oceans may have begun before the onset of glaciation. Perhaps continental extension and rifting during the Neoproterozoic and the creation of many shallow epicontinental seaways at low paleolatitudes created environments that were particularly favorable for the deposition of phosphorites (Donnelly et al., 1990).

Some of the Neoproterozoic BIFs and associated rock units are also quite enriched in P_2O_5. For instance, the P_2O_5 content of the Rapitan iron formation in Canada and its associated hematitic mudstones ranges from 0.49% to 2.16% (Klein and Beukes, 1993). It can readily be shown, however, that the phosphate output from the oceans into the known phosphorites and BIFs is a small fraction of the phosphate metabolism of the oceans as a whole between 800 Ma and 600 Ma. This observation does not eliminate the possibility that phosphate removal into other sedimentary rocks was abnormally rapid during the two phosphogenic periods between 800 Ma and 600 Ma. Such abnormally rapid phosphate removal as a constituent of apatite would have decreased the availability of phosphate for deposition with organic matter. This would have produced a decrease in the δ^{13}C value of carbonates as observed before the onset of the snowball Earth glaciations. It would probably also have reduced the rate of methane generation, the methane concentration in the atmosphere, and the global temperature. If this, in turn, led to the onset of glaciation, the decrease in the rate of weathering would have further restricted the riverine flow of phosphate and thence to a decrease in $\delta^{13}C_{carb}$ and the global temperature. This scenario is highly speculative, but it does seem to account at least for the onset of the glaciations.

It seems very likely that the continents were largely ice covered during the Neoproterozoic glaciations. The state of the oceans is still a matter of debate. The Hoffman–Schrag Snowball Earth

hypothesis posits that the oceans were completely, or nearly completely, ice covered. This seems unlikely. Leather *et al.* (2002) have pointed out that the sedimentology and stratigraphy of the Neoproterozoic glacials of Arabia were more like those of the familiar oscillatory glaciations of the Pleistocene than those required by the Snowball Earth hypothesis. Similarly, Condon *et al.* (2002), who studied the stratigraphy and sedimentology of six Neoproterozoic glaciomarine successions, concluded that the Neoproterozoic seas were not totally frozen, and that the hydrologic cycle was functioning during the major glaciations. This suggests that the tropical oceans were ice free or only partially ice covered. Perhaps an Earth in such a state might be called a frostball, rather than a snowball. Chemical weathering on the continents in this state would have been very minor. CO_2 released from volcanoes would have built up in the atmosphere and in the oceans until its partial pressure was high enough to overcome the low albedo of the Earth at the height of the glacial episodes. In the Hoffman–Schrag model, some 10 Ma of CO_2 buildup are needed to raise the atmospheric CO_2 pressure sufficiently to overcome the low albedo of a completely ice-covered Earth. The only test of this timescale has been provided by the Bowring *et al.* (2003) data for the duration of the Gaskiers glacial deposits in Newfoundland. This unit is often described as a Varanger-age glaciomarine deposit. It is locally overlain by a thin cap carbonate bed with a highly negative carbon isotopic signature. The U–Pb geochronology of zircons separated from ash beds below, within, and above the glacial deposits indicates that these glacial deposits accumulated in less than 1 Ma. The short duration of this episode may be more consistent with a frostball than with a snowball Earth.

At the very low stand of sea level during the heights of these glaciations, the release of methane from clathrates might have contributed significantly to the subsequent warming and to the negative value of $\delta^{13}C_{CARB}$ in the ocean–atmosphere system (Kennedy *et al.*, 2001). Intense weathering after the retreat of the glaciers would—among other products—have released large quantities of phosphate. This might have speeded the recovery of photosynthesis and the return of the $\delta^{13}C$ of marine carbonates to their large positive values along the course of the 800–600 Ma positive $\delta^{13}C$ excursion.

Between the end of the positive $\delta^{13}C$ excursion and the beginning of the Cambrian, several large marine evaporites were deposited. These are still preserved and offer the earliest opportunity to use the mineralogy of marine evaporites and the composition of fluid inclusions in halite to reconstruct the composition of the contemporaneous seawater. Horita *et al.* (2002) have used this approach to show that the sulfate concentration in latest Neoproterozoic seawater was ~ 23 mmol kg^{-1}, i.e., only slightly less than in modern seawater, and significantly greater than during some parts of the Phanerozoic. By the latest Proterozoic, a new sulfur regimen had been installed. The cycling of seawater through MORs had probably reached present-day levels, the S/C ratio in volcanic gases had therefore risen, and the proportion of volcanic sulfur converted to constituents of sulfides and sulfates had approached unity as demanded by the composition of average Phanerozoic volcanic gases (Holland, 2002). The conversion of the composition of sedimentary rocks from their pre-GOE to their modern composition had been nearly completed.

The level of atmospheric O_2 seems to have been the last of the redox parameters to approach modern values. The evidence for this comes from the changes in the biota that occurred between the latest Proterozoic and the middle of the Cambrian period. These changes are discussed in the next section. Although a good deal of progress has been made since 1980 in our understanding of the atmosphere and oceans during the Proterozoic Era, we are still woefully ignorant of even the most basic oceanographic data for Precambrian seawater.

6.21.5 THE PHANEROZOIC

6.21.5.1 Evidence from Marine Evaporites

Our understanding of the chemical evolution of Phanerozoic seawater has increased enormously since the end of World War II. Rubey's (1951) presidential address to the Geological Society of America was aptly entitled "The geologic history of seawater, an attempt to state the problem." During the following year, Barth (1952) introduced the concept of the characteristic time in his analysis of the chemistry of the oceans, and this can, perhaps, be considered the beginning of the application of systems analysis to marine geochemistry. Attempts were made by the Swedish physical chemist Lars Gunnar Sillén to apply equilibrium thermodynamics to define the chemical history of seawater, but, as he pointed out, "practically everything that interests us in and around the sea is a symptom of nonequilibrium… What we can hope is that an equilibrium model may give a useful first approximation to the real system, and that the deviations of the real system may be treated as disturbances" (Sillén, 1967). Similar sentiments were expressed by Mackenzie and Garrels (1966) and by Garrels and Mackenzie (1971). They proposed that there has been little change in seawater composition since 1.5–2 Ga, although they were concerned by the discovery by Ault and Kulp (1959), Thode *et al.* (1961),

Thode and Monster (1965), and Holser and Kaplan (1966) of very significant fluctuations in the isotopic composition of sulfur in seawater during the Phanerozoic.

A good deal of optimism regarding the constancy or near constancy of the composition of seawater during the Phanerozoic was, however, permitted by the Holser (1963) discovery that the Mg/Cl and Br/Cl ratios in brines extracted from fluid inclusions in Permian halite from Hutchinson, Kansas were close to those of modern brines. Holland (1972) published his analysis of the constraints placed by the constancy of the early mineral sequence in marine evaporites during the Phanerozoic. This paper showed that most of the seawater compositions permitted by the precipitation sequence $CaCO_3$–$CaSO_4$–$NaCl$ in marine evaporites fall within roughly twice and half of the concentration of the major ions in seawater today. These calculations were extended by Harvie *et al.* (1980) and Hardie (1991) to include the later, more complex mineral assemblages of marine evaporites. Their calculations explained the mineral sequence in modern evaporites, and confirmed that the composition of Permian seawater was similar to that of modern seawater.

The development of a method to extract brines from fluid inclusions in halite and to obtain quantitative analyses by means of ion chromatography (Lazar and Holland, 1988) led to a study of the composition of trapped brines in halite from several Permian marine evaporites (Horita *et al.*, 1991). Their results together with those of Stein and Krumhansl (1988) confirmed that the composition of modern seawater is similar to that of Permian seawater, and suggested that the composition of seawater has been quite conservative during the Phanerozoic. This suggestion, however, has turned out to be far off the mark. Analyses of fluid inclusions in halite of the Late Silurian Salina Group of the Michigan Basin (Das *et al.*, 1990), the Middle Devonian Prairie Formation in the Saskatchewan Basin (Horita *et al.*, 1996), and a growing number of other marine evaporites (for a summary of the results of other groups, see Horita *et al.* (2002)) have shown that the similarity between Permian and modern seawater is the exception rather than the rule. Only the fluid inclusions in halite of the latest Neoproterozoic Ara Formation in Oman (Horita *et al.*, 2002) are similar to their Permian and modern equivalents. All of the other fluid inclusions contain brines which are very significantly depleted in Mg^{2+} and SO_4^{2-} relative to modern seawater. Their composition is consistent with the mineralogy of the associated evaporites. The difference between these inclusion fluids and their modern counterparts is either due to significant differences in the composition of the seawater from which they were derived or to

reactions which depleted the Mg^{2+} and SO_4^{2-} content of the brines along their evaporation path. The Silurian and Devonian evaporites which we studied are associated with large carbonate platforms. The dolomitization of $CaCO_3$ followed by the deposition of gypsum and/or anhydrite during the passage of seawater across such platforms can deplete the evaporating brines in Mg^{2+} and SO_4^{2-}. Their composition can then become similar to that of the brines in the Silurian and Devonian halites. We opted for this interpretation of the fluid inclusion data, wrongly as it turned out. An obvious test of the proposition that the differences were due to dolomitization and $CaSO_4$ precipitation was to analyze fluid inclusions in halite from marine evaporites which are not associated with extended carbonate platforms. Zimmermann's (2000) work on Tertiary evaporites did just that. Her analyses showed that in progressively older Tertiary evaporites the composition of the seawater from which the brines in these evaporites developed was progressively more depleted in Mg^{2+} and SO_4^{2-} (Figure 17). As shown in Figure 18, this trend continued into the Cretaceous and was not reversed until the Triassic or latest Permian. The composition of fluid inclusion brines in marine halite is, therefore, a reasonably good guide to the composition of their parent seawater. However, changes due to the reaction of evaporating seawater with the sediments across which it passes en route to trapping have almost certainly occurred and cannot be neglected.

6.21.5.2 The Mineralogy of Marine Oölites

The proposed trend of the Mg/Ca ratio of seawater (Figure 17) during the Tertiary is supported by two independent lines of evidence: the mineralogy of marine oölites and the magnesium content of foraminifera. Sandberg (1983, 1985) discovered that the mineralogy of marine oölites has alternated several times between dominantly calcitic and dominantly aragonitic (see Figure 18). On this basis he divided the Phanerozoic into periods of calcitic and aragonitic seas. He suggested that the changes in mineralogy were related to changes in atmospheric P_{CO_2} or to changes in the Mg/Ca ratio of seawater. The experiments by Morse *et al.* (1997) have shown that changes in the Mg/Ca ratio are the most likely cause of the changes in oölite mineralogy. The most recent switch in oölite mineralogy occurred near the base of the Tertiary (see Figures 17 and 18). Unfortunately, the Mg/Ca ratio of seawater at the time of this switch can be defined only roughly, because the change in oölite mineralogy from calcite to aragonite depends on temperature as well as on the Mg/Ca ratio of
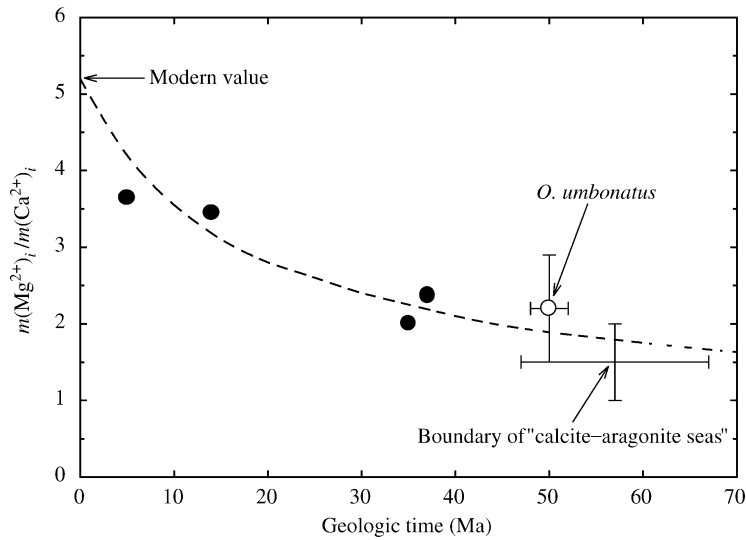
Figure 17 $m(Mg^{2+})_i/m(Ca^{2+})_i$ ratio in seawater during the Tertiary based on analyses of fluid inclusions in marine halite (● and dashed line), compared with data based on the Mg/Ca ratio of *O. umbonatus* (○) (Lear *et al.*, 2000) and the boundary of "aragonite-calcite seas" of Sandberg (1985) (source Horita *et al.*, 2002).
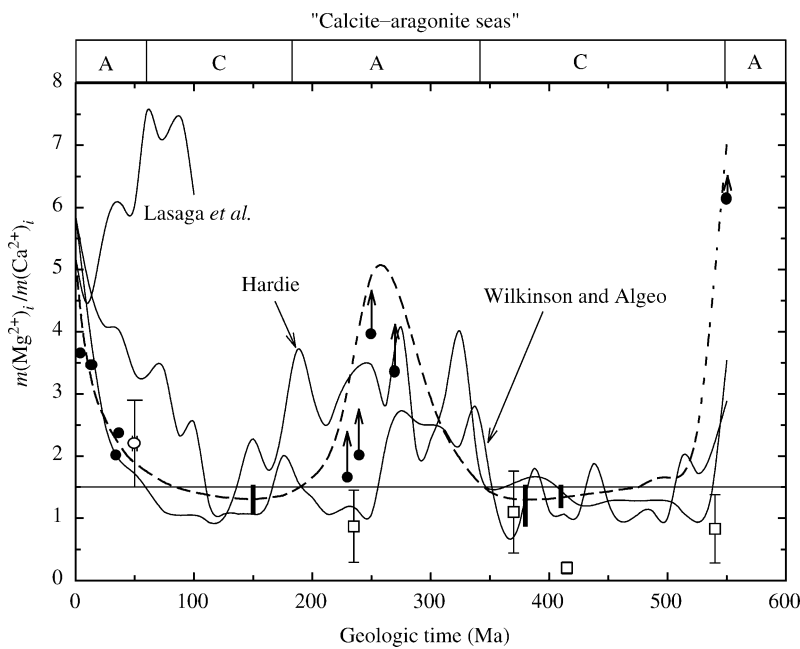
Figure 18 $m(Mg^{2+})_i/m(Ca^{2+})_i$ ratio in seawater during the Phanerozoic based on analyses of fluid inclusions in marine halite (solid symbols and dashed line), compared with the data based on Mg/Ca of *O. umbonatus* (○) (Lear *et al.*, 2000) and of abiogenic marine carbonate cements (□) (Cicero and Lohmann, 2001). Also shown are the results of modeling by Lasaga *et al.* (1985), Wilkinson and Algeo (1989), and Hardie (1996). "A" and "C" at the top indicate "aragonite seas" and "calcite seas" of Sandberg (1985) (source Horita *et al.*, 2002).

seawater, and probably also on other compositional and kinetic factors.

6.21.5.3 The Magnesium Content of Foraminifera

The magnesium content of foraminifera supplies another line of evidence in support of a low Mg/Ca ratio in Early Tertiary seawater. Lear *et al.* (2000) found that the magnesium content of *O. umbonatus* decreased progressively with increasing age during the Tertiary. This change in composition is due in large part to changes in seawater temperature and in the Mg/Ca ratio of seawater, but it can also be overprinted by diagenetic processes. Much more data are needed

to define the course of the Mg/Ca ratio of seawater on the basis of paleontologic data, but it is encouraging that its rather uncertain course during the Tertiary is consistent with that derived from the two other lines of evidence.

The correlation between the mineralogy of marine oölites and the Mg/Ca ratio of seawater as inferred from the composition of fluid inclusion brines extends throughout the Phanerozoic. This is also true for the correlation of the temporal distribution of the taxa of major calcite and aragonite reef builders and the temporal distribution of KCl-rich and MgSO$_4$-rich marine evaporites (Figure 19; Stanley and Hardie, 1998). There is no reason, therefore, to doubt that the composition of seawater has changed significantly during the Phanerozoic. As shown in Figures 20–23, only the concentration of potassium seems to have remained essentially constant. Lowenstein et al. (2001) have confirmed these trends and have shown that ancient inclusion fluids in halite had somewhat lower Na$^+$ concentrations and higher Cl$^-$ concentrations during halite precipitation than present-day halite-saturated seawater brines.

Figures 20–23 compare the changes in the composition of seawater during the Phanerozoic that have been proposed by various authors since the early 1980s. Some of these differences are

sizable. The Berner–Lasaga–Garrels (BLAG) box model developed by Berner et al. (1983) and Lasaga et al. (1985) included most of the major geochemical processes that affect the composition of seawater. Their changes in the concentration of Mg^{2+} and Ca^{2+} during the past 100 Ma are, however, much smaller than the estimates of Horita et al. (2002). The differences are due, in part, to the absence of dolomite as a major sink of Mg^{2+} in the BLAG model. However, Wallmann (2001) proposed concentrations of Ca^{2+} much higher than those of Horita et al. (2002), because he assumed, as an initial value in his model, that at 150 Ma the Ca^{2+} concentration in seawater was twice that of modern seawater.

The effect of penecontemporaneous dolomite deposition on the chemical evolution of seawater was included in the model published by Wilkinson and Algeo (1989), which was based on Given and Wilkinson's (1987) compilation of the distribution of limestones and dolomites in Phanerozoic sediments. Their calculations suggest that the concentration of Ca^{2+} in seawater remained relatively constant (±20%) during the Phanerozoic, but that the concentration of Mg^{2+} changed significantly, largely in phase with their proposed dolomite-age curve. The changes that they proposed for the concentration of both elements differ significantly from those of
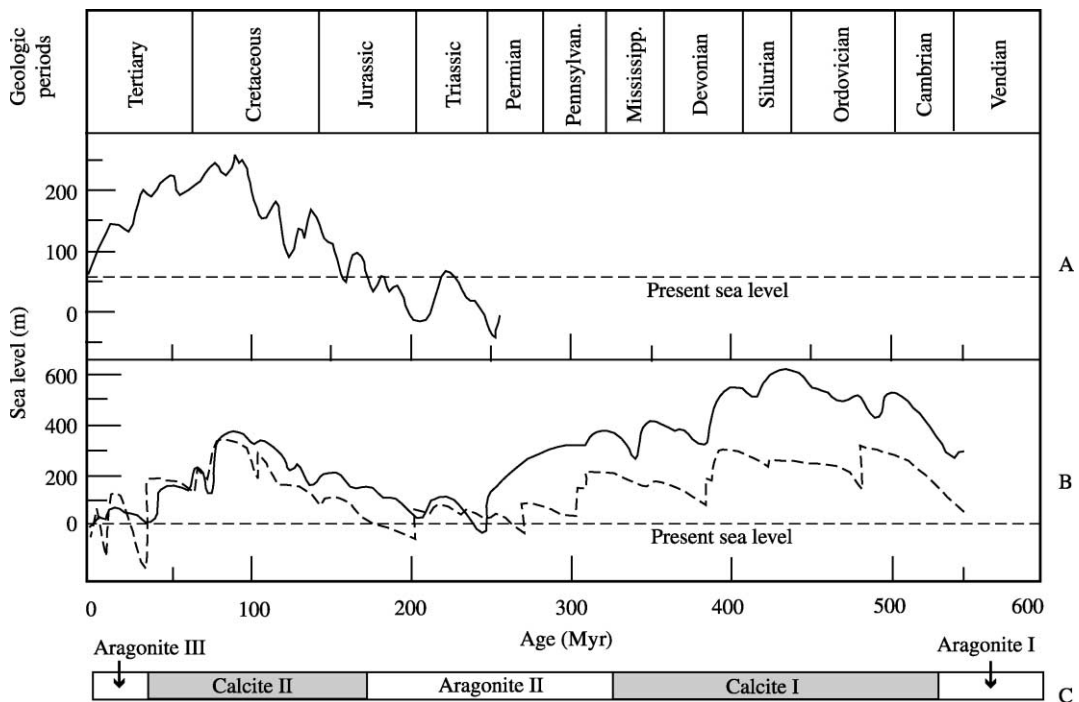
Figure 19 Sea-level changes and secular variations in the mineralogy of marine carbonates (Holland and Zimmermann, 2000): A—mean sea level during the Mesozoic and Cenozoic (Haq et al., 1987); B—mean sea level during the Phanerozoic ((– –) Vail et al., 1977; (—) Hallam, 1984); and C—secular variation in the mineralogy of Phanerozoic nonskeletal marine carbonates (source Stanley and Hardie, 1998).
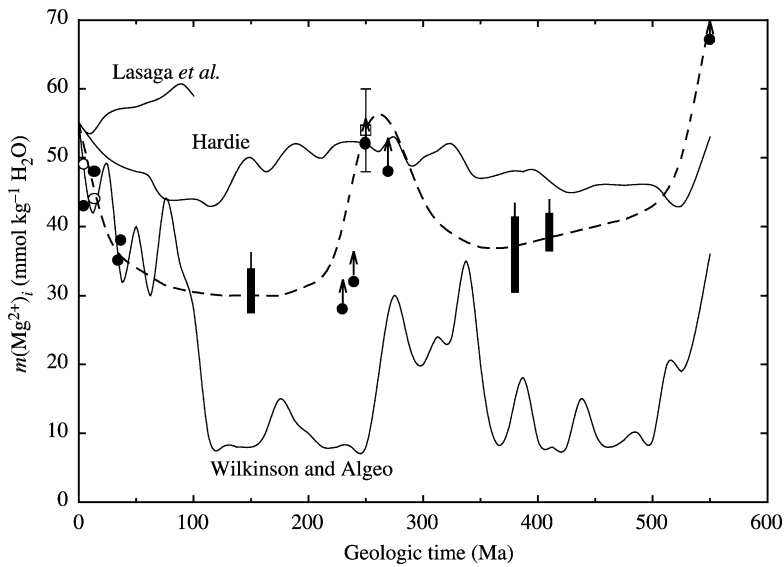
Figure 20 Concentration of Mg^{2+} in seawater during the Phanerozoic based on analyses of fluid inclusions in marine halite (solid symbols): thick and thin vertical bars are based on the assumption of different values for $m(Ca^{2+})_i/m(SO_4^{2-})_i$. Dashed line is our best estimate of age curve: (□)—Horita *et al.* (1991) and (○)—Zimmermann (2000). Also shown are the results of modeling by Lasaga *et al.* (1985), Wilkinson and Algeo (1989), and Hardie (1996) (source Horita *et al.*, 2002).
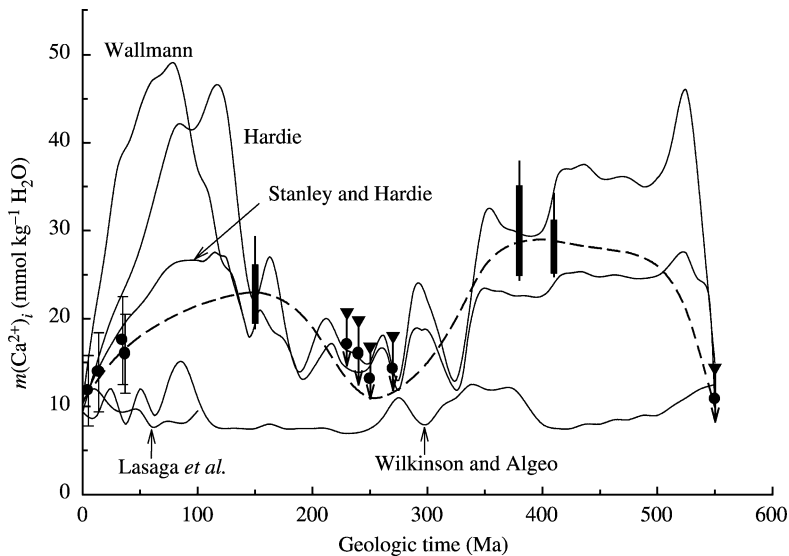
Figure 21 Concentration of Ca^{2+} in seawater during the Phanerozoic based on analyses of fluid inclusions in marine halite (solid symbols): circles–triangles and thick–thin vertical bars are based on the assumption of different values for $m(Ca^{2+})_i m(SO_4^{2-})_i$. Dashed line is our best estimate of age curve. Also shown are the results of modeling by Lasaga *et al.* (1985), Wilkinson and Algeo (1989), Hardie (1996), Stanley and Hardie (1998), and Wallmann (2001) (source Horita *et al.*, 2002).

Horita *et al.* (2002), in part because of their incomplete compilation of Phanerozoic carbonate rocks (Holland and Zimmermann, 2000).

6.21.5.4 The Spencer–Hardie Model

A very different approach to estimating the composition of seawater during the Phanerozoic was taken by Spencer and Hardie (1990) and Hardie (1996). These authors proposed that the composition of seawater was determined by the mixing ratio of river water and mid-ocean ridge solutions coupled with the precipitation of solid $CaCO_3$ and SiO_2 phases. They accepted Gaffin's (1987) curve for the secular variation of ocean crust production, which is based on the Exxon first-order
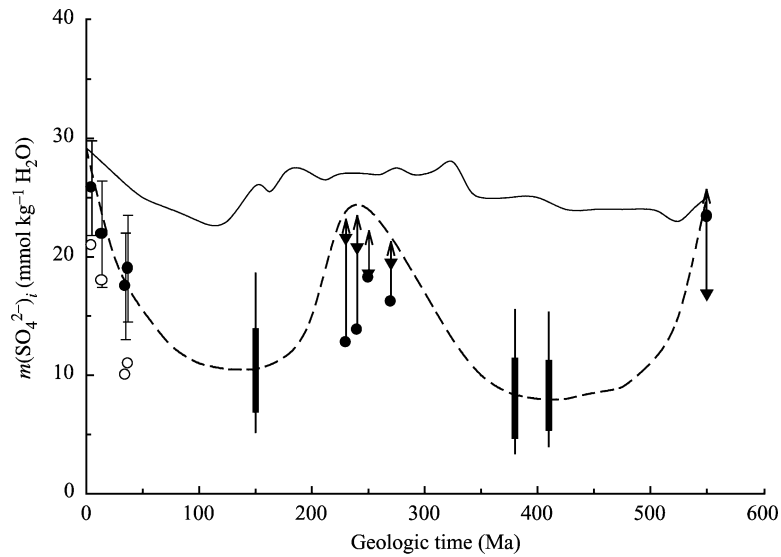
Figure 22 Concentration of SO_4^{2-} in seawater during the Phanerozoic based on analyses of fluid inclusions in marine halite (solid symbols): circles–triangles and thick–thin vertical bars are based on the assumption of different values for $m(Ca^{2+})_i, m(SO_4^{2-})_i$. Dashed line is our best estimate of age curve. Data in open and filled circles are from Zimmermann (2000). Also shown are the results of modeling by Hardie (1996) (source Horita *et al.*, 2002).
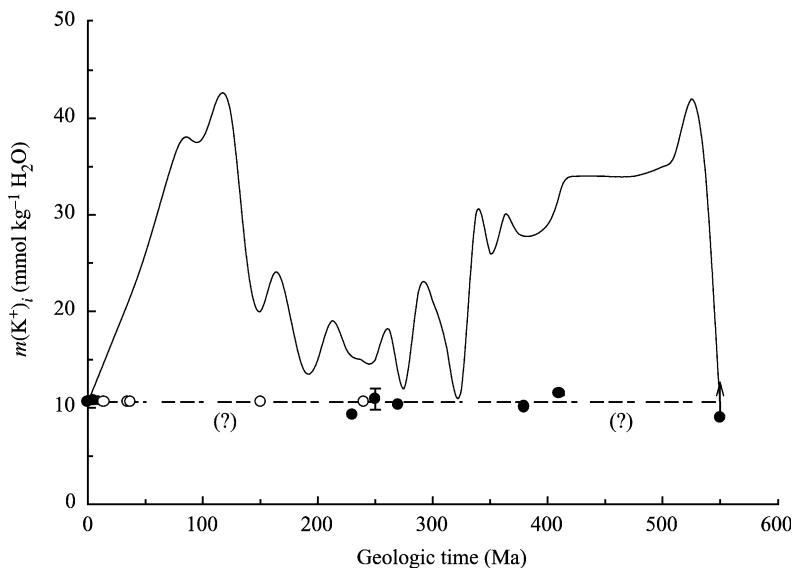
Figure 23 Concentration of K^+ in seawater during the Phanerozoic based on analyses of fluid inclusions in marine halite (solid symbols): circles–triangles and thick–thin vertical bars are based on the assumption of different values for $m(Ca^{2+})_i, m(SO_4^{2-})_i$. Dashed line is our best estimate of age curve. Open circles are from Zimmermann (2000). Also shown are the results of modeling by Hardie (1996) (source Horita *et al.*, 2002).

global sea-level curve (Vail *et al.*, 1977). They assumed that, as a first approximation, the MOR flux of hydrothermal brines has scaled linearly with the rate of ocean crust production as estimated from the sea-level curves. Spencer and Hardie (1990) and Hardie (1996) then applied their mixing model to estimate the course of the composition of seawater during the Phanerozoic.

The sea-level curves in Figure 19 have two maxima. In the Hardie (1996) model these maxima are taken to coincide with maxima in the rate of seawater cycling through MORs and hence to minima in the concentration of Mg^{2+} and SO_4^{2-} in the contemporaneous seawater. To that extent the predictions of the Hardie (1996) model agree well with the fluid inclusion data

and represented a distinct advance in understanding the chemical evolution of seawater during the Phanerozoic.

There are, however, rather serious discrepancies between the Hardie (1996) model and the fluid inclusion data of Horita et al. (2002). The most glaring is the difference between the large variations in the K^+ concentration predicted by Hardie (1996) and the essentially constant value of the K^+ concentration indicated by the fluid inclusion data. The reasons for the near constancy of the K^+ concentration in Phanerozoic seawater are not completely understood. They must, however, be related to the mechanisms by which K^+ is removed from seawater. The most important of these are almost certainly the uptake of K^+ by riverine clays and by silicate phases produced during the alteration of oceanic crust by seawater at temperatures below 100 °C. Neither process is included in the Hardie (1996) model.

The Hardie (1996) model has also been criticized on several other grounds (Holland et al., 1996; Holland and Zimmermann, 1998). At present it is, perhaps, best regarded as a rough, first-order approximation. Currently the fluid inclusion data for brines in marine halite are probably the best indicators of the composition of seawater during the Phanerozoic. However, these data are much in need of improvement. The coverage of the Phanerozoic era is still quite spotty, and a large number of additional measurements are needed before anything more can be claimed than a preliminary outline of the Phanerozoic history of seawater. Even the presently available data are not above suspicion. The assumptions that underlie the data points in Figures 17–23 were detailed by Horita et al. (2002). They are reasonable but not necessarily correct. The composition of brines trapped in halite is far removed from that of their parent seawater. Reconstructing the evolution of these brines is a considerable challenge, given the complexity of the precipitation, dissolution, reprecipitation, and mixing processes in evaporite basins.

6.21.5.5 The Analysis of Unevaporated Seawater in Fluid Inclusions

Analyses of unevaporated seawater are probably essential for defining precisely the evolution of seawater during the Phanerozoic. Johnson and Goldstein (1993) have described single-phase fluid inclusions in low-magnesium calcite cement of the Wilberns Formation in Texas. These almost certainly contain Cambro–Ordovician seawater. The salinity of the inclusion fluids ranges from 31‰ to 47‰. This is essentially identical to the range of seawater salinity observed in shallow-water marine settings today, and is consistent with the precipitation of the calcite cements within slightly restricted environments. Banner has reported a similar salinity range for fluid inclusions in low-magnesium calcite cements in the Devonian Canning Basin of Australia. The fluid inclusions in both areas have diameters ≤30 μm. They are large enough for making heating–freezing measurements but too small until now to serve for quantitative chemical analysis. The recent development of analytical techniques based on ICPMS technology brings the analysis of these fluid inclusions within reach. It will be important to determine whether their composition agrees with the composition of seawater that has been inferred from studies of the composition of inclusion fluids in halite from marine evaporites.

6.21.5.6 The Role of the Stand of Sea Level

The correlation between the composition of seawater and the sea-level curves in Figure 19 is quite striking. The reasons for the correlation are not entirely clear. Hardie (1996) suggested that the stand of sea level reflects the rate of ocean crust formation, that this determines the rate of seawater cycling through MORs, and hence the mixing ratio of hydrothermally altered seawater with average river water. However, the rate of seafloor spreading has apparently not changed significantly during the last 40 Ma (Lithgow-Bertelloni et al., 1993), and Rowley's (2002) analysis of the rate of plate creation and destruction indicates that the rate of seafloor spreading has not varied significantly during the past 180 Ma. If this is correct, the rate of ridge production has been essentially constant since the Early Jurassic. Since the rate of seawater cycling through MORs is probably proportional to this rate, other changes in the Earth system have been responsible for the changes in sea level and in the composition of seawater during the past 180 Ma. Holland and Zimmermann (2000) have pointed out that marine carbonate sediments deposited during the past 40 Ma contain, on average, less dolomite than Proterozoic and Paleozoic carbonates. The lower dolomite content of the more recent carbonate sediments is due to the increase in the deposition of $CaCO_3$ in the deep sea, where dolomitization only takes place in unusual circumstances. The decrease in the rate of Mg^{2+} output from the oceans due to dolomite formation has been balanced by an increase in the output of oceanic Mg^{2+} by the reaction of

seawater with clay minerals and with ocean-floor basalts, mainly at MORs. The increase in the output of Mg^{2+} into these reservoirs has been brought about by an increase in the Mg^{2+} concentration of seawater. A simple quantitative model of these processes (Holland and Zimmermann, 2000) can readily account for the observed increase in the Mg^{2+} and SO_4^{2-} concentration of seawater during the Tertiary.

This explanation cannot account for the changes in seawater chemistry before the development of abundant open-ocean $CaCO_3$ secreting organisms. Coccolithophores first appeared in the Jurassic and diversified tremendously during the Cretaceous. The foraminifera radiated explosively during the Jurassic and Cretaceous. Prior to the evolution of coccoliths and planktonic foraminifera, carbonate sediments were largely or entirely deposited on the continents and in shallow-water marine settings. It is likely, therefore, that changes in seawater composition before ca. 150 Ma were related either to changes in the rate of seafloor spreading or to the mineralogy of continental and near-shore carbonate sediments. There are not enough data to rule out the first alternative. However, the apparent near-constancy of the rate of ocean crust formation during the past 180 Ma (Rowley, 2002) is not kind to the notion of major changes in this rate during the first part of the Phanerozoic. The second alternative is more attractive. Flooding of the continents was extensive during high stands of sea level, and dolomitization, which is favored in warm, shallow evaporative settings, must have been widespread. During low stands of sea level, carbonate deposition on the continents was probably replaced by deposition on rims along continental margins, where dolomitization was kinetically less favored. One can imagine that this is the major reason for the correlation of the Mg^{2+} and SO_4^{2-} concentration of seawater and the stand of sea level. The relationship may, however, be more complicated. During the Tertiary, sea level fell, yet the shallow water, near-shore carbonates deposited during the last 40 Ma are strongly and extensively dolomitized. It is not clear why this should not have happened equally enthusiastically during the Permian and Late Neoproterozoic low stands of sea level.

6.21.5.7 Trace Elements in Marine Carbonates

Many attempts have been made to relate the trace element distribution in marine minerals, particularly in carbonates, to the rate of seawater cycling through MORs, and to tectonics in general. The concentration of lithium and the concentration and isotopic composition of strontium have been studied particularly intensively. In their paper on the lithium and strontium content of foraminiferal shells, Delaney and Boyle (1986) proposed that the Li/Ca ratio has varied rather little during the past 116 Ma, but that the Sr/Ca ratio increased significantly during this time period. More recent measurements by Lear et al. (2003) on a very large number of foraminifera have shown that the Sr/Ca ratio of benthic foraminifera has had a more complicated history during the past 75 Ma. Relating the Sr/Ca ratio of foraminiferal shells to the Sr/Ca ratio in seawater is complicated, because the Sr/Ca ratio in foraminifera is a rather strong function of temperature, shell size, and pressure, and because it is species specific (Elderfield et al., 2000, 2002). Lear et al. (2003) have taken all these factors into account, have combined their data for a variety of benthic foraminifera, and have proposed the course shown in Figure 24 for the Sr/Ca ratio in seawater during the last 75 Ma. The ratio decreased rapidly between 75 Ma and 40 Ma; during the last 40 Ma it climbed significantly, but the increase was interrupted by a decrease between 15 Ma and 7 Ma.

The data in Figure 24 can be combined with those in Figure 21 for the course of the calcium concentration in seawater to yield the course of the strontium concentration of seawater during the last 75 Ma. At 75 Ma, the strontium concentration was $\sim 22 \times 10^{-5}$ mol kg^{-1} H$_2$O. At 40 Ma, it was $\sim 11 \times 10^{-5}$ mol kg^{-1} H$_2$O. At present it is 8.5×10^{-5} mol kg^{-1} H$_2$O. The 60% decrease in the strontium concentration during the last 75 Ma exceeds the decrease of the calcium concentration (45%).

Reconstructing the course of the Sr/Ca concentration in seawater from the composition of fossils is limited by the effects of diagenesis. These are particularly disturbing in carbonates older than 100 Ma. Figure 25 shows Steuber and Veizer's (2002) data for the strontium content of Phanerozoic biological low-magnesium calcites. The averages of the strontium concentrations indicate a course similar to that of the changes in sea level during the Phanerozoic; but the scatter in their data is so large that the significance of their average curve is somewhat in doubt. Lear et al. (2003) have attempted to interpret the changes in the concentration and the isotopic composition of strontium in seawater during the last 75 Ma. The rise of the Himalayas and perhaps of other major mountain chains, the lowering of sea level, and the transfer of a significant fraction of marine $CaCO_3$ deposition from shallow to deep waters have all played a role in the changes in seawater composition during the Tertiary. A quantitative treatment of the available data for strontium is
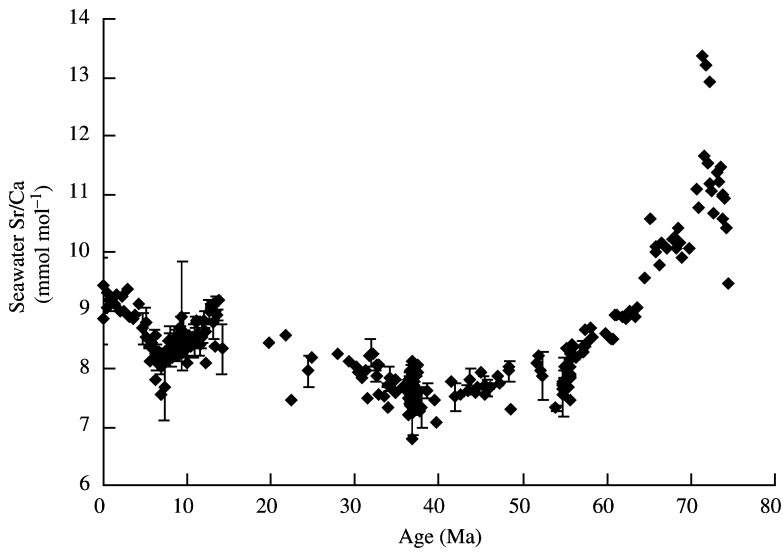
Figure 24 Seawater Sr/Ca record for the Cenozoic (source Lear *et al*., 2003).
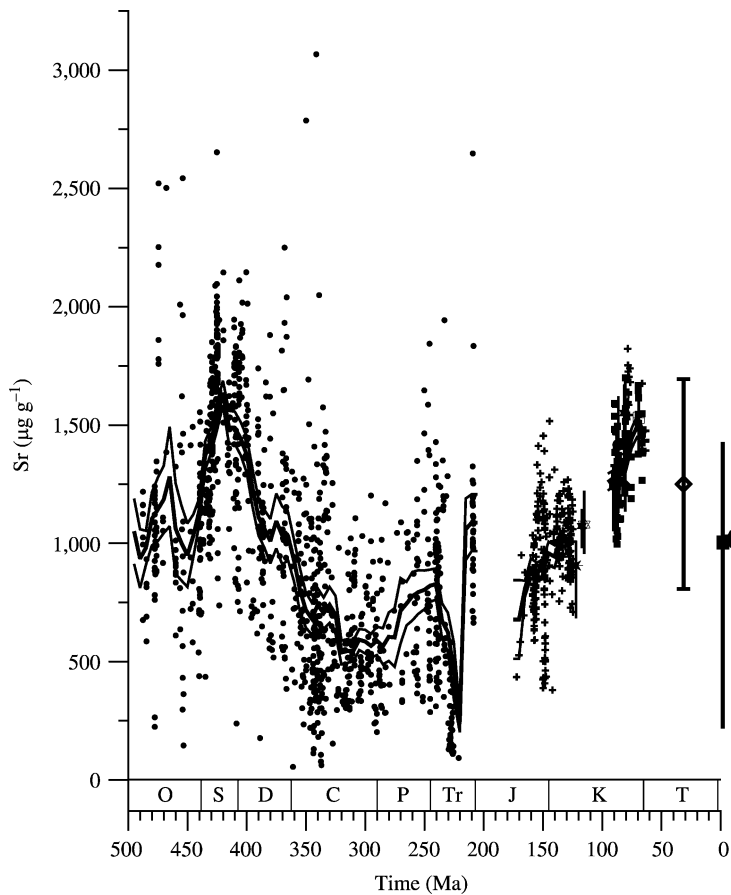
Figure 25 Sr concentrations in biological low-Mg calcite of brachiopods (dots), belemnites (crosses) and rudist bivalve (boxes). Mean values (bold curve) and two standard errors (thin curves) were calculated by moving a 20 Myr window in 5 Myr intervals across the data set. Ranges (vertical lines) and mean values (stars) of intrashell variations for concentrations in single rudist shells are also shown, but were not used in calculation of running means (source Steuber and Veizer, 2002).

still quite difficult; there are still too many poorly defined parameters in the controlling equations.

6.21.5.8 The Isotopic Composition of Boron in Marine Carbonates

The isotopic composition of several elements in marine mineral phases is a much better indicator of oceanic conditions than their concentration in these phases. The $^{11}B/^{10}B$ ratio of living planktonic foraminifera is related to the pH of seawater (Sanyal *et al.*, 1996). This relationship has opened the possibility of using the $^{11}B/^{10}B$ ratio in foraminifera to infer the pH of seawater in the past (Spivack *et al.*, 1993) and thence the course of past P_{CO_2}. This approach has been applied by Pearson and Palmer (1999, 2000) and by Palmer *et al.* (2000) to estimate the pH of seawater and P_{CO_2} during the Cenozoic. The results are, however, somewhat uncertain, because they depend rather heavily on the assumed value of the isotopic composition of boron in Cenozoic seawater, and because the fractionation of the boron isotopes during the uptake of this element in foraminifera is somewhat species specific (Sanyal *et al.*, 1996).

6.21.5.9 The Isotopic Composition of Strontium in Marine Carbonates

A very important contribution to paleoceanography has been made by measurements of the isotopic composition of strontium in Phanerozoic

carbonates. The Burke *et al.* (1982) compilation of the isotopic composition of strontium in 744 Phanerozoic marine carbonates has now been expanded by a factor of ~6. Figure 26 is taken from the summary of these data by Veizer *et al.* (1999). The major features of the Burke curve have survived, and many of its features have been sharpened considerably. The curve in Figure 26 is quite robust, and our view of variations in the $^{87}Sr/^{86}Sr$ ratio of seawater during the Phanerozoic is unlikely to change significantly. The $^{87}Sr/^{86}Sr$ ratio of seawater has fluctuated quite significantly. The overall decrease from its high value during the Cambrian to a minimum in the Jurassic and the return to its Early Paleozoic value during the Tertiary does not mirror the two megacycles of the sea-level curve. There is an obvious second-order correlation with orogenies, but their effect on the $^{87}Sr/^{86}Sr$ ratio of seawater has been overshadowed by changes in the isotopic composition and the flux of river strontium to the oceans. The very rapid rise of the $^{87}Sr/^{86}Sr$ ratio in seawater during the Tertiary must be related to the weathering of rocks of very high $^{87}Sr/^{86}Sr$ ratios, and changes in the $^{87}Sr/^{86}Sr$ ratio of rocks undergoing weathering have probably played a major role in determining the fluctuations in the $^{87}Sr/^{86}Sr$ ratio of seawater during the entire Phanerozoic.

6.21.5.10 The Isotopic Composition of Osmium in Seawater

Large changes in the composition of rocks undergoing weathering must also be invoked to
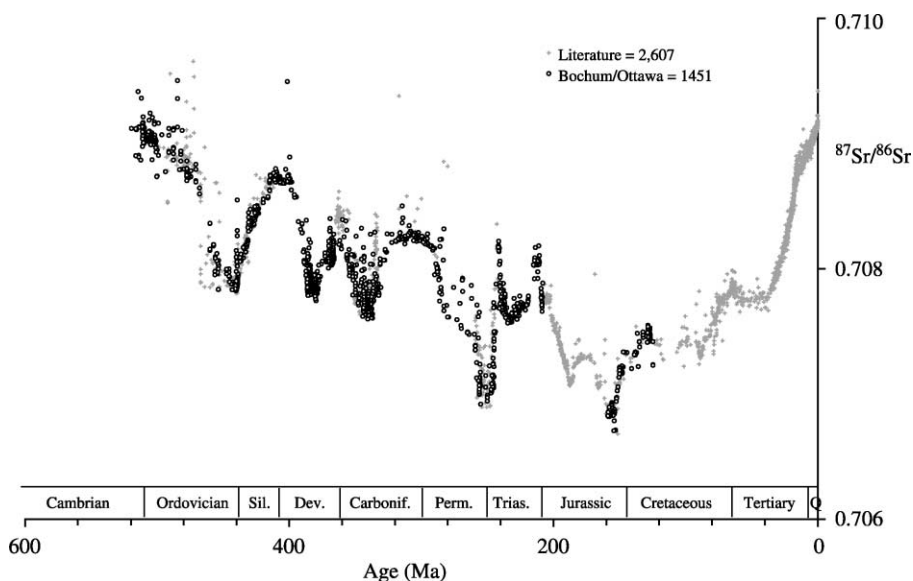
Figure 26 $^{87}Sr/^{86}Sr$ variations for the Phanerozoic based on 4,055 samples of brachiopods ("secondary" layer only for the new Bochum/Ottawa measurements), belemnites, and conodonts (source Veizer *et al.*, 1999).

explain the major changes in the $^{187}Os/^{186}Os$ ratio of seawater during the Cenozoic (see Figure 27) (Pegram and Turekian, 1999; Peucker-Ehrenbrink et al., 1995).

6.21.5.11 The Isotopic Composition of Sulfur and Carbon in Seawater

Interestingly, the first-order variation of the isotopic composition of sulfur and carbon in seawater during the Phanerozoic is qualitatively similar to that of strontium. The value of $\delta^{34}S$ at the base of the Phanerozoic is highly positive. It drops to a minimum in the Permian and then rises again to its present, intermediate level (Figures 28 and 29). The variation of $\delta^{13}C$ during the Phanerozoic is nearly the inverse of the $\delta^{34}S$ curve (Figure 30). Both describe a half-cycle rather than a two-cycle path. The inverse variation of $\delta^{34}S$ and $\delta^{13}C$ strongly suggests that the geochemical cycles of the two elements are closely linked, as suggested
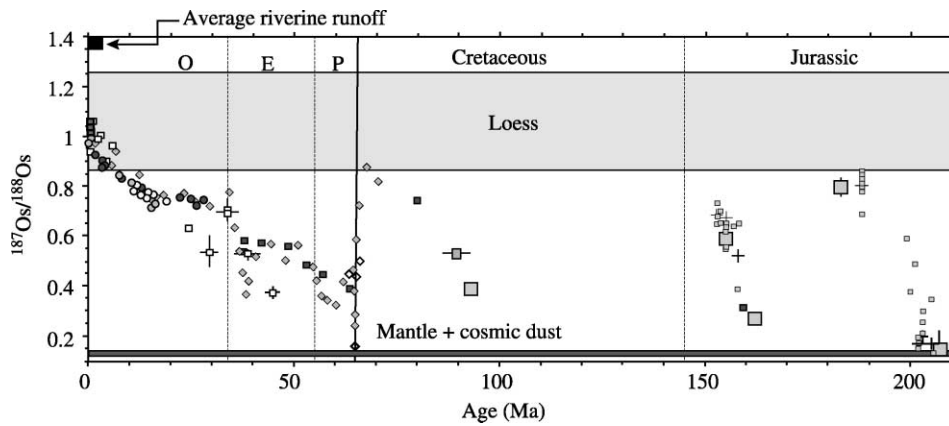
Figure 27 The marine Os isotope record during the last 200 Ma (source Peucker-Ehrenbrink and Ravizza, 2000).
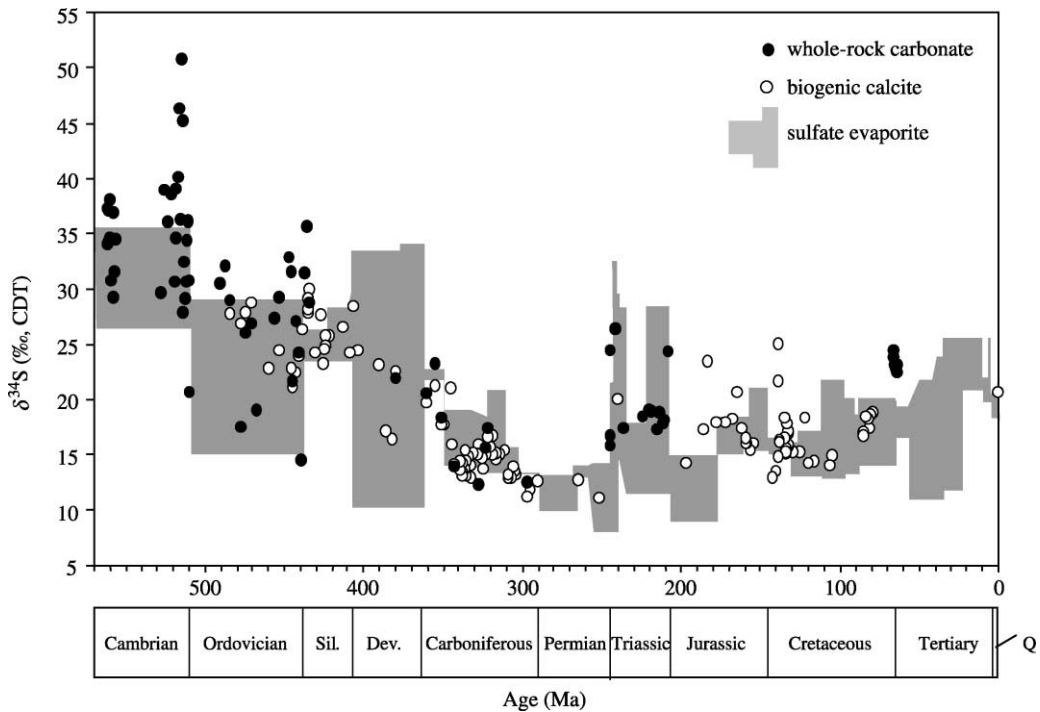
Figure 28 The sulfur isotopic composition of Phanerozoic seawater sulfate based on the analysis of structurally substituted sulfate in carbonates (Kampschulte and Strauss, in press) and evaporite based δ^{34} data (source Strauss, 1999).
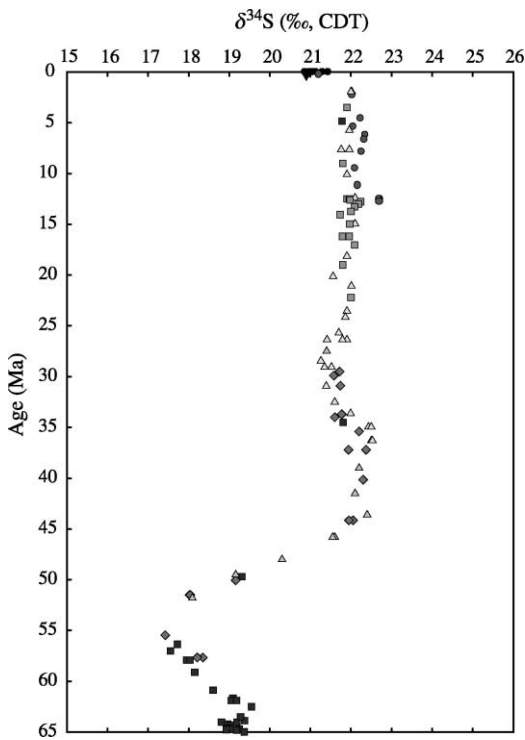
Figure 29 Isotopic composition of seawater sulfate during the past 65 Ma (Paytan *et al*., 1998, 2002) with ages modified somewhat (sources Paytan, personal communication, 2003).

by Holland (1973) and Garrels and Perry (1974). Since that time the database for assessing the variation of the isotopic composition of both elements has been enlarged very considerably, and the literature dealing with the linkage between their geochemistry has grown apace (e.g., Veizer *et al*., 1980; Holser *et al*., 1988, 1989; Berner, 1989; Kump, 1993; Carpenter and Lohmann, 1997; Petsch and Berner, 1998). Nevertheless, a truly quantitative understanding of the linkage has not yet been achieved. The inputs of sulfur and carbon to the oceans as well as the functional relationships that relate the composition of these reservoirs to their outputs into the rock record are still not very well defined. The large difference between the residence time of HCO_3^- and SO_4^{2-} in the oceans has invited deviations from steady state both in their concentration in seawater and in the isotopic composition of their constituents.

6.21.5.12 The Isotopic Composition of Oxygen in Seawater

The use of the isotopic composition of oxygen in marine carbonates as a means of reconstructing the course of the $\delta^{18}O$ value of seawater during the Phanerozoic has been a

matter of considerable contention. The $\delta^{18}O$ value of carbonates and cherts tends to become more negative with increasing geologic age (see, e.g., Figure 31). In many instances this decrease is clearly due to diagenetic changes involving reactions with isotopically light water. However, the $\delta^{18}O$ of carbonates which have been chosen carefully to avoid overprinting by diagenetic alteration also tends to decrease with increasing geologic age.

The strongest argument in favor of a near-constant $\delta^{18}O$ value of seawater during much of Earth history is based on an analysis of the effects of seawater cycling through MORs at high temperatures (Muehlenbachs and Clayton, 1976; Holland, 1984; Muehlenbachs, 1986). Changes in the high-temperature cycling of seawater through mid-ocean ridges do not seem to be capable of accounting for major changes in the $\delta^{18}O$ of seawater. At present the only promising mechanism for explaining large changes in the $\delta^{18}O$ of seawater is a major change in the ratio of low-temperature to high-temperature alteration of the oceanic crust (Lohmann and Walker, 1989). The $\delta^{18}O$ of high-temperature vent fluids (200–400 °C) scatter from +0.2‰ to +2.15‰ with an average value of +1.0‰ with respect to the entering seawater (Bach and Humphris, 1999). $\delta^{18}O$ data for basement fluids at temperatures below 100 °C are few. Elderfield *et al*. (1999) have shown that thermally driven seawater in an 80 km transect across the eastern flank of the Juan de Fuca Ridge at 48° latitude has temperatures between 15.5 °C and 62.8 °C and $\delta^{18}O$ values, on average, −1.05‰ with respect to the entering seawater. About 5% of the global ridge flank heat flux would have to be associated with exchange of $\delta^{18}O$ in the ridge flanks to balance the enrichment in seawater $\delta^{18}O$ due to high-temperature hydrothermal activity. The estimate of 5% is similar to that proposed by Mottl and Wheat (1994) (see also Mottl, 2003). It remains to be seen whether the large changes in the balance between low-temperature and high-temperature alteration of the oceanic crust that seem to be required to shift the $\delta^{18}O$ values of seawater to −8‰ have actually occurred. Even if they have not, the Earth's total hydrologic system is so complex that major changes in the $\delta^{18}O$ of seawater during the history of the planet should not be dismissed out of hand.

6.21.6 A BRIEF SUMMARY

The large amount of research that has been completed since the early 1980s has done much to clarify our understanding of the chemical evolution of seawater. In the Precambrian, major advances have centered on the effects of the rise
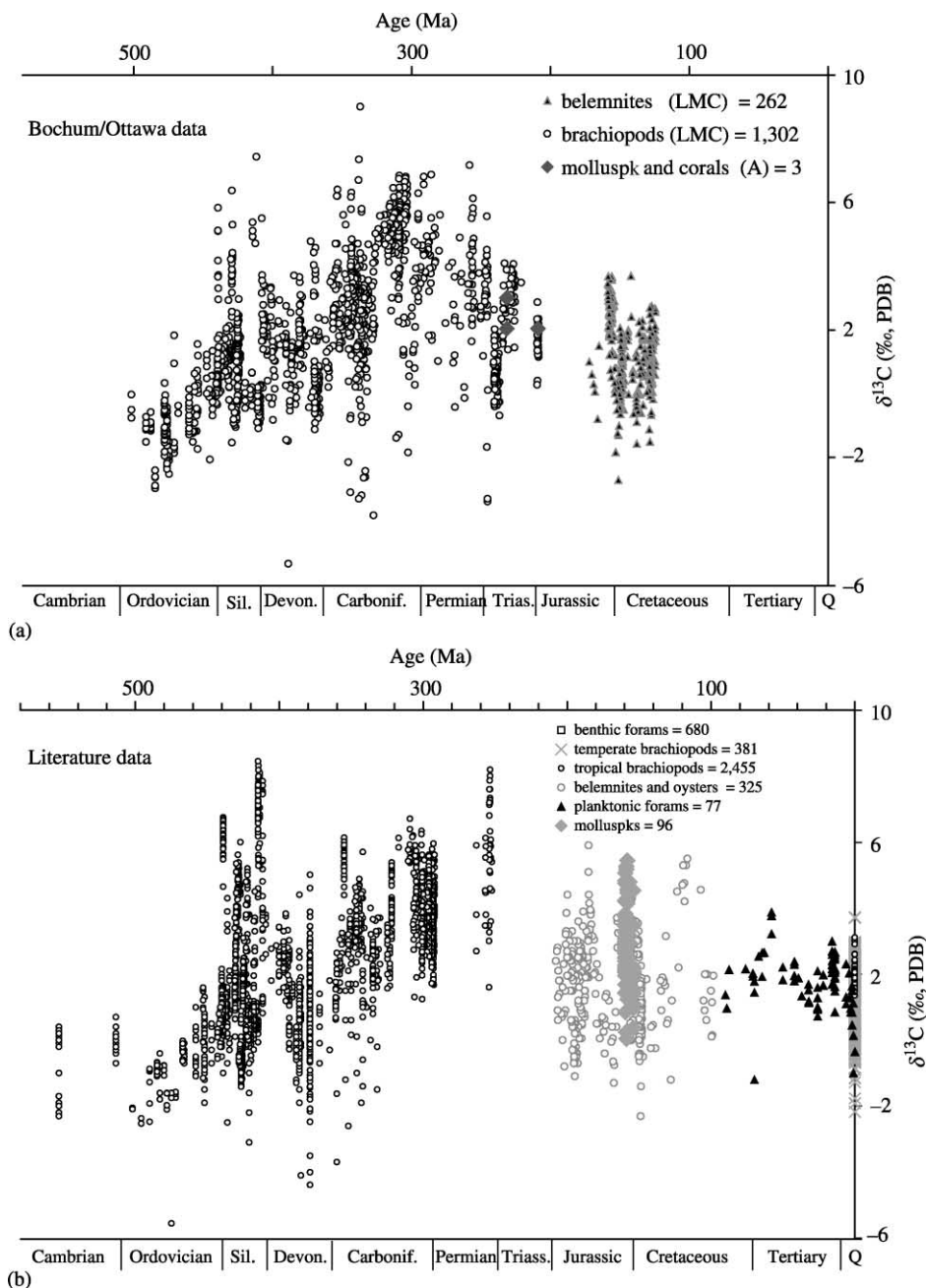
Figure 30 Carbon isotope composition of Phanerozoic low-Mg calcitic shells (source Veizer *et al.*, 1999).

of oxygen on the marine geochemistry of sulfur and the redox sensitive elements. In the Phanerozoic the definition, albeit imprecise, of the concentration of the major constituents of seawater and of the relationship between changes in their concentration, isotopic composition, tectonics, and biological evolution represent a major advance.

Despite this progress our knowledge of the ancient oceans is miniscule compared to our knowledge of the modern ocean. Even the

course of the major element concentrations in Phanerozoic seawater is still rather poorly defined, and estimates of their concentration in Precambrian seawater are little more than guesswork. The most promising avenue to a more satisfactory paleoceanography is probably the analysis of fluid inclusions containing unevaporated seawater. This presents formidable analytical problems. If they can be solved, and if a sufficient number of such inclusions spanning a large fraction of Earth history are analyzed, the
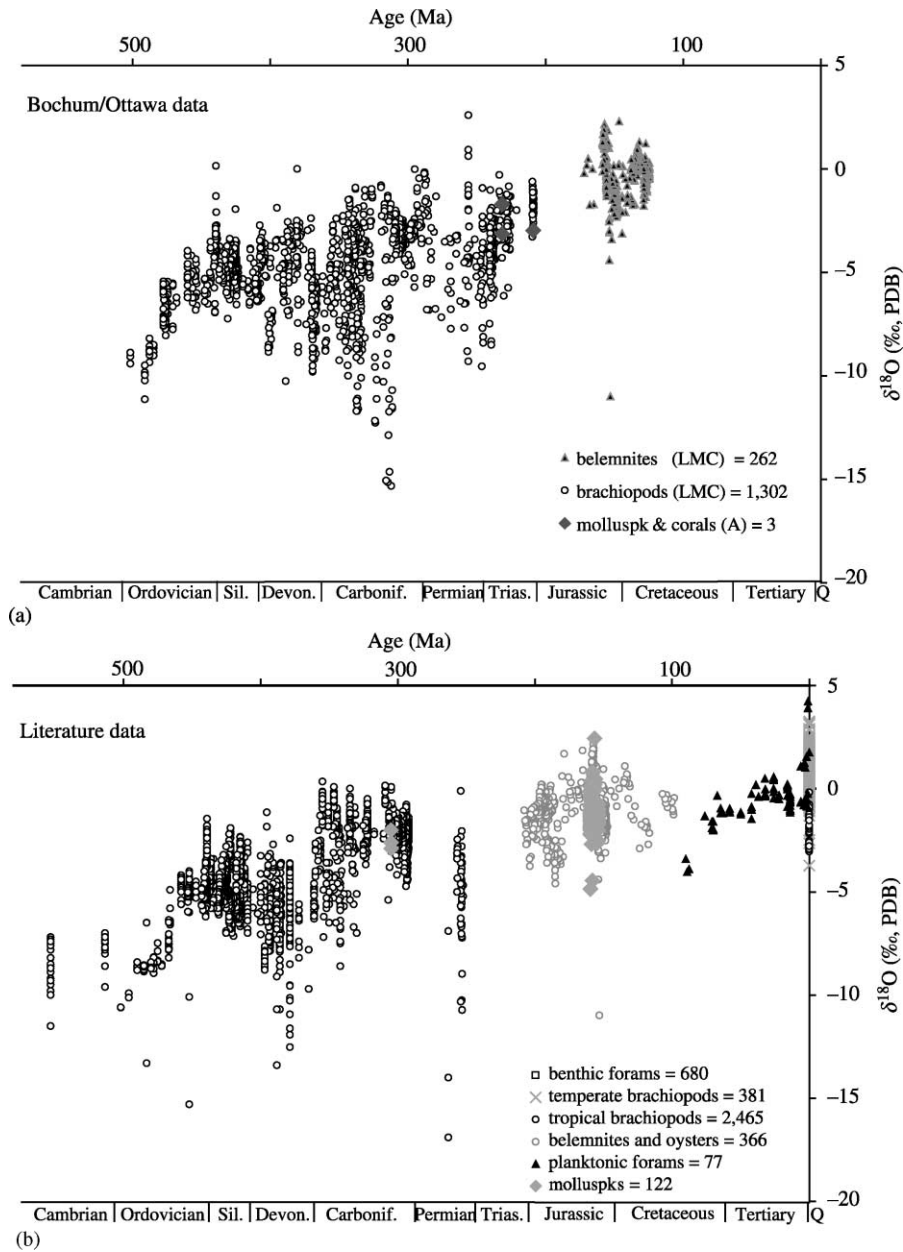
Figure 31 Oxygen isotope composition of Phanerozoic low-Mg calcitic shells (source Veizer *et al.*, 1999).

state of paleoceanography will be improved dramatically.

ACKNOWLEDGMENTS

REFERENCES

Allègre C., Manhès G., and Göpel C. (1995) The age of the Earth. *Geochim. Cosmochim. Acta* **59**, 1445–1456.
Anbar A. D. and Holland H. D. (1992) The photochemistry of manganese and the origin of banded iron formations. *Geochim. Cosmochim. Acta* **56**, 2595–2603.
Anbar A. D. and Knoll A. H. (2002) Proterozoic ocean chemistry and evolution: a bioinorganic bridge? *Science* **297**, 1137–1142.

Anbar A. D., Zahnle K. J., Arnold G. L., and Mojzsis S. J. (2002) Extraterrestrial iridium, sediment accumulation and the habitability of the early Earth's surface. *J. Geophys. Res.* **106**, 3219–3236.

Appel P. W. U. (1983) Rare earth elements in the Early Archean Isua iron-formation, West Greenland. *Precamb. Res.* **20**, 243–258.

Appel P. W. U. and Moorbath S. (1999) Exploring Earth's oldest geological record in Greenland. *EOS, Trans., AGU* **80**, 257, 261, 264.

Armstrong R. A., Lee G. F., Hedges J. I., Honjo S., and Wakeham A. (2002) A new mechanistic model for organic carbon fluxes in the ocean based on the quantitative association of POC with ballast minerals. *Deep-Sea Res.* **49**, 219–236.

Arnold G. L., Anbar A. D., and Barling J. (2002) Oxygenation of Proterozoic oceans: insight from molybdenum isotopes (abstr.). *Geochim. Cosmochim. Acta* **66** (15A), A30 (abstracts of the 12th V. M. Goldschmidt Conference, Davos, Switzerland, August 18–23, 2002).

Ault W. U. and Kulp J. L. (1959) Isotopic geochemistry of sulfur. *Geochim. Cosmochim. Acta* **16**, 201–235.

Bach W. and Humphris S. E. (1999) Relationship between the Sr and O isotope compositions of hydrothermal fluids and the spreading and magma-supply rates at oceanic spreading centers. *Geology* **27**, 1067–1070.

Barth T. F. W. (1952) *Theoretical Petrology*. Wiley, New York.

Bau M. and Möller P. (1993) Rare earth element systematics of the chemically precipitated component in Early Precambrian iron formations and the evolution of the terrestrial atmosphere–hydrosphere–lithosphere system. *Geochim. Cosmochim. Acta* **57**, 2239–2249.

Bekker A., Kaufman A. J., Karhu J. A., Beukes N. J., Swart Q. D., Coetzee L. L., and Eriksson K. A. (2001) Chemostratigraphy of the Paleoproterozoic Duitschland Formation, South Africa: implications for coupled climate change and carbon cycling. *Am. J. Sci.* **301**, 261–285.

Bekker A., Holland H. D., Rumble D., Yang W., Wang P.-L., and Coetzee L. L. (2002) MIF of S, oölitic ironstones, redox sensitive elements in shales, and the rise of atmospheric oxygen (abstr.). *Geochim. Cosmochim. Acta* **66**, A64.

Bekker A., Holland H. D., Young G. M., and Nesbitt H. W. (2003) The fate of oxygen during the early Paleoproterozoic carbon isotope excursion. *Astrobiology* **2**(4), 477.

Berner R. A. (1989) Biogeochemical cycles of carbon and sulfur and their effect on atmospheric oxygen over Phanerozoic time. *Paleogeogr. Paleoclimatol. Paleoecol.* **75**, 97–122.

Berner R. A., Lasaga A. C., and Garrels R. M. (1983) The carbonate-silicate geochemical cycle and its effect on atmospheric carbon dioxide. *Am. J. Sci.* **283**, 641–683.

Beukes N. J. (1978) Die Karbonaatgesteentes en Ysterformasies van die Ghaap-Groep van die Transvaal-Supergroep in Noord-Kaapland. PhD Thesis, Rand Afrikaans University.

Beukes N. J. (1983) Palaeoenvironmental setting of iron-formations in the depositional basin of the Transvaal Supergroup, South Africa. In *Iron Formation: Facts and Problems* (eds. A. F. Trendall and R. C. Morris). Elsevier, Amsterdam, pp. 131–209.

Beukes N. J. and Klein C. (1990) Geochemistry and sedimentology of a facies transition from micro-banded to granular iron-formation in the early Proterozoic Transvaal Supergroup, South Africa. *Precamb. Res.* **47**, 99–139.

Beukes N. J. and Klein C. (1992) Time distribution, stratigraphy, and sedimentologic setting, and geochemistry of Precambrian iron-formations. In *The Proterozoic Biosphere* (eds. J. W. Schopf and C. Klein). Cambridge University Press, Cambridge, pp. 139–146.

Beukes N. J., Dorland H., and Gutzmer J. (2002a) Pisolitic ironstone and ferricrete in the 2.22–2.4 Ga Timeball Hill Formation, Transvaal Supergroup: implications for the history of atmospheric oxygen (abstr.). *2002 Annual Meeting of the Geological Society of America*, 283p.

Beukes N. J., Dorland H., Gutzmer J., Nedachi M., and Ohmoto H. (2002b) Tropical laterites, life on land, and the history of atmospheric oxygen in the Paleoproterozoic. *Geology* **30**, 491–494.

Birch T. (1756) *A History of the Royal Society of London* (ed. A. Millar). London, vol. 1.

Black R. C. (1966) *The Younger John Winthrop*. Columbia University Press, New York.

Boak J. L. and Dymek R. F. (1982) Metamorphism of the ca. 3, 800 Ma supercrustal rocks at Isua, West Greenland: implications for early Archaean crustal evolution. *Earth Planet. Sci. Lett.* **59**, 155–176.

Boetius A., Ravenschlag K., Schubert C. J., Rickert D., Widdel F., Gieseke A., Amann R., Jørgensen B. B., Witte U., and Pfannkuche O. (2000) A marine microbial consortium mediating anaerobic oxidation of methane. *Nature* **407**, 623–626.

Bowring S. A. and Williams I. S. (1999) Priscoan (4.00–4.03) orthogneiss from northwestern Canada. *Contrib. Mineral. Petrol.* **134**, 3–16.

Bowring S. A., Landing E., Myrow P., and Ramenzavi J. (2003) Geochronological constraints on the terminal Neo-proterozoic events and the rise of Metazoans. *Astrobiology* **2**(4), 457–458.

Brasier M. D., Green O. R., Steele A., Van Kranendonk M., Jephcoat A. P., Kleppe A. K., Lindsay J. F., and Grassineau N. V. (2002) Questioning the evidence for Earth's oldest fossils. In *Astrobiology Science Conference, NASA Ames Research Center, April 7–11, 2002*.

Braterman P. S., Cairns-Smith A. G., and Sloper R. W. (1983) Photo-oxidation of hydrated Fe^{+2}—significance for banded iron formations. *Nature* **303**, 163–164.

Braterman P. S., Cairns-Smith A. G., Sloper R. W., Truscott T. G., and Craw M. (1984) Photooxidation of iron (II) in water between pH 7.4 and 4.0. *J. Chem. Soc.: Dalton Trans.*, 1441–1445.

Bridgewater D., Keto L., McGregor V. R., and Myers J. S. (1976) Archaean gneiss complex in Greenland. In *Geology of Greenland*, Geological Survey of Greenland (eds. A. Escher and W. S. Watt). Copenhagen, pp. 20–75.

Brocks J. J., Logan G. A., Buick R., and Summons R. E. (1999) Archean molecular fossils and the early rise of Eukaryotes. *Science* **285**, 1033–1036.

Brocks J. J., Summons R. E., Logan G. A., and Buick R. (2002) Molecular fossils in Archean Rocks: constraints on the oxygenation of the upper water column (abstr.). In *Astrobiology Science Conference, NASA Ames Research Center, April 7–11, 2002*.

Bruno J., Wersin P., and Stumm W. (1992) On the influence of carbonate in mineral dissolution: II. The stability of $FeCO_3(s)$ at 25° and 1 atm. total pressure. *Geochim. Cosmochim. Acta* **56**, 1149–1155.

Burke W. H., Denison R. E., Heatherington E. A., Koepnick R. B., Nelson H. F., and Otto J. B. (1982) Variation of seawater $^{87}Sr/^{86}Sr$ throughout Phanerozoic time. *Geology* **10**, 516–519.

Cairns-Smith A. G. (1978) Precambrian solution photochemistry-inverse segregation and banded iron formations. *Nature* **276**, 807–808.

Canfield D. E. (1998) A new model for Proterozoic ocean chemistry. *Nature* **396**, 450–452.

Canfield D. E. (2001) Biogeochemistry of Sulfur Isotopes. In *Stable Isotope Geochemistry*, Reviews in Mineralogy and Geochemistry (eds. J. W. Valley and D. R. Cole). Washington, DC, vol. 43, pp. 607–636.

Canfield D. E. and Raiswell R. (1999) The evolution of the sulfur cycle. *Am. J. Sci.* **299**, 697–729.

Canfield D. E., Habicht K., and Thamdrup B. (2000) The Archean sulfur cycle and the early history of atmospheric oxygen. *Science* **288**, 658–661.

Canil D. (1997) Vanadium partitioning and the oxidation state of Archaean Komatiite magmas. *Nature* **389**, 842–845.

Canil D. (1999) Vanadium partitioning between orthopyroxene, spinel and silicate melt and the redox states of mantle source regions for primary magmas. *Geochim. Cosmochim. Acta* **63**, 557–572.

Canil D. (2002) Vanadium in peridotites, mantle redox and tectonic environments: Archean to present. *Earth Planet. Sci. Lett.* **195**, 75–90.

Carpenter S. J. and Lohmann K. C. (1997) Carbon isotope ratios of Phanerozoic marine cements: re-evaluating the global carbon and sulfur systems. *Geochim. Cosmochim. Acta* **61**, 4831–4846.

Catling D. C., Zahnle K. J., and McKay C. P. (2001) Biogenic methane, hydrogen escape, and the irreversible oxidation of early Earth. *Science* **293**, 839–843.

Chyba C. F. (1993) The violent emergence of the origin of life: progress and uncertainties. *Geochim. Cosmochim. Acta* **57**, 3351–3358.

Cicero A. D. and Lohmann K. C. (2001) Sr/Mg variation during rock-water interaction: implications for secular changes in the elemental chemistry of ancient seawater. *Geochim. Cosmochim. Acta* **65**, 741–761.

Clarke F. W. (1911) *The Data of Geochemistry,* 2nd edn. The Government Printing Office, Washington, DC.

Cloud P. E., Jr. (1968) Atmospheric and hydrospheric evolution on the primitive Earth. *Science* **160**, 729–736.

Cloud P. E., Jr. (1972) A working model for the primitive Earth. *Am. J. Sci.* **272**, 537–548.

Colman A. S. and Holland H. D. (2000) The global diagenetic flux of phosphorus from marine sediments to the oceans: redox sensitivity and the control of atmospheric oxygen levels. In *Marine Authigenesis: From Global to Microbiol*, SEPM Special Publication No. 66 (eds. C. R. Glenn, L. Prévôt-Lucas, and J. Lucas). Tulsa, UK, pp. 53–75.

Compston W. and Pidgeon R. T. (1986) Jack Hills, evidence of more very old detrital zircons in Western Australia. *Nature* **321**, 766–769.

Condon D. J., Prave A. R., and Benn D. I. (2002) Neoproterozoic glacial-rainout intervals: observations and implications. *Geology* **30**, 35–38.

Conway E. J. (1943) The chemical evolution of the ocean. *Proc. Roy. Irish Acad.* **48B**(8), 161–212.

Conway E. J. (1945) Mean losses of Na, Ca, etc. in one weathering cycle and potassium removal from the ocean. *Am. J. Sci.* **243**, 583–605.

Cook P. J. and McElhinny M. W. (1979) A reevaluation of the spatial and temporal distribution of sedimentary phosphate deposits in the light of plate tectonics. *Econ. Geol.* **74**, 315–330.

Cook P. J. and Shergold J. H. (1984) Phosphorus, phosphorites and skeletal evolution at the Precambrian–Cambrian boundary. *Nature* **308**, 231–236.

Cook P. J. and Shergold J. H. (1986) Proterozoic and Cambrian phosphorites—nature and origins. In *Phosphate Deposits of the World: Volume 1. Proterozoic and Cambrian Phosphorites* (eds. P. J. Cook and J. H. Shergold). Cambridge University Press, Cambridge, pp. 369–386.

Crick I. H. (1992) Petrological and maturation characteristics of organic matter from the Middle Proterozoic McArthur Basin, Australia. *Austral. J. Earth Sci.* **39**, 501–519.

Dalrymple G. B. and Ryder G. (1996) Argon-40/argon-39 age spectra of Apollo 17 highlands breccia samples by laser step heating and the age of the Serenitatis basin. *J. Geophys. Res.* **101**, 26069–26084.

Das N., Horita J., and Holland H. D. (1990) Chemistry of fluid inclusions in halite from the Salina Group of the Michigan Basin: implications for Late Silurian seawater and the origin of sedimentary brines. *Geochim. Cosmochim. Acta* **54**, 319–327.

Delaney M. L. and Boyle F. A. (1986) Lithium in foraminiferal shells: implications for high-temperature hydrothermal circulation fluxes and oceanic crustal generation rates. *Earth Planet. Sci. Lett.* **80**, 91–105.

Delano J. W. (2001) Redox history of the Earth's interior: implications for the origin of life. *Origins Life Evol. Biosphere* **31**, 311–334.

De Long E. F. (2000) Resolving a methane mystery. *Nature* **407**, 577–579.

De Ronde C. E. J., de Wit M. J., and Spooner E. T. C. (1994) Early Archean (>3.2 Ga) iron-oxide-rich hydrothermal discharge vents in the Barberton greenstone belt. *South Africa Geol. Soc. Am. Bull.* **106**, 86–104.

De Ronde C. E. J., Channer R. M., Faure de R., Bray C. J., and Spooner E. T. C. (1997) Fluid chemistry of Archean seafloor hydrothermal vents: implications for the composition of circa 3.2 Ga seawater. *Geochim. Cosmochim. Acta* **61**, 4025–4042.

Donnelly T. H. and Jackson M. J. (1988) Sedimentology and geochemistry of a mid-Proterozoic lacustrine unit from Northern Australia. *Sedim. Geol.* **58**, 145–169.

Donnelly T. H., Shergold J. H., Southgate P. N., and Barnes C. J. (1990) Events leading to global phosphogenesis around the Proterozoic–Cambrian boundary. In *Phosphorite Research and Development*, Geological Society Special Publication No. 52 (eds. A. J. G. Notholt and I. Jarvis). London, pp. 273–287.

Dymek R. F. and Klein C. (1988) Chemistry, petrology and origin of banded iron-formation lithologies from the 3,800 Ma Isua supracrustal belt. *West Greenland. Precamb. Res.* **39**, 247–302.

Elderfield H., Wheat C. G., Mottle M. J., Monnin C., and Spiro B. (1999) Fluid and geochemical transport through oceanic crust: a transect across the eastern flank of the Juan de Fuca Ridge. *Earth Planet. Sci.* **172**, 151–165.

Elderfield H., Cooper M., and Ganssen G. (2000) Sr/Ca in multiple species of planktonic foraminifera: implications for reconstructions of seawater Sr/Ca. *Geochem. Geophys. Geosys.* **1**, paper number 1999GC000031.

Elderfield H., Vautravers M., and Cooper M. (2002) The relationship between cell size and Mg/Ca, Sr/Ca, $\delta^{18}O$ and $\delta^{13}C$ of species of planktonic foraminifera. *Geochem. Geophys. Geosys.* **3**(8), paper number 10.1029/2001GC000194.

Farquhar J., Bao H., and Thiemens M. (2000) Atmospheric influence of Earth's earliest sulfur cycle. *Science* **289**, 756–758.

Farquhar J., Savarino J., Airieau S., and Thiemens M. (2001) Observation of wavelength-sensitive mass-independent sulfur isotope effect during SO_2 photolysis: implications for the early atmosphere. *J. Geophys. Res.* **106**, 32829–32839.

Feather C. E. (1980) Some aspects of Witwatersrand mineralization with special reference to uranium minerals: Prof. Paper. *US Geol. Surv.*, 1161-M.

Fedo C. M. and Whitehouse M. J. (2002) Metasomatic origin of quartz-pyroxene rock, Akilia, Greenland, and implications for Earth's earliest life. *Science* **296**, 1448–1452.

François L. M. (1986) Extensive deposition of banded iron formations was possible without photosynthesis. *Nature* **320**, 352–354.

François L. M. (1987) Reducing power of ferrous iron in the Archean ocean: 2. Role of $Fe(OH)^+$ photo-oxidation. *Paleoceanography* **2**, 395–408.

Froude D. O. (1983) Ion microprobe identification of 4,100–4,200 Myr old terrestrial zircons. *Nature* **304**, 616–618.

Fryer B. J. (1983) Rare-earth elements. In *Iron Formation: Facts and Problems* (eds. A. F. Trendall and R. C. Morris). Elsevier, Amsterdam, pp. 345–358.

Gaffin S. (1987) Ridge volume dependence on sea floor generation rate and inversion using long-term sea level change. *Am. J. Sci.* **287**, 596–611.

Garrels R. M. and Mackenzie F. T. (1971) *Evolution of Sedimentary Rocks*. W.W. Norton, New York.

Garrels R. M. and Perry E. C., Jr. (1974) Cycling of carbon, sulfur and oxygen through geologic time. In *The Sea* (ed. E. D. Goldberg). Wiley, New York, vol. 5, pp. 303–336.

Given R. K. and Wilkinson B. H. (1987) Dolomite abundance and stratigraphic age: constraints on rates and mechanisms of Phanerozoic dolostone formation. *J. Sedim. Petrol.* **57**, 1068–1078.

Grandstaff D. E. (1976) A kinetic study of the dissolution of uraninite. *Econ. Geol.* **71**, 1493–1506.

Grandstaff D. E. (1980) Origin of uraniferous conglomerates at Elliott Lake, Canada and Witwatersrand, South Africa: implications for oxygen in the Precambrian atmosphere. *Precamb. Res.* **13**, 1–26.

Grotzinger J. P. (1989) Facies and evolution of Precambrian carbonate depositional systems: emergence of the modern platform archetype. In *Controls on Carbonate Platform and Basin Development*, Special Publication No. 44 (eds. P. D. Crevello, J. L. Wilson, J. F. Sarg, and J. F. Read). The Society of Economic Paleontologists and Mineralogists, Tulsa, UK, pp. 79–106.

Grotzinger J. P. and Kasting J. F. (1993) New constraints on Precambrian ocean composition. *J. Geol.* **101**, 235–243.

Grundl T. and Delwiche J. (1993) Kinetics of ferric oxyhydroxide precipitation. *J. Contamin. Hydrol.* **14**, 71–87.

Habicht K. S., Gade M., Thamdrup B., Berg P., and Canfield D. E. (2002) Calibration of sulfate levels in Archean ocean. *Science* **298**, 2372–2374.

Hallam A. (1984) Pre-quaternary sea level changes. *Ann. Rev. Earth Planet. Sci.* **12**, 205–243.

Hallbauer D. K. (1986) The mineralogy and geochemistry of Witwatersrand pyrite, gold, uranium and carbonaceous matter. In *Mineral Deposits of Southern Africa* (eds. C. R. Anhaeusser and S. Maske). Geological Society of South Africa, Johannesburg, SA, pp. 731–752.

Halley E. (1715) A short account of the cause of the saltness of the ocean, and of the several lakes that emit no rivers; with a proposal, by help thereof, to discover the Age of the World. *Phil. Trans. Roy. Soc. London* **29**, 296–300.

Halliday A. N. (2000) Terrestrial accretion rates and the origin of the Moon. *Earth Planet. Sci. Lett.* **176**, 17–30.

Halliday A. N. (2001) In the beginning. *Nature* **409**, 144–145.

Halverson G. P. (2003) Towards an integrated stratigraphic and carbon isotopic record for the Neoproterozoic. Doctoral Dissertation, Department of Earth and Planetary Sciences, Harvard University, Cambridge, MA.

Hambrey M. J. and Harland W. B. (1981) *Earth's Pre-Pleistocene Glacial Record*. Cambridge University Press, Cambridge.

Han T.-M. (1982) Iron formations of Precambrian age: hematite–magnetite relationships in some Proterozoic iron deposits—a microscopic observation. In *Ore Genesis—The State of the Art* (eds. G. C. Amstutz, A. E. Goresy, G. Frenzel, C. Kluth, G. Moh, A. Wauschkuhn, and R. A. Zimmermann). Springer, Berlin, pp. 451–459.

Han T.-M. (1988) Origin of magnetite in iron-formations of low metamorphic grade. In *Proceedings of the 7th Quadrennial IAGOD Symposium*, pp. 641–656.

Haq B. U., Hardenbol J., and Vail P. R. (1987) Chronology of fluctuating sea levels since the Triassic. *Science* **235**, 1156–1167.

Hardie L. A. (1967) The gypsum-anhydrite equilibrium at one atmosphere pressure. *Am. Mineral.* **52**, 171–200.

Hardie L. A. (1991) On the significance of evaporites. *Ann. Rev. Earth Planet. Sci.* **19**, 131–168.

Hardie L. A. (1996) Secular variation in seawater chemistry: an explanation for the coupled variation in the mineralogies of marine limestones and potash evaporites over the past 600 my. *Geology* **24**, 279–283.

Harrison A. G. and Thode H. G. (1958) Mechanisms of the bacterial reduction of sulfate from isotope fractionation studies. *Trans. Faraday Soc.* **53**, 84–92.

Hartmann W. K., Ryder G., Grinspoon D., and Dones L. (2000) The time-dependent intense bombardment of the primordial Earth/Moon system. In *Origin of the Earth and Moon* (eds. R. M. Canup and K. Righter). University of Arizona Press, Tucson, pp. 493–512.

Harvie C. E., Weare J. H., Hardie L. A., and Eugster H. P. (1980) Evaporation of seawater: calculated mineral sequences. *Science* **208**, 498–500.

Hoehler T. M. and Alperin M. J. (1996) Anaerobic methane oxidation by a methanogen-sulfate reducer consortium: geochemical evidence and biochemical considerations. In *Microbial Growth in C1 Compounds* (eds. M. E. Lindstrom and F. R. Tabita). Kluwer Academic, San Diego.

Hoffman P. F. and Schrag D. P. (2002) The snowball earth hypothesis: testing the limits of global change. *Terra Nova* **14**, 129–155.

Hoffman P., Kaufman A. J., Halverson G. P., and Schrag D. P. (1998) A Neoproterozoic snowball Earth. *Science* **281**, 146–1342.

Holland H. D. (1962) Model for the evolution of the Earth's atmosphere. In *Petrologic Studies: A Volume to Honor A. F. Buddington* (eds. A. E. J. Engel, H. L. James, and B. F. Leonard). Geological Society of America, pp. 447–477.

Holland H. D. (1972) The geologic history of seawater: an attempt to solve the problem. *Geochim. Cosmochim. Acta* **36**, 637–651.

Holland H. D. (1973) Systematics of the isotopic composition of sulfur in the oceans during the Phanerozoic and its implications for atmospheric oxygen. *Geochim. Cosmochim. Acta* **37**, 2605–2616.

Holland H. D. (1984) *The Chemical Evolution of the Atmosphere and Oceans*. Princeton University Press, Princeton, NJ, 582p.

Holland H. D. (1994) Early Proterozoic atmospheric change. In *Early Life on Earth*, Nobel Symposium 84 (ed. S. Bengtson). Columbia University Press, New York, pp. 237–244.

Holland H. D. (1997) Evidence for life on Earth more than 3, 850 million years ago. *Science* **275**, 38–39.

Holland H. D. (2002) Volcanic gases, black smokers, and the Great Oxidation Event. *Geochim. Cosmochim. Acta* **66**, 3811–3826.

Holland H. D. and Beukes N. J. (1990) A paleoweathering profile from Griqualand West, South Africa: evidence for a dramatic rise in atmospheric oxygen between 2.2 and 1.9 BYBP. *Am. J. Sci.* **290**, 1–34.

Holland H. D. and Zbinden E. A. (1988) Paleosols and the evolution of the atmosphere: Part I. In *Physical and Chemical Weathering in Geochemical Cycles* (eds. A. Lerman and M. Meybeck). Kluwer Academic, San Diego, pp. 61–82.

Holland H. D. and Zimmermann H. (1998) On the secular variations in the composition of Phanerozoic marine potash evaporites: Comment and reply. *Geology* **26**, 91–92.

Holland H. D. and Zimmermann H. (2000) The dolomite problem revisited. *Int. Geol. Rev.* **42**, 481–490.

Holland H. D., Horita J., and Seyfried W. E. (1996) On the secular variations in the composition of Phanerozoic marine potash evaporites. *Geology* **24**, 993–996.

Holser W. T. (1963) Chemistry of brine inclusions in Permian salt from Hutchinson, Kansas. In *Symposium on Salt (First)* (ed. A. C. Bersticker). Northern Ohio Geol. Soc., Cleveland, OH, pp. 86–95.

Holser W. T. and Kaplan I. R. (1966) Isotope geochemistry of sedimentary sulfates. *Chem. Geol.* **1**, 93–135.

Holser W. T., Schidlowski M., Mackenzie F. T., and Maynard J. B. (1988) Biogeochemical cycles of carbon and sulfur. In *Chemical Cycles in the Evolution of the Earth* (eds. C. B. Gregor, R. M. Garrels, F. T. Mackenzie, and J. B. Maynard). Wiley-Interscience, New York, pp. 105–173.

Holser W. T., Maynard J. B., and Cruikshank K. M. (1989) Modelling the natural cycle of sulphur through Phanerozoic

time. In *Evolution of the Global Biogeochemical Sulphur Cycle* (eds. P. Brimblecombe and A. Y. Lein). Wiley, New York, chap 2, pp. 21–56.

Horita J., Friedman T. J., Lazar B., and Holland H. D. (1991) The composition of Permian seawater. *Geochim. Cosmochim. Acta* **55**, 417–432.

Horita J., Weinberg A., Das N., and Holland H. D. (1996) Brine inclusions in halite and the origin of the Middle Devonian Prairie Evaporites of Western Canada. *J. Sedim. Res.* **66**, 956–964.

Horita J., Zimmermann H., and Holland H. D. (2002) The chemical evolution of seawater during the Phanerozoic: implications from the record of marine evaporites. *Geochim. Cosmochim. Acta* **66**, 3733–3756.

Iglesias-Rodriguez M. D., Armstrong R. A., Feely R., Hood R., Kleypas J., Milliman J. D., Sabine C., and Sarmiento J. L. (2002) Progress made in study of ocean's calcium carbonate budget. *EOS* **83**, 365, 374–375.

Iversen N. and Jørgensen B. B. (1985) Anaerobic methane oxidation rates at the sulfate-methane transition in marine sediments from Kattegat and Skagerrak (Denmark). *Limnol. Oceanogr.* **30**, 944–955.

Jackson M. J. and Raiswell R. (1991) Sedimentology and carbon–sulfur geochemistry of the Velkerry Formation, a mid-Proterozoic potential oil source in Northern Australia. *Precamb. Res.* **54**, 81–108.

Jackson M. J., Muir M. D., and Plumb K. A. (1987) Geology of the southern McArthur Basin, Northern Territory. *Bureau of Mineral Resources, Geology and Geophysics*. Bulletin 220.

Jacobsen S. B. and Kaufman A. J. (1999) The Sr, C, and O isotopic evolution of Neoproterozoic seawater. *Chem. Geol.* **161**, 37–57.

James H. L. (1983) Distribution of banded iron-formation in space and time. In *Iron Formation: Facts and Problems* (eds. A. F. Trendall and R. C. Morris). Elsevier, Amsterdam, pp. 471–490.

James H. L. (1992) Precambrian iron-formations: nature, origin, and mineralogical evolution from sedimentation to metamorphism. In *Diagenesis III: Developments in Sedimentology* (eds. K. H. Wolf and G. V. Chilingarian). Elsevier, Amsterdam, pp. 543–589.

Johnson W. J. and Goldstein R. H. (1993) Cambrian seawater preserved as inclusions in marine low-magnesium calcite cement. *Nature* **362**, 335–337.

Joly J. (1899) An estimate of the geological age of the Earth. *Sci. Trans. Roy. Dublin Soc.* **7**(II), 23–66.

Kakegawa T., Kawai H., and Ohmoto H. (1998) Origins of pyrite in the .5 Ga Mt. McRae Shale, the Hamersley District, Western Australia. *Geochim. Cosmochim. Acta* **62**, 3205–3220.

Karhu J. A. (1993) Paleoproterozoic evolution of the carbon isotope ratios of sedimentary carbonates in the Fennoscandian Shield. *Geol. Soc. Finland Bull.* **371**, 87.

Karhu J. A. and Holland H. D. (1996) Carbon isotopes and the rise of atmospheric oxygen. *Geology* **24**, 867–870.

Kasting J. F., Eggler D. H., and Raeburn S. P. (1993) Mantle redox evolution and the state of the Archean atmosphere. *J. Geol.* **101**, 245–257.

Kasting J. F., Pavlov A. A., and Siefert J. L. (2001) A coupled ecosystem-climate model for predicting the methane concentration in the Archean atmosphere. *Origin Life Evol. Biosphere* **31**, 271–285.

Kennedy M. J., Christie-Blick N., and Sohl L. E. (2001) Are Proterozoic cap carbonates and isotopic excursions a record of gas hydrate destabilization following Earth's coldest intervals? *Geology* **29**, 443–446.

Kinsman D. J. J. (1966) Gypsum and anhydrite of Recent age, Trucial Coast, Persian Gulf. In *2nd Symposium on Salt* (ed. J. L. Rau). The Northern Ohio Geological Society, Cleveland, OH, vol. 1, pp. 302–326.

Kirk J., Ruiz J., Chesley J., Titley S., and Walshe J. (2001) A detrital model for the origin of gold and sulfides in the Witwatersrand basin based on Re–Os isotopes. *Geochim. Cosmochim. Acta* **65**, 2149–2159.

Kirschvink J. L. (1992) Late Proterozoic low-latitude glaciation: the snowball earth. In *The Proterozoic Biosphere* (eds. J. W. Schopf and C. Klein). Cambridge University Press, Cambridge, pp. 51–52.

Klein C. and Beukes N. J. (1989) Geochemistry and sedimentology of a facies transition from limestone to iron-formation deposition in the Early Proterozoic Transvaal Supergroup, South Africa. *Econ. Geol.* **84**, 1733–1774.

Klein C. and Beukes N. J. (1993) Sedimentology and geochemistry of the glaciogenic Late Proterozoic Rapitan iron-formation in Canada. *Econ. Geol.* **88**, 542–565.

Kleine T., Münker C., Mezger K., and Palme H. (2002) Rapid accretion and early core formation on asteroids and the terrestrial planets from Hf–W chronometry. *Nature* **418**, 952–955.

Knoll A. H. (1992) Biological and biogeochemical preludes to the Edeacaran radiation. In *Origin and Early Evolution of the Metazoa* (eds. J. H. Lipps and P. W. Signor). Plenum, New York, chap. 4.

Konhauser K. O., Hamade T., Raiswell R., Morris R. C., Ferris F. G., Southam G., and Canfield D. E. (2002) Could bacteria have formed the Precambrain banded iron formations? *Geology* **30**, 1079–1082.

Kump L. R. (1993) The coupling of the carbon and sulfur biogeochemical cycles over Phanerozoic time. In *Interactions of C, N, P, and S Biogeochemical Cycles and Global Change* (eds. R. Wollast, F. T. Mackenzie, and L. Chou). Springer, pp. 475–490.

Lasaga A. C., Berner R. A., and Garrels R. M. (1985) An improved geochemical model of atmospheric CO_2 fluctuations over the past 100 million years. In *The Carbon Cycle and Atmospheric CO_2, Natural Variations Archean to Present*, Geophysical Monograph 32 (eds. E. T. Sundquist and W. S. Broecker). American Geophysical Union, Washington, DC, pp. 397–411.

Lazar B. and Holland H. D. (1988) The analysis of fluid inclusions in halite. *Geochim. Cosmochim. Acta* **52**, 485–490.

Lear C. H., Elderfield H., and Wilson P. A. (2000) Cenozoic deep-sea temperatures and global ice volumes from Mg/Ca in benthic foraminiferal calcite. *Science* **287**, 269–272.

Lear C. H., Elderfield H., and Wilson P. A. (2003) A Cenozoic seawater Sr/Ca record from benthic foraminiferal calcite and its application in determining global weathering fluxes. *Earth Planet. Sci. Lett.* **208**, 69–84.

Leather J., Allen P. A., Brasier M. D., and Cozzi A. (2002) Neoproterozoic snowball Earth under scrutiny: evidence from the Fig glaciation of Oman. *Geology* **30**, 891–894.

Lithgow-Bertelloni C., Richards M. A., Ricard Y., O'Connell R. J., and Engebretson D. C. (1993) Toroidal–poloidal partitioning of plate motions since 120 Ma. *Geophys. Res. Lett.* **20**, 375–378.

Logan G. A., Hayes J. M., Hieshima G. B., and Summons R. E. (1995) Terminal Proterozoic reorganization of biogeochemical cycles. *Nature* **376**, 53–56.

Lohmann K. C. and Walker C. G. (1989) The $\delta^{18}O$ record of Phanerozoic abiotic marine calcite cements. *Geophys. Res. Lett.* **16**, 319–322.

Lowenstein T. K., Timofeeff M. N., Brennan S. T., Hardie L. A., and Demicco R. V. (2001) Oscillations in Phanerozoic seawater chemistry: evidence from fluid inclusions in salt deposits. *Science* **294**, 1086–1088.

Lugmaier G. W. and Shukolyukov A. (1998) Early solar system timescales according to $^{53}Mn–^{53}Cr$ systematics. *Geochim. Cosmochim. Acta* **62**, 2863–2886.

Lyons T. W., Gellatly A. M., and Kah L. C. (2002) Paleoenvironmental significance of trace sulfate in sedimentary carbonates. In *Abstracts Volume, 6th International Symposium on the Geochemistry of the Earth's*

Surface, May 20–24, 2002, Honolulu, Hawaii, pp. 162–165.

Mackenzie F. T. and Garrels R. M. (1966) Chemical mass balance between rivers and oceans. *Am. J. Sci.* **264**, 507–525.

Melezhik V. A., Gorokhov I. M., Kuznetsov A. B., and Fallick A. E. (2001) Chemostratigraphy of neoproterozoic carbonates: implications for "blind" dating. *Terra Nova* **13**, 1–11.

Michaelis W., Seifert R., Nauhaus K., Treude T., Thiel V., Blumenberg M., Knittel K., Gieseke A., Peterknecht K., Pape T., Boetius A., Amann R., Jørgensen B. B., Widdel F., Peckmann J., Pimenov N., and Gulin M. (2002) Microbial reefs in the Black Sea fueled by anaerobic oxidation of methane. *Science* **297**, 1013–1015.

Millero F. J., Sotolongo S., and Izaguirre M. (1987) The oxidation kinetics of Fe(II) in seawater. *Geochim. Cosmochim. Acta* **51**, 793–801.

Mojzsis S. J., Arrhenius G., McKeegan K. D., Harrison T. M., Nutman A. P., and Friend C. R. L. (1996) Evidence for life on Earth before 3,800 million years ago. *Nature* **384**, 55–59.

Mojzsis S. J., Harrison T. M., and Pidgeon R. T. (2001) Oxygen-isotope evidence from ancient zircons for liquid water at the Earth's surface 4,300 Myr ago. *Nature* **409**, 178–181.

Morse J., Millero F. J., Thurmond V., Brown E., and Ostlund H. G. (1984) The carbonate chemistry of Grand Bahama Bank waters: after 18 years another look. *J. Geophys. Res.* **89**, 3604–3614.

Morse J. W., Wang Q., and Tsio M.-Y. (1997) Influences of temperature and Mg:Ca ratio on $CaCO_3$ precipitates from seawater. *Geology* **25**, 85–87.

Mottl M. J. (2003) Partitioning of energy and mass fluxes between mid-ocean ridge axes and flanks at high and low temperature. In *Energy and Mass Transfer in Marine Hydrothermal Systems* (eds. P. E. Halbach, V. Tunnicliffe, and J. R. Hein). Dahlem University Press, pp. 271–286.

Mottl M. J. and Wheat C. G. (1994) Hydrothermal circulation through mid-ocean ridge flanks: fluxes of heat and magnesium. *Geochim. Cosmochim. Acta* **58**, 2225–2237.

Muehlenbachs K. (1986) Alteration of the oceanic crust and the ^{18}O history of seawater. In *Stable Isotopes in High Temperature Geological Processes*, Reviews in Mineralogy (eds. J. W. Valley, H. P. Taylor, Jr., and J. R. O'Neil). Mining Society of America, Chelsea, MI, vol. 16, chap. 12, pp. 425–444.

Muehlenbachs K. and Clayton R. N. (1976) Oxygen isotope composition of the oceanic crust and its bearing on seawater. *J. Geophys. Res.* **81**, 4365–4369.

Muir M. D. (1979) A sabkha model for deposition of part of the Proterozoic McArthur Group of the Northern Territory, and implications for mineralization. *BMR J. Austral. Geol. Geophys.* **4**, 149–162.

Myers J. S. (2001) Protoliths of the 3.8–3.7 Ga Isua greenstone belt, West Greenland. *Precamb. Res.* **105**, 129–141.

Naraoka H., Ohtake M., Maruyama S., and Ohmoto H. (1996) Non-biogenic graphite in 3.8-Ga metamorphic rocks from the Isua district, Greenland. *Chem. Geol.* **133**, 251–260.

Nelson D. R., Trendall A. F., and Altermann W. (1999) Chronological correlations between the Pilbara and Kaapvaal cratons. *Precamb. Res.* **97**, 165–189.

Nelson D. R., Robinson B. W., and Myers J. S. (2000) Complex geological histories extending for ≥4.0 Ga deciphered from xenocryst zircon microstructures. *Earth Planet. Sci.* **181**, 89–102.

Nutman A. P., Kinny P. D., Compston W., and Williams J. S. (1991) Shrimp U–Pb zircon geochronology of the Narryer Gneiss Complex, Western Australia. *Precamb. Res.* **52**, 275–300.

Nutman A. P., McGregor V. R., Friend C. R. L., Bennett V. C., and Kinny P. D. (1996) The Itsaq Gneiss complex of southern West Greenland: the world's most extensive record of early crustal evolution (3,900–3,600 Ma). *Precamb. Res.* **78**, 1–39.

Nutman A. P., Bennett V. C., Friend C. R. L., and Rosing M. T. (1997) 3,710 and >3,790 Ma volcanic sequences in the Isua (Greenland) supracrustal belt: structural and Nd isotope implications. *Chem. Geol. (Isotope Geosci.)* **141**, 271–287.

Nutman A. P., Friend C. R. L., and Bennett V. (2002) Evidence for 3,650–3,600 Ma assembly of the northern end of the Itsaq Gneiss Comples, Greenland: implication for early Archaean tectonics. *Tectonics* **21**, 1–28.

Oehler D. Z. and Smith J. W. (1977) Isotopic composition of reduced and oxidized carbon in early Archaean rocks from Isua, Greenland. *Precamb. Res.* **5**, 221–228.

Ohmoto H. (1996) Evidence in pre-2.2 Ga paleosols for the early evolution of the atmospheric oxygen and terrestrial biota. *Geology* **24**, 1135–1138.

Ohmoto H. (1999) Redox state of the Archean atmosphere: evidence from detrital heavy minerals in ca. 3,250–2,750 Ma sandstones from the Pilbara Craton, Australia: Comment. *Geology* **27**, 1151–1152.

Ohmoto H., Kakegawa T., and Lowe D. R. (1993) 3.4-billion-year-old biogenic pyrites from Barberton, South Africa: sulfur isotope evidence. *Science* **262**, 555–557.

Ono S. (2002) Detrital uraninite and the early Earth's atmosphere: SIMS analyses of uraninite in the Elliot Lake district and the dissolution kinetics of natural uraninite. Doctoral Dissertation, Pennsylvania State University, State College, PA.

Orphan V. J., House C. H., Hinrichs K. U., McKeegan K. D., and DeLong E. F. (2001) Methane-consuming archaea revealed by directly coupled isotopic and phylogenetic analysis. *Science* **293**, 484–487.

Palmer H. R., Pearson P. N., and Cobb S. J. (2000) Reconstructing past ocean pH-depth profiles. *Science* **282**, 1468–1471.

Pavlov A. A. and Kasting J. F. (2002) Mass-independent fractionation of sulfur isotopes in Archean sediments: strong evidence for an anoxic Archean atmosphere. *Astrobiology* **2**, 27–41.

Pavlov A. A., Kasting J. F., Brown L. L., Rages K. A., and Freedman R. (2000) Greenhouse warming by CH_4 in the atmosphere of early Earth. *J. Geophys. Res.* **105**, 11981–11990.

Pavlov A. A., Hurtgen M., Kasting J. F., and Arthur M. A. (2003) A methane-rich Proterozoic atmosphere? *Geology* **31**, 87–90.

Paytan A., Kastner M., Campbell D., and Thiemens M. (1998) Sulfur isotopic composition of Cenozoic seawater sulfate. *Science* **282**, 1459–1462.

Paytan A., Mearon S., Cobb K., and Kastner M. (2002) Origin of marine barite deposits: Sr and S characterization. *Geology* **30**, 747–750.

Pearson P. N. and Palmer M. R. (1999) Middle Eocene seawater pH and atmospheric carbon dioxide concentrations. *Science* **284**, 1824–1826.

Pearson P. N. and Palmer M. R. (2000) Atmospheric carbon dioxide concentrations over the past 60 million years. *Nature* **406**, 695–699.

Peck W. H., Valley J. W., Wilde S. A., and Geraham C. M. (2001) Oxygen isotope ratios and rare earth elements in 3.3 to 4.4 Ga zircons: ion microprobe evidence for high $\delta^{18}O$ continental crust and oceans in the early Archean. *Geochim. Cosmochim. Acta* **65**, 4215–4229.

Pegram W. J. and Turekian K. K. (1999) The Osmium isotopic composition change of Cenozoic seawater as inferred from a deep-sea core corrected for meteoritic contributions. *Geochim. Cosmochim. Acta* **63**, 4053–4058.

Perry E. C., Jr. and Ahmad S. N. (1977) Carbon isotope composition of graphite and carbonate minerals from the 3.8-AE metamorphosed sediments, Isukasia, Greenland. *Earth Planet. Sci. Lett.* **36**, 281–284.

Petsch S. T. and Berner R. A. (1998) Coupling the geochemical cycles of C, P, Fe, and S: the effect on atmospheric O_2 and the isotopic records of carbon and sulfur. *Am. J. Sci.* **298**, 246–262.

Peucker-Ehrenbrink B. and Ravizza G. (2000) The marine osmium isotope record. *Terra Nova* **12**, 205–219.

Peucker-Ehrenbrink B., Ravizza G., and Hofmann A. W. (1995) The marine $^{187}Os/^{186}Os$ record of the past 80 million years. *Earth Planet. Sci. Lett.* **130**, 155–167.

Phillips G. N., Law J. D. M., and Myers R. E. (2001) Is the redox state of the Archean atmosphere constrained? *Soc. Econ. Geologists SEG Newslett.* **47**(1), 9–18.

Pinto J. P. and Holland H. D. (1988) Paleosols and the evolution of the atmosphere: Part II. In *Paleosols and Weathering Through Geologic Time*, Geol. Soc. Am. Spec. Pap. 216 (eds. J. Reinhardt and W. Sigleo), pp. 21–34.

Plummer L. N. and Busenberg E. (1982) The solubilities of calcite, aragonite and vaterite in CO_2–H_2O solutions between 0° and 90°, and an evaluation of the aqueous model for the system $CaCO_3$–CO_2–H_2O. *Geochim. Cosmochim. Acta* **46**, 1011–1040.

Porcelli D., Cassen P., Woolum D., and Wasserburg G. J. (1998) Acquisition and early losses of rare gases from the deep Earth. In *Origin of the Earth and Moon: Lunar Planetary Institute Contribution, Report 957*, pp. 35–36.

Porter S. M. and Knoll A. H. (2000) Testate amoebae in the Neoproterozoic era: evidence from vase-shaped microfossils in the Chuar Group, Grand Canyon. *Paleobiology* **26**, 360–385.

Porter S. M., Meisterfeld R., and Knoll, A. H. (2003) Vase-shaped microfossils from the Neoproterozoic Chuar Group, Grand Canyon: a classification guided by modern Testate amoebae. *J. Paleontol.* **77**, 205–255.

Ramdohr P. (1958) Die Uran-und Goldlagerstätten Witwatersrand-Blind River District-Dominion Reef-Serra de Jacobina: erzmikroskopische Untersuchungen und ein geologischer Vergleich. *Abh. Deutschen Akad. Wiss Berlin* **3**, 1–35.

Rasmussen B. and Buick R. (1999) Redox state of the Archean atmosphere: evidence from detrital heavy minerals in ca. 3,250–2,750 Ma sandstones from the Pilbara Craton, Australia. *Geology* **27**, 115–118.

Rasmussen B., Buick R., and Holland H. D. (1999) Redox state of the Archean atmosphere: evidence from detrital heavy minerals in ca. 3,250–2,750 Ma sandstones from the Pilbara Craton, Australia: Reply. *Geology* **27**, 1152.

Reeburgh W. S., Ward B. B., Whalen S. C., Sandbeck K. A., Kilpatrick K. A., and Kerkhof L. J. (1991) Black Sea methane geochemistry. *Deep-Sea Res.* **38**(suppl. 2), 1189–1210.

Rosing M. T. (1999) ^{13}C-depleted carbon microparticles in >3,700-Ma sea-floor sedimentary rocks from West Greenland. *Science* **283**, 674–676.

Rosing M. T., Rose N. M., Bridgewater D., and Thomsen H. S. (1996) Earliest part of Earth's stratigraphic record: a reappraisal of the >3.7 Ga Isua (Greenland) supracrustal sequence. *Geology* **24**, 43–46.

Rowley D. B. (2002) Rate of plate creation and destruction: 180 Ma to present. *Geol. Soc. Am. Bull.* **114**, 927–933.

Rubey W. W. (1951) Geologic history of seawater, an attempt to state the problem. *Bull. Geol. Soc. Am.* **62**, 1111–1147.

Ryder G. (1990) Lunar samples, lunar accretion and the early bombardment of the Moon. *EOS, Trans., AGU* **71**(10), 313, 322–323.

Rye R. and Holland H. D. (1998) Paleosols and the evolution of the atmosphere: a critical review. *Am. J. Sci.* **298**, 621–672.

Rye R., Kuo P. H., and Holland H. D. (1995) Atmospheric carbon dioxide concentration before 2.2 billion years ago. *Nature* **378**, 603–605.

Sandberg P. A. (1983) An oscillating trend in Phanerozoic non-skeletal carbonate mineralogy. *Nature* **305**, 19–22.

Sandberg P. A. (1985) Nonskeletal aragonite and pCO2 in the Phanerozoic and Proterozoic. In *The Carbon Cycle and Atmospheric CO2, Natural Variations Archean to Present*, Geophysical Monograph 32 (eds. E. T. Sundquist and W. S. Broecker) American Geophysical Union, Washington, DC, pp. 585–594.

Sanyal A., Hemming N. G., Broecker W. S., Lea D. W., Spero H. J., and Hanson G. N. (1996) Oceanic pH control on the boron isotopic composition of foraminifera: evidence from culture experiments. *Paleoceanography* **11**, 513–517.

Sarmiento J. L., Dunne J., Gnanadesikan A., Key R. M., Matsumoto K., and Slater R. (2002) A new estimate of the $CaCO_3$ to organic carbon export ratio. *Global Biogeochem. Cycles* **16**(4), 54-1–54-12.

Sasaki S. and Nakazawa K. J. (1986) Metal–silicate fractionation in the growing Earth: energy source for the terrestrial Magma Ocean. *J. Geophys. Res.* **91**, B9231–B9238.

Schidlowski M. (1966) Beiträge zur Kenntnis der radioactiven Bestandteile der Witwatersrand-Konglomerate. I Uranpecherz in den Konglomeraten des Oranje-Freistaat-Goldfeldes. *N. Jb. Miner Abh.* **105**, 183–202.

Schidlowski M., Appel P. W. U., Eichmann R., and Junge C. E. (1979) Carbon isotope geochemistry of the 3.7×10^9 yr-old Isua sediments, West Greenland: implications for the Archaean carbon and oxygen cycles. *Geochim. Cosmochim. Acta* **43**, 189–199.

Schidlowski M., Hayes J. M., and Kaplan I. R. (1983) Isotopic inferences of ancient biochemistries: carbon, sulfur, hydrogen, and nitrogen. In *Earth's Earliest Biosphere, Its Origin and Evolution* (ed. J. W. Schopf). Princeton University Press, Princeton, NJ, chap. 7, pp. 149–186.

Schopf J. W. (1983) Microfossils of the Early Archean Apex Chert: new evidence for the antiquity of life. *Science* **260**, 640–646.

Schopf J. W. and Packer B. M. (1987) Early Archean (3.3-billion to 3.5-billion-year-old) microfossils from Warrawoona Group, Australia. *Science* **237**, 70–73.

Schopf J. W., Kudryatsev A. B., Agresti D. G., Czaja A. D., and Widowiak T. J. (2002) Laser-Raman imagery of the oldest fossils on Earth. In *Astrobiology Science Conference, NASA Ames Research Center, April 7–11, 2002*.

Sellwood B. W. (1986) Shallow marine carbonate environments. In *Sedimentary Environments and Facies* (ed. H. G. Reading). Blackwell, UK, chap. 10, pp. 283–342.

Shen Y., Buick R., and Canfield D. E. (2001) Isotopic evidence for microbial sulphate reduction in the early Archaean era. *Nature* **410**, 77–81.

Shen Y., Canfield D. E., and Knoll A. H. (2002) Middle Proterozoic ocean chemistry: evidence from the McArthur Basin, Northern Australia. *Am. J. Sci.* **302**, 81–109.

Shields G. and Veizer J. (2002) Precambrian marine carbonate isotope database: version 1.1. *Geochem. Geophys. Geosys.* **3**, doi: 10.1029/2001GC000266.

Shimizu H., Umemoto N., Masuda A., and Appel P. W. U. (1990) Sources of iron-formations in the Archean Isua and Malene supracrustals, West Greenland: evidence from La–Ce and Sm–Nd isotopic data and REE abundances. *Geochim. Cosmochim. Acta* **54**, 1147–1154.

Sillén L. G. (1967) The ocean as a chemical system. *Science* **156**, 1189–1197.

Sleep N. H., Zahnle K. J., Kasting J. F., and Morowitz H. J. (1989) Annihilation of ecosystems by large asteroid impacts on the early Earth. *Nature* **342**, 139–142.

Southgate P. N., Bradshaw B. E., Domagala J., Jackson M. J., Idnurm M., Krassay A. A., Page R. W., Sami T. T., Scott D. L., Lindsay J. F., McConachie B. A., and Tarlowski C. (2000) Chronostratigraphic basin framework for Paleoproterozoic rocks (1,730–1,575 Ma) in northern Australia and implications for base-metal mineralization. *Austral. J. Earth Sci.* **47**, 461–483.

Spencer R. J. and Hardie L. A. (1990) Control of seawater composition by mixing of river waters and mid-ocean ridge hydrothermal brines. In *Fluid–Mineral Interactions: A Tribute to H. P. Eugster*. Special Publication 2 (eds. R. J. Spencer and I.-M. Chou). Geochemical Society, San Antonio, TX, pp. 409–419.

Spivack A. J., You C.-F., and Smith H. J. (1993) Foraminiferal boron isotope ratios as a proxy for surface ocean pH over the past 21 Myr. *Nature* **363**, 149–151.

Stanley S. M. and Hardie L. A. (1998) Secular oscillations in the carbonate mineralogy of reef-building and

sediment-producing organisms driven by tectonically forced shifts in seawater chemistry. *Paleogeogr. Paleoclimatol. Paleoecol.* **144**, 3–19.

Stein C. L. and Krumhansl J. L. (1988) A model for the evolution of brines in salt from the lower Salado Formation, southeastern New Mexico. *Geochim. Cosmochim. Acta* **52**, 1037–1046.

Steuber T. and Veizer J. (2002) Phanerozoic record of plate tectonic control of seawater chemistry and carbonate sedimentation. *Geology* **30**, 1123–1126.

Strauss H. (1993) The sulfur isotopic record of Precambrian sulfates: new data and a critical evaluation of the existing record. *Precamb. Res.* **63**, 225–246.

Strauss H. (1999) Geological evolution from isotope proxy signals-sulfur. *Chem. Geol.* **161**, 89–101.

Strauss H., DesMarais D. J., Hayes J. M., and Summons R. E. (1992) The carbon-isotopic record. In *The Proterozoic Biosphere* (eds. J. W. Schopf and C. Klein). Cambridge University Press, Cambridge, chap. 3, pp. 117–127.

Stumm W. and Lee G. F. (1961) Oxygenation of ferrous iron. *Ind. Eng. Chem.* **53**, 143–146.

Stumm W. and Morgan J. J. (1996) *Aquatic Chemistry: Chemical Equilibria and Rates in Natural Waters*. Wiley-Interscience, New York.

Suess E. (1980) Particulate organic carbon flux in the oceans—surface productivity and oxygen utilization. *Nature* **288**, 260–263.

Summons R. E., Jahnke L. L., Hope J. M., and Logan G. A. (1999) 2-methylhopanoids as biomarkers for cyanobacterial oxygenic photosynthesis. *Nature* **400**, 554–557.

Thode H. G. and Monster J. (1965) Sulfur isotope geochemistry of petroleum, evaporites, and ancient seas. In *Fluids in Subsurface Environments, Mem. 4*. Am. Assoc. Petrol. Geol., Tulsa, OK, pp. 367–377.

Thode H. G., Monster J., and Sunford H. B. (1961) Sulfur isotope geochemistry. *Geochim. Cosmochim. Acta* **25**, 159–174.

Vail P. R., Mitchum R. W., and Thompson S. (1977) Seismic stratigraphy and global changes of sea level 4, Global cycles of relative changes of sea level. *AAPG Memoirs* **26**, 82–97.

Van Zuilen M. A., Lepland A., and Arrhenius G. (2002) Reassessing the evidence for the earliest traces of life. *Nature* **418**, 627–630.

Veizer J., Holser W. T., and Wilgus C. K. (1980) Correlation of ^{13}C/^{12}C and ^{34}S/^{32}S secular variations. *Geochim. Cosmochim. Acta* **44**, 579–587.

Veizer J., Hoefs J., Lowe D. R., and Thurston P. C. (1989) Geochemistry of Precambrian carbonates: II. Archean greenstone belts and Archean seawater. *Geochim. Cosmochim. Acta* **53**, 859–871.

Veizer J., Ala D., Azmy K., Bruckschen P., Buhl D., Bruhn F., Carden G. A. F., Diener A., Ebneth S., Godderis Y., Jasper T., Korte C., Pawellek F., Podlaha O. G., and Strauss H. (1999) ^{87}Sr/^{86}Sr, δ^{13}C and δ^{18}O evolution of Phanerozoic seawater. *Chem. Geol.* **161**, 59–88.

Walker J. (1966) *Lectures on Geology*. The University of Chicago Press, Chicago, IL.

Walker R. N., Muir M. D., Diver W. L., Williams N., and Wilkins N. (1977) Evidence of major sulphate evaporite deposits in the Proterozoic McArthur Group, Northern Territory, Australia. *Nature* **265**, 526–529.

Wallmann K. (2001) Controls on the Cretaceous and Cenozoic evolution of seawater composition, atmospheric CO_2 and climate. *Geochim. Cosmochim. Acta* **65**, 3005–3025.

Walter M. R., Veevers J. J., Calver C. R., Gorjan P., and Hill A. C. (2000) Dating the 840–544 Neoproterozoic interval by isotopes of strontium, carbon, and sulfur in seawater and some interpretative models. *Precamb. Res.* **100**, 371–433.

Werne J. P., Sageman B. B., Lyons T. W., and Hollander D. J. (2002) An intergrated assessment of a "type euxinic" deposit: evidence for multiple controls on black shale deposition in the Middle Devonian Oatka Creek formation. *Am. J. Sci.* **302**, 110–143.

Wilde S. A., Valley J. W., Peck W. H., and Graham C. M. (2001) Evidence from detrital zircons for the existence of continental crust and oceans on the Earth 4.4 Gyr ago. *Nature* **409**, 175–178.

Wilkinson B. H. and Algeo T. J. (1989) Sedimentary carbonate record of calcium-magnesium cycling. *Am. J. Sci.* **289**, 1158–1194.

Winefield P. R. (2000) Development of late Paleoproterozoic aragonitic sea floor cements in the McArthur Group, Northern Australia. In *Carbonate Sedimentation and Diagenesis in the Evolving Precambrian World*, SEPM Special Publication 67 (eds. J. P. Grotzinger and N. P. James). pp. 145–159.

Yang W. and Holland H. D. (2002) The redox sensitive trace elements Mo, U, and Re in Precambrian carbonaceous shales: indicators of the Great Oxidation Event (abstr.). *Geol. Soc. Am. Ann. Mtng.* **34**, 382.

Yang W. and Holland H. D. (2003) The Hekpoort paleosol profile in Strata 1 at Gaborone, Botswana: soil formation during the Great Oxidation Event. *Am. J. Sci.* **303**, 187–220.

Yin Q., Jacobsen S. B., Yamashita K., Blichert-Toft J., Télouk P., and Albarède F. (2002) A short timescale for terrestrial planet formation from Hf–W chronometry of meteorites. *Nature* **418**, 852–949.

Young G. M. (1969) Geochemistry of Early Proterozoic tillites and argillites of the Gowganda Formation, Ontario, Canada. *Geochim. Cosmochim. Acta* **33**, 483–492.

Young G. M. (1976) Iron-formation and glaciogenic rocks of the Rapitan Group, Northwest Territories, Canada. *Precamb. Res.* **3**, 137–158.

Zimmermann H. (2000) Tertiary seawater chemistry—implications from fluid inclusions in primary marine halite. *Am. J. Sci.* **300**, 723–767.